

Contract No:

This document was prepared in conjunction with work accomplished under Contract No. DE-AC09-08SR22470 with the U.S. Department of Energy (DOE) Office of Environmental Management (EM).

Disclaimer:

This work was prepared under an agreement with and funded by the U.S. Government. Neither the U. S. Government or its employees, nor any of its contractors, subcontractors or their employees, makes any express or implied:

- 1) warranty or assumes any legal liability for the accuracy, completeness, or for the use or results of such use of any information, product, or process disclosed; or
- 2) representation that such use or results of such use would not infringe privately owned rights; or
- 3) endorsement or recommendation of any specifically identified commercial product, process, or service.

Any views and opinions of authors expressed in this work do not necessarily state or reflect those of the United States Government, or its contractors, or subcontractors.

We put science to work.™



**Savannah River
National Laboratory™**

OPERATED BY SAVANNAH RIVER NUCLEAR SOLUTIONS

A U.S. DEPARTMENT OF ENERGY NATIONAL LABORATORY • SAVANNAH RIVER SITE • AIKEN, SC

Evaluation of Simple Chemical Interactions in the Defense Waste Processing Facility (DWPF) Chemical Process Cell (CPC) Under the Glycolic Acid Flowsheet

W. H. Woodham

J. R. Zamecnik

June 2018

SRNL-STI-2017-00318, Revision 0

SRNL.DOE.GOV

DISCLAIMER

This work was prepared under an agreement with and funded by the U.S. Government. Neither the U.S. Government or its employees, nor any of its contractors, subcontractors or their employees, makes any express or implied:

1. warranty or assumes any legal liability for the accuracy, completeness, or for the use or results of such use of any information, product, or process disclosed; or
2. representation that such use or results of such use would not infringe privately owned rights; or
3. endorsement or recommendation of any specifically identified commercial product, process, or service.

Any views and opinions of authors expressed in this work do not necessarily state or reflect those of the United States Government, or its contractors, or subcontractors.

Printed in the United States of America

**Prepared for
U.S. Department of Energy**

Keywords: *Glycolic, Mercury, Nitrite,
CPC, DWPF*

Retention: *Permanent*

Evaluation of Simple Chemical Interactions in the Defense Waste Processing Facility (DWPF) Chemical Process Cell (CPC) Under the Glycolic Acid Flowsheet

W. H. Woodham
J. R. Zamecnik

June 2018

Prepared for the U.S. Department of Energy under
contract number DE-AC09-08SR22470.



REVIEWS AND APPROVALS

AUTHORS:

W. H. Woodham, Process Technology Programs, SRNL Date

J. R. Zamecnik, Process Technology Programs, SRNL Date

TECHNICAL REVIEW:

J. D. Newell, Process Technology Programs, SRNL, Reviewed per E7 2.60 Date

D. P. Lambert, Process Technology Programs, SRNL, Reviewed per E7 2.60 Date

APPROVAL:

F. M. Pennebaker, Chemical Processing Technologies, SRNL Date

D. E. Dooley, Director Date
Chemical Processing Technologies, SRNL

R. E. Edwards, Manager Date
Nuclear Safety and Engineering Integration, SRR

E. J. Freed, Manager Date
Defense Waste Processing Facility and Saltstone Facility Engineering

ACKNOWLEDGEMENTS

The authors wish to thank Jon Duvall, Phyllis Workman, and Vickie Williams for their consistent support and invaluable experience as laboratory technicians throughout this testing. The authors would also like to express gratitude to Whitney Riley, Beverly Wall, Kim Wyszynski, and Kandice Miles for their timely analysis of samples generated through the testing described herein. Additionally, the authors would like to acknowledge the work of Andy Foreman and Gary Dobos for their work in modifying the small-scale J-Kem apparatus used during this testing, the work of Holly Hall in coordinating and scheduling the tasks performed, the assistance of Amy Blunt in assessment and disposal of the waste generated as a result of the testing herein described, and the work of Matt Williams in analyzing and processing offgas data generated during experimentation. Finally, the authors would like to thank Savannah River Remediation for the support of this project, the aim of which is and has always been to enhance safety in the field of radioactive waste treatment and disposal by means of increased understanding of the chemical interactions present in nuclear waste slurries.

EXECUTIVE SUMMARY

This report describes results from testing developed for the increased understanding of simple chemical interactions relevant to the processing and vitrification of radioactive waste at the Savannah River Site (SRS) in Aiken, SC. This work is outlined in task 3 of the Technical Task Request X-TTR-S-00024, Rev. 0 and task 4 of the Task Technical & Quality Assurance Plan SRNL-RP-2014-01183 Rev. 0. The testing was conducted from May 2016 through February 2017 at the Aiken County Technology Laboratory (ACTL) and performed by Savannah River National Laboratory (SRNL) personnel. This testing involved the investigation of simple reactions and interactions of glycolic or nitric acids with combinations of sodium nitrite, manganese dioxide, mercuric oxide, and noble metals (silver, palladium, rhodium, and ruthenium). The aim of this testing was to better understand the reactions and chemical phenomena previously observed in the Sludge Receipt and Adjustment Tank (SRAT) cycle of the Chemical Process Cell (CPC) in the Defense Waste Processing Facility (DWPF).

Glycolic acid has been recommended as an alternative to formic acid due to the lowered production of flammable hydrogen gas during processing in the CPC relative to that produced under formic acid processing. Among other things, the testing described herein seeks to better understand by what mechanism the glycolic acid flowsheet can allow processing with production of minimal H₂ despite the generation of formate and the presence of the same noble metals necessary for catalytic formic acid dehydrogenation.

Four series of tests (nineteen tests in total) were conducted to investigate the reactions of sodium nitrite, mercuric oxide, and manganese dioxide with glycolic acid with and without noble metals. These species were chosen for study because they are major species that undergo REDuction/OXidation (REDOX) reactions in the CPC. To avoid the complication of using a solid species that does not dissolve, iron hydroxides were not studied in this initial work even though they can possibly participate in REDOX reactions at high acid stoichiometries. The reactions were studied as functions of acid stoichiometry, the percent of acid added as reducing acid, reaction headspace to sludge volume, reagent concentrations, and acid addition rates. Tests were performed with single species and with several combinations of species.

Anion conversions, metal solubilities, mercury reduction, and offgas generation were monitored as a function of time for most of these runs. The following conclusions have been made from this testing:

- The destruction of nitrite to form NO_x gases and nitrate occurs almost totally by internal disproportionation of the nitrous acid formed and not by REDOX reactions with glycolic acid.
- The acid stoichiometry of nitrite destruction is 2/3 mole of any acid per mole of nitrite.
- Scrubbed NO₂ gas recycled as HNO₂ and HNO₃ reduced the effective acid requirement to ½ mole of any acid per mole of nitrite.
- Lower acid feedrates result in higher nitrite-to-nitrate conversions because relatively more NO₂ is scrubbed to recycle HNO₂ and HNO₃.
- The generation of HNO₂ and HNO₃ in the Mercury Water Wash Tank (MWWT) has the potential to dissolve previously collected Hg⁰ metal.
- An offgas condensate that was caustic quenched showed the presence of both HNO₂ and HNO₃, whereas unquenched samples (that had been stored several days or more) showed only the presence of HNO₃, indicating that HNO₂ is probably lost as NO_x gas during storage. Condensates to be analyzed for nitrogen species other than ammonia should be caustic quenched.
- The reduction of nitrite by glycolic acid produces very small quantities of N₂O, indicating a REDOX reaction does occur but to a very low extent.

- The reduction of one mole of MnO_2 by glycolic acid requires 2.33-2.50 moles of any acid, consumes 0.33 to 0.50 moles of glycolate, but requires about 0.90 moles of glycolate, which is an excess of 100-140% depending on the reaction stoichiometry chosen.
- The reduction of MnO_2 by glycolic acid produces varying amounts of formate. Due to the limited scope of this work, the dependence of the conversion to formate on reaction parameters was not determined.
- No oxalate is generated in the reduction of MnO_2 alone or nitrite alone, or in the dissolution of HgO alone by glycolic acid.
- Oxalate is generated transiently when mixtures of MnO_2 , nitrite, and HgO are reacted with glycolic acid, indicating that there are additional reactions occurring when these three species are present together that do not occur with the individual species.
- This work did not, due to its limited scope, determine the reactions with full sludge simulants that generate measurable quantities of oxalate at the end of the SRAT cycle.
- The reduction of MnO_2 can be accomplished with nitrite and nitric acid, showing that a reducing acid is not required to reduce MnO_2 . In this reaction, nitrous acid acts as a reductant rather than an oxidant as it commonly does. It is unclear what effects this reaction has on acid stoichiometry.
- Most of the formic acid generated in the reduction of MnO_2 is consumed when HgO and nitrite are present.
- It was not determined if the reaction of MnO_2 and glycolic acid to generate two moles of CO_2 per mole of glycolate proceeds directly or through the generation of formate which subsequently reacts with MnO_2 to generate CO_2 .
- There is some evidence that the reduction of MnO_2 by glycolic acid may proceed through glyoxylic acid. Several tests showed more glycolate destruction than could be accounted for by formate and CO_2 generated.
- The presence of glyoxylic acid in samples could be missed by the Ion Chromatography (IC) method with caustic quenching if the glyoxylic acid is unstable in caustic solutions.
- Possible intermediate species that are non-ionic are not currently measured. If these species are unstable or volatile in caustic solutions (e.g., formaldehyde), the caustic quench preparation would remove them.
- HgO is readily dissolved by both nitric and glycolic acids.
- In the presence of MnO_2 and HgO , the reduction of nitrite by glycolic acid is delayed until these species are both dissolved.
- The presence of noble metals had no measurable effect on any of the reactions studied.
- Low generation of formate in the presence of noble metals *and* Hg in CPC demonstrations with sludge is due to the presence of Hg and not the noble metals.
- The measurement of dissolved Mn^{2+} in the presence of glycolic acid appears to be biased low by up to 30%.
- A GMA minimum acid equation similar to the KMA or Hsu equation can be developed for the NG flowsheet that will account for the actual chemical reactions occurring in the NG flowsheet.
- The Hsu equation appears to provide a better basis for the development of a GMA equation.

- The Hsu and KMA equations are tentatively acceptable for prediction of the acid window with the acceptable range being between 100 and 115% minimum acid.
- An additional additive term is needed in a GMA equation to account for the additional acid necessary to achieve specific rheological properties.

The following recommendations are divided into three categories: 1) additional fundamental R&D on simplified chemistry testing, should SRR choose to fund; 2) testing that would be incorporated into other SRR requested testing such as sludge batch qualification for the NG flowsheet; 3) flowsheet optimization that would occur after transition to the NG flowsheet and throughout one or more sludge batches. None of the recommendations need to be completed prior to implementation of the NG flowsheet in DWPF.

1) Fundamental R&D:

- a. Further testing targeting the role of direct oxidation of nitrite by manganese and other metal oxides in the CPC should be investigated.
- b. Samples for IC analysis should be taken without the Caustic Quench preparation and immediately be analyzed by IC to determine if glyoxylic acid is present. If glyoxylic acid is found, its stability in caustic quenched samples should be investigated.
- c. Tests with only MnO_2 and HgO and with only HgO and nitrite should be performed to understand the effect of each on the chemistry.
- d. The reaction of HgO with glycolic acid should be studied with prior addition of nitric acid to dissolve the HgO to determine if Hg^0 is formed and if the presence of nitrate is sufficient to cause HgO reduction.
- e. The reduction reactions of MnO_2 , HgO and nitrite should be studied further using full supernate simulants to better understand what conditions can result in reduction of HgO . Addition of Fe^{3+} as $\text{Fe}(\text{OH})_3$ solids should also be considered since significant Fe dissolution occurs at high acid stoichiometries, which might indicate reduction of Fe^{3+} to Fe^{2+} .
- f. Examination of additional historical data for the NG flowsheet (other than SB9-NG) should be included in analyses of data similar to that done in this work.
- g. Three full sludge demonstrations should be performed with 1) both noble metals and Hg present; 2) with only noble metals present; and 3) with only Hg present to verify that it is the presence of Hg that results in low conversion of glycolate to formate.

2) Incorporated into other planned testing:

- a. Future testing should cover the range of KMA values from 100–115% because this appears to be the range that may result in acceptable rheological properties.
- b. Because the results for SB9-NG indicate that acid requirements from the KMA or 2 Hsu GMA equations between 100-115% may be optimal for melter feed rheology, the basis for increasing the amount of acid above that from the KMA or one of the proposed GMA equations should be studied further. It appears that this increased acid may be needed to dissolve Fe (and possibly other metals) to a certain extent that results in the desired rheology.
- c. The cause of the low bias in soluble Mn concentration measurements in supernate samples containing glycolic acid should be determined, and a method developed to assure accurate measurements.
- d. When analyzing condensate samples for nitrite and nitrate, the samples should be caustic quenched to prevent decomposition of nitrous acid during storage. Comparison to unquenched samples should be performed. (Condensate samples should probably not be caustic quenched

if the intended analysis is for species that are potentially volatile under caustic conditions (e.g., ammonia, formaldehyde).

3) Flowsheet optimization:

- a. Further work on the relationships of Mn solubility, Fe solubility, yield stress, and consistency should be performed with additional sludge compositions to develop correlations between these variables and acid requirement.
- b. More real waste data is needed because the dissolution of Fe is likely to be different than in simulants.

TABLE OF CONTENTS

LIST OF TABLES	xii
LIST OF FIGURES	xii
LIST OF ABBREVIATIONS.....	xiv
1.0 Quality Assurance.....	1
2.0 Introduction.....	1
2.1 Proposed Nitrite Chemistry	4
2.2 Proposed MnO ₂ Chemistry.....	5
2.2.1 Reactivity of Reducing Acids with MnO ₂	8
2.3 Proposed HgO Chemistry.....	8
2.4 Proposed Roles of Noble Metals	9
2.5 Acid Requirements and Minimum Acid Requirement Equations	10
3.0 Experimental Procedure.....	12
3.1 Experimental Set-up.....	12
3.1.1 Initial Nitrite Tests.....	12
3.1.2 J-Kem Tests	14
3.1.3 Combined Species Tests	15
3.2 Solution/Slurry Preparation.....	16
3.3 Offgas Sampling and Analysis.....	16
3.4 Liquid Sampling and Analysis	17
3.5 pH Measurement	17
4.0 Results and Discussion	18
4.1 Destruction of Nitrite.....	18
4.1.1 Effect of Acid Selection.....	20
4.1.2 Behavior of Nitrogen Oxide Gases in Offgas System	26
4.1.3 Effect of MnO ₂ on Nitrite	30
4.1.4 Summary of Observed Nitrogen Chemistry	31
4.2 Reduction of MnO ₂	33
4.2.1 Reduction by Glycolic Acid	34
4.2.2 Generation of Oxalate and Formate.....	35
4.3 Reduction of HgO	35
4.3.1 Reaction of HgO with Glycolic Acid	36
4.3.2 Reaction of HgO with Formic Acid.....	36
4.4 Combined Species Testing	37

4.4.1 Reduction of HgO in Supernate Only Tests from 2012.....	47
4.5 Minimum Acid Equations for the NG Flowsheet.....	49
5.0 Conclusions.....	58
6.0 Recommendations.....	59
7.0 References.....	61
Appendix A Equations for the Prediction of Glycolate Destruction, Nitrite to Nitrate Conversion, and Conversions to Formate and Oxalate.....	64

LIST OF TABLES

Table 2-1. Dissociation Constants and Molecular Weights for Acids Anticipated in the CPC.....	4
Table 2-2 Comparison of Minimum Acid Equation Terms and Coefficients.....	10
Table 3-1. Derivation of Target Concentrations Used Throughout Testing.....	16
Table 3-2. Offgas Components by Analysis Technique.....	17
Table 4-1. Run Parameters and Results for Nitrite-Only Tests.....	19
Table 4-2. Run Parameters and Additional Results for Nitrite-Only Tests.....	20
Table 4-3. Selected Results from Initial Nitrite Testing.....	26
Table 4-4. Run Parameters and Results for J-Kem MnO ₂ Testing.....	34
Table 4-5. Run Parameters and Results for J-Kem HgO Testing.....	36
Table 4-6. Comparison of Stoichiometric Requirements.....	37
Table 4-7. Run Parameters and Results from Combined Species Testing.....	38
Table 4-8. Composition of Supernate Simulant for Runs GF39a–GF39e.....	47
Table 4-9. Runs GF39a-e Parameters and Results.....	48
Table 4-10. Concentration Inputs for Table 4-11.....	52
Table 4-11. Calculated Minimum Acid for Proposed Equations.....	53

LIST OF FIGURES

Figure 2-1. Possible Reaction Pathways of Glycolic Acid.....	6
Figure 2-2. Order of Reactivity of Glycolic Acid and Products towards MnO ₂ Reduction.....	8
Figure 3-1. Photograph of 4-L SRAT Apparatus Used for CPC Simulations.....	12
Figure 3-2. Schematic of 4-L Apparatus Used for Initial Nitrite Testing.....	13
Figure 3-3. Photograph of J-Kem Vessel Used in Testing.....	14
Figure 3-4. Photograph of Machined Teflon Cap for J-Kem Reactor Vessels.....	15
Figure 4-1. pH Profiles of Initial Nitrite Tests 1A-5A (Nitric Acid) & 6A-7A (Glycolic Acid).....	21
Figure 4-2. Concentrations of Nitrite & Nitrate, NO _x Rate, and pH During Run 4A.....	22
Figure 4-3. OLI Models of Reactions in Run 4A.....	24
Figure 4-4. Concentrations of Nitrite & Nitrate, NO _x Rate, and pH During Run 1A.....	25

Figure 4-5. Production Rates of NO During Initial Nitrite Tests..... 27

Figure 4-6. Consumption Rates of O₂ During Initial Nitrite Tests 1A-7A. 28

Figure 4-7. Photograph of Bubbles Forming in MWWT Condensate During CPC Run SB9-NG57..... 30

Figure 4-8. Photographs of MnO₂/Nitrite Slurry Before and After Treatment with Nitric Acid..... 31

Figure 4-9. Proposed Model for Nitrite Destruction by Nitrous Acid Disproportionation in the Absence of Other Reactants. 32

Figure 4-10. Proposed Model for Nitrite Destruction in the Presence of MnO₂ Particles. 33

Figure 4-11. Photograph of HgO-Glycolic Acid Solution After Treatment with Formic Acid..... 37

Figure 4-12. Anion Conversions, Offgas Production, Metal Solubilities, and pH of Run 1D as a Function of Processing Time..... 40

Figure 4-13. Species Quantities for Run 1D as a Function of Processing Time..... 41

Figure 4-14. Anion Conversions, Offgas Production, Metal Solubilities, and pH of Run 2D as a Function of Processing Time..... 42

Figure 4-15. Anion Conversions, Offgas Production, Metal Solubilities, and pH of Run 3D as a Function of Processing Time..... 46

Figure 4-16. Photos of Runs GF39a and 39b Before and After HgO Dissolution..... 48

Figure 4-17. Requirement for Any Acid for MnO₂ versus HgO..... 51

Figure 4-18. GMA Minimum Acid Stoichiometry Based on KMA Equation..... 54

Figure 4-19. GMA Minimum Acid Stoichiometry Based on Hsu Equation..... 55

Figure 4-20. SB9-NG and SC-18 Yield Stress and Consistency versus Koopman Minimum Acid..... 56

LIST OF ABBREVIATIONS

ACTL	Aiken County Technology Laboratory
CPC	Chemical Process Cell
DWPF	Defense Waste Processing Facility
ELN	Electronic Laboratory Notebook
FAVC	Formic Acid Vent Condenser
FTIR	Fourier Transform Infrared Spectrometer
GC	Gas Chromatograph
GMA	Glycolic Minimum Acid
HSV	Headspace Volume
IC	Ion Chromatography
ICP-AES	Inductively-Coupled Plasma-Atomic Emission Spectroscopy
KMA	Koopman Minimum Acid Stoichiometry
MS	Mass Spectrometer
MSE	Mixed Solvent Electrolyte
MWWT	Mercury Water Wash Tank
NA	Not Applicable
NF	Nitric-Formic
NG	Nitric-Glycolic
OD	Outside diameter
PRA	Percent Reducing Acid
PSAL	Process Science Analytical Laboratory
REDOX	REDuction / OXidation Potential
R&D	Research and Development
SB	Sludge Batch
SC	Shielded Cells
SME	Slurry Mix Evaporator
SMECT	Slurry Mix Evaporator Condensate Tank
SRAT	Sludge Receipt and Adjustment Tank
SRNL	Savannah River National Laboratory
SRR	Savannah River Remediation
SRS	Savannah River Site
TS	Total Solids

1.0 Quality Assurance

This work is outlined in task 3 of the Technical Task Request¹ and task 4 of the Task Technical & Quality Assurance Plan.² Additional details are given in the Chemistry Path Forward document.³

Requirements for performing reviews of technical reports and the extent of review are established in Manual E7, Procedure 2.60.⁴ Savannah River National Laboratory (SRNL) documents the extent and type of review using the SRNL Technical Report Design Checklist contained in WSRC-IM-2002-00011, Rev. 2.⁵ This report has received design verification by document review.

Experimental data are recorded in the Electronic Laboratory Notebook (ELN) experiment T7909-00035-15.⁶

2.0 Introduction

In recent years, Savannah River Remediation (SRR) has worked to implement the nitric-glycolic (NG) flowsheet as a processing improvement over the current nitric-formic (NF) flowsheet for the pretreatment and vitrification of radioactive waste in the Defense Waste Processing Facility (DWPF) at the Savannah River Site (SRS) in Aiken, SC. The use of glycolic acid in place of formic acid has been shown to decrease the production of flammable H₂ and ammonia in both the Chemical Process Cell (CPC) and the melter.⁷⁻¹⁰

The incorporation of glycolic acid in the CPC is an improvement over the use of formic acid in terms of hazard mitigation, but is not without its own challenges. Several challenges relate to the understanding of the actual chemical reactions of glycolic acid in this system.

The average oxidation state of each carbon in glycolic acid is +1, whereas the oxidation state of carbon in formic acid is +2, which means that glycolic acid is capable of reducing three times as much oxidant as formic acid upon full conversion to CO₂. In other words, formic acid can transfer two electrons for reduction while glycolic acid can transfer six. The Koopman Minimum Acid¹¹ (KMA) and Hsu Minimum Acid^{12,13} equations which define the amounts of nitric and formic acids needed in the NF flowsheet were developed for formic acid as the reductant. To expect that the same number of moles of glycolic acid would be needed compared to formic acid is incorrect because glycolic acid has three times the reducing capacity. Shielded Cells (SC) Run SC-18¹⁰ and several NG flowsheet (SB9-NG) simulant runs¹⁴ were performed with glycolic acid at 78% KMA acid requirement and demonstrated sufficient destruction of nitrite, whereas 100% KMA would have been required for formic acid. Therefore, a better understanding of the underlying chemistry of glycolic acid is needed to define a chemically sound minimum acid requirement equation for glycolic acid. (Note that the *requirements* for such an equation might be different; e.g., destruction of nitrite might no longer be important, or the SME slurry rheology might be important.) The Minimum Acid Equation will be discussed in light of the current work in Section 4.5.

The important parameters for the NF flowsheet are nitrite destruction, peak hydrogen generation rate, nitrite to nitrate conversion, formic acid destruction, and Slurry Mix Evaporator (SME) slurry rheology. The degree of nitrite destruction may not be important, and hydrogen generation is minimal under all conditions tested in the NG flowsheet. For both flowsheets, the relative amounts of oxidants and reductants in the SME product are important, so formic and glycolic acid destruction and nitrite to nitrate conversion are important. Prediction of the glass product REDUction/OXidation (REDOX) state of the SME product (or SRAT product with frit added if a SME cycle is not performed; this is only applicable to simulant testing) depends on the aforementioned parameters. The REDOX is defined in terms of chemical composition according to the following semi-empirical electron equivalents model:¹⁵⁻¹⁸

$$\text{REDOX} = \frac{\text{Fe}^{2+}}{\sum \text{Fe}} = 0.2358 + 0.1999(2[\text{F}] + 4[\text{C}] + 4[\text{O}_T] + 6[\text{G}] + 2.88[\text{A}] - 5[\text{N}] - m[\text{Mn}]) \frac{45}{T} \quad [1]$$

where [F] = formate (mol/kg feed)

[C] = coal (carbon) (mol/kg feed)

[O_T] = total oxalate (soluble and insoluble) (mol/kg feed)
[G] = glycolate (mol/kg feed)
[A] = antifoam (mol C/kg feed)
[N] = nitrate + nitrite (mol/kg feed)
m = coefficient (0 for the NG flowsheet)
[Mn] = manganese (mol/kg feed)
T = total solids (wt %)

Prediction of the amount of each acid required to satisfactorily treat the sludge is required. In the NF flowsheet, both formic acid destruction and nitrite to nitrate conversion are relatively constant within certain ranges and the values used in testing have generally been estimated from past experience. For the NG flowsheet, nitrite to nitrate conversion is not constant, and differences in glycolate destruction affect the REDOX more because the coefficient on glycolate is 6 versus the formate value of 2.

It has also been observed that glycolic acid leads to the production of formate and oxalate in CPC simulation experiments, adding a complexity in REDOX prediction that is not present in the NF flowsheet.^{8,9,19,20} Glycolate has also been observed to be more chemically stable in CPC simulations than formate, typically yielding measurably lower acid destruction values and increasing the theoretical and actual REDOX measurement values. The greater stability of glycolate relative to formate results in lower and more stable pH values. The lower and more stable pH increases pH-dependent properties such as metal solubility (and is also enhanced by coordination and complex formation with glycolate) and increases the degree of acid-dependent reduction reactions.

The factors mentioned above necessitated the development of glycolic flowsheet-specific correlations for the prediction of the product concentrations of glycolate, nitrate, oxalate, and formate. Two reports on modeling have been written about the development of such correlations, endeavoring to explain historical observations of anion conversions in terms of independent experimental parameters.^{19,20} These correlation equations are given in Appendix A. Glycolate destruction was reported to have a strong dependence on acid stoichiometry and lesser dependencies on mercury and nitrate concentrations. Conversion of glycolic acid to formate when noble metals and mercury are present was found to be dependent on acid stoichiometry, with greater generation of formate at lower acid stoichiometries. Experiments without noble metals and mercury have yielded significantly higher conversions to formate. Conversion of glycolic acid to oxalate was shown to have a dependence on acid stoichiometry, and either the initial concentration of nitrite or the type of ruthenium catalyst precursor used. Conversion of nitrite to nitrate depended on acid stoichiometry, percent reducing acid, and initial nitrite concentrations or initial mercury concentration. The glycolate to formate conversion with noble metals and mercury present was inversely dependent on the acid stoichiometry.

In parallel with the development of the correlations described above, SRNL was tasked with conducting a fundamental chemical study to better understand the basis and meaning of these apparent relationships. To categorize and prioritize interactions of interest, anticipated CPC reactions were divided into two classes: 1) acid-base reactions, and 2) REDOX reactions.

The major species involved in REDOX reactions in the CPC are the metals Mn, Fe, and Hg, and the anion nitrite. To lesser extents the metals Ni, Cu and Pd and the anion nitrate may participate in REDOX reactions. In this work, the REDOX reactions of Mn, Hg, and nitrite have been studied since these are three of the major species. Although REDOX reactions of Fe can possibly be significant at high acid stoichiometries, measurement of the distribution of Fe³⁺ and Fe²⁺ in solution would require development of a new analytical method, and was thus beyond the specified scope of this work. Also, glycolic acid is generally a two electron donor in REDOX reactions, so reduction of Fe³⁺ to Fe²⁺ by glycolic (or glyoxylic or formic) acid is less likely and Fe³⁺ dissolution by glycolic acid may be due to only complexation. Distinguishing between the oxidation states of Mn and Hg are possible visually since Mn⁴⁺ is insoluble as MnO₂ and Mn²⁺ is soluble, and Hg²⁺ is present either as orange HgO or soluble Hg²⁺ while elemental Hg⁰ mostly exists in a separate

liquid phase. The oxides of nitrogen can be measured as nitrite and nitrate in solution by Ion Chromatography (IC) and the gaseous oxides by gas analyzers.

Acid-base reactions (such as those shown in Reactions [2]–[5] for hydroxide, carbonates, alumina, and alkaline earth metal hydroxides) are relatively simple and are not expected to have any significant effect on anion conversions important to REDOX prediction.



An important exception to this assumption of insignificant impact on anion conversion is the proposed acid-enhanced disproportionation of nitrite shown in Reactions [6] and [7], where formation of HNO_2 from nitrite and acid has been assumed. These reactions are important for REDOX prediction, not because of any reduction or oxidation of another species taking place, but rather because of the variable amount of conversion to nitric acid (HNO_3). Note that these reactions are “internal” REDOX reactions because nitrogen is both reduced and oxidized. For Reaction [6], nitrous acid N(III) is converted to nitric acid N(V) and nitric oxide N(II), and for Reaction [7] it is converted to nitric oxide N(II) and nitrogen dioxide N(IV).



Reactions [6] and [7] are overall reactions that are actually comprised of several elementary reactions. The generally accepted mechanism for HNO_2 disproportionation is:²¹⁻²⁵



These elementary reactions can be shown to reduce to Reaction [6].

Five avenues of investigation were initially proposed to investigate the simple chemical interactions of the major actors in REDOX chemistry (manganese and mercury) and anion conversions (nitrite):

- The reactivity of nitrite with total acid
- The reactivity of nitrite with glycolic acid
- The reactivity of MnO_2 with glycolic acid
- The reactivity of HgO with glycolic acid
- The effects of noble metals in simple mixtures of nitrite, HgO , and MnO_2 with glycolic acid

2.1 Proposed Nitrite Chemistry

In the NF flowsheet, it has been previously reported that approximately 75% of nitrite destruction with formic acid was expected to proceed by nitrous acid disproportionation as shown in Reaction [6].¹¹ Given that this reaction is not dependent on the type of acid used to initiate the reaction but rather the availability of protonated nitrite (nitrous acid), it was not expected that this reaction should be greatly affected by the substitution of formic acid with glycolic acid (given the relatively similar pKa values for the acids, shown in Table 2-1).

Table 2-1. Dissociation Constants and Molecular Weights for Acids Anticipated in the CPC.

Acid	pKa	MW
Glycolic Acid (C ₂ H ₄ O ₂)	3.83	76.052
Oxalic Acid (COOH) ₂	1.25, 3.81	90.035
Formic Acid (HCO ₂ H)	3.75	46.026
Glyoxylic Acid (C ₂ H ₂ O ₃)	3.18	74.036
Nitric Acid (HNO ₃)	-1.3	63.013
Nitrous Acid (HNO ₂)	3.29	47.013

By Reaction [6], the only nitrogen oxide gas produced from reaction is nitric oxide, NO. If true, this implies that variations in nitrite-to-nitrate conversions could effectively be eliminated (fixing the value at 33%) by the removal of oxygen present in purge air; the role of oxygen is expected to be that of an oxidizer of NO, allowing for subsequent scrubbing of NO₂ and formation of additional nitrate, as shown in Reactions [12] through [14].



Analysis of condensate from previous CPC simulations has measured negligible amounts of nitrite, suggesting that Reaction [14] has negligible effect on nitrogen oxide behavior in the CPC offgas train (but not necessarily in the Sludge Receipt and Adjustment Tank (SRAT) vessel itself). However, results from this work indicate that Reaction [14] may actually predominate, while Reaction [13] is negligible. A condensate sample was inadvertently caustic quenched and analysis showed both nitrite and nitrate present. This result will be discussed further in Section 4.1.2.

In addition to the reactions above, it has also been proposed that nitrite destruction may occur by reductive mechanisms to form NO or N₂O while oxidizing the reducing acid. Such mechanisms for the NF flowsheet were proposed to account for a small portion of NO generation and all of the N₂O generation.¹¹ The presence of reductive routes for NO and N₂O formation would add considerable complexity to the understanding of the glycolic acid-nitrite interactions. During reduction of nitrite by formic acid, the only carbon-containing product is CO₂, whereas for these reactions either glycolic acid, formate and oxalate can also be produced by partial oxidation of the glycolic acid. These reactions are shown in Reactions [15]–[17] for producing NO and in Reactions [18]–[20] for producing N₂O.



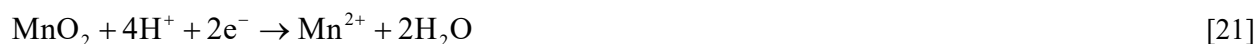


The following questions were studied in this work:

- How important is the re-formation of HNO_2 and HNO_3 by hydrolysis of NO_2 generated in the headspace or condenser?
- How does glycolic acid reduce nitrite to form N_2O ?
- How many moles of acid per mole of nitrite is required to destroy all nitrite?
 - Is the amount required different for glycolic and nitric acids?
- Is there a reductive (non-disproportionation) path to formation of NO ?

2.2 Proposed MnO_2 Chemistry

Unlike nitrite destruction, the dissolution of manganese in the CPC is expected to happen by reductive/oxidative mechanisms. REDOX mechanisms are expected because the oxidation state of manganese in the CPC is primarily Mn(IV) , which is believed to be insoluble in all forms. In preparation of MnO_2 by reaction of sodium permanganate with manganese (II) nitrate, some small portion of the final product can be Mn(III) oxide (Mn_2O_3). In this report, the oxides of Mn will generally be referred to as MnO_2 since it is the predominant species. To be dissolved, the Mn oxides must first be reduced to Mn(II) , which is known to be more soluble. The half-reaction for the reduction of MnO_2 is given in Reaction [21]:



Because two electrons are needed to convert Mn(IV) to Mn(II) , reagents that successfully reduce MnO_2 are expected to undergo two-electron transfer oxidation. Possible reactions of glycolic acid are shown in Figure 2-1. In this diagram, the electrons and hydrogen ions above or below the equilibrium lines indicate the number of electrons and hydrogen ions gained or lost in the reaction. These electrons would reduce the oxidant species in a reaction (such as MnO_2 to Mn^{2+}). Note that the reactions of glycolic acid (carbon oxidation states -1 and +3) to form glyoxylic acid or formaldehyde generate the same number of electrons (2) for reduction. (Because of the electron-withdrawing capability of the hydroxyl group, the hydroxyl carbon's oxidation state may be closer to zero and the carboxylate carbon may be closer to +2.) Glyoxylic acid carbons are in oxidation states +1 and +3 (maybe closer to +2 each), whereas formaldehyde and CO_2 are in oxidation states 0 and +4, respectively, so the net oxidation state of the products is the same (+4).

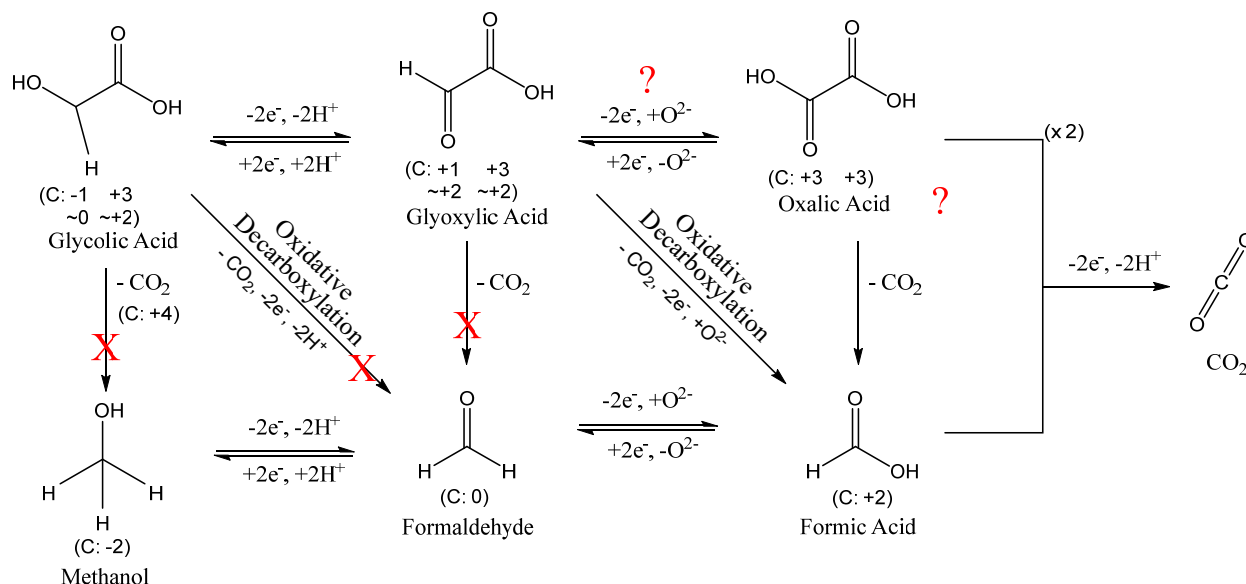


Figure 2-1. Possible Reaction Pathways of Glycolic Acid

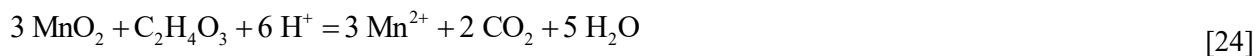
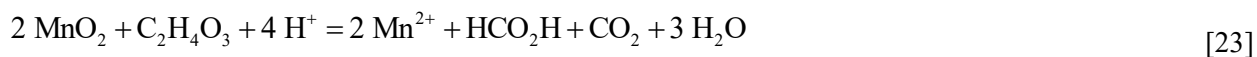
There is no experimental evidence for the formation of glyoxylic acid, methanol, or formaldehyde. Glyoxylic acid can be resolved by the PSAL IC technique but none has ever been found; it could exist as a short-lived intermediate with a concentration too low to detect. It could also be possible that the caustic quench method for preventing further reaction of samples and for IC preparation could cause the decomposition of glyoxylic acid to form CO₂, which would escape, and formic acid, or formaldehyde, which would not be measured.

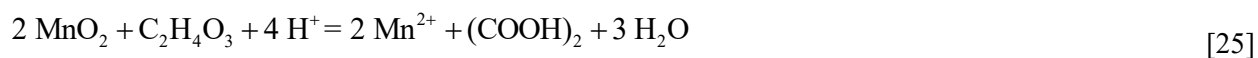
Recommendation: Samples for IC analysis should be taken without the Caustic Quench preparation and immediately be analyzed by IC to determine if glyoxylic acid is present.

Recommendation: If glyoxylic acid is found, its stability in caustic quenched samples should be investigated.

Neither methanol nor formaldehyde have been analyzed for in SRAT products or offgas condensates. Both methanol and formaldehyde could be detected by the FTIR if present in the offgas, but none has been found; however, both are soluble enough in water to be removed in the SRAT or FAVC condenser or the ammonia scrubber, such that no detectable amounts may have reached the FTIR in the gas phase. Note that although formaldehyde is an impurity in glycolic acid, it has not been detected in the offgas.²⁶ Therefore, this lack of evidence for generation of methanol or formaldehyde does not necessarily indicate they are not formed. Nonetheless, it appears that at most negligible amounts could be formed.

Excluding the formation of methanol and formaldehyde, the possible reactions of MnO₂ with glycolic acid and its decomposition products are shown below. Reactions [22]–[24] produce glyoxylic acid (C₂H₃O₃), formic acid and CO₂, and CO₂, respectively. Oxalic acid could also be produced as shown in Reaction [25]. It is known that formate and oxalate are also formed as end products during SRAT-cycle processing, indicating that complete oxidation of glycolic acid to CO₂ does not necessarily occur in CPC chemistry.^{19,20}





As noted in Figure 2-1, the direct oxidation of glycolic acid to oxalic acid is likely to proceed through glyoxylic acid as an intermediate via Reaction [26]:



For each of reactions [22]–[25], the first step is most likely the protonation of MnO_2 by hydrogen ions:



This step would then be followed by reduction by glycolic or other reducing acid.

Reactions [23] and [24] are most likely overall reactions because as written they require two and three moles, respectively, of MnO_2 to react with glycolic acid. The reaction of glycolic acid with MnO_2 is more likely a series of three steps where the oxidized organic product of one reaction becomes the reductant for a subsequent reaction. Reactions [22], [28], and [29] show the sequential reduction of three MnO_2 molecules.



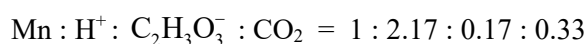
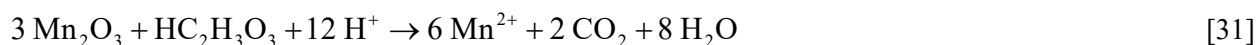
Adding Reactions [22] and [28] gives the overall Reaction [23], and adding [22], [28], and [29] gives Reaction [24]. Reaction [29] is the MnO_2 reduction reaction in the NF flowsheet.

Reaction [24] suggests a stoichiometric requirement of 1 equivalent of glycolate and 7 equivalents of acid are required per 3 equivalents of manganese in order to achieve complete reduction of three moles of MnO_2 :



with CO_2 as the oxidized carbon product. Glycolic acid is ~14% of the total acid required. It had previously been expected that the dissolution of MnO_2 would correlate with the percent reducing acid (PRA; percent of total acid that is glycolic) with higher PRA resulting in measurably more dissolution. However, the stoichiometry of Reaction [30] shows that ~86% of the acid requirement can be any acid, so unless the PRA values used in a sludge test were varied quite significantly, any difference in dissolution would be small and difficult to detect.

Note that for Mn_2O_3 , the any acid requirement is the same while the glycolic acid required is half, as shown in Reaction [31]. The amount of CO_2 produced per Mn is also half.



For Reaction [23] that generates formic acid and CO_2 as products, the stoichiometry is:



and glycolic acid is 20% of the total acid required.

Both formate and oxalate can also reduce MnO_2 , adding complexity to the kinetic profiles of dissolution and estimation of minimum theoretical stoichiometry. It becomes important, then, to better understand the effects of process parameters on the final product distribution of glycolate oxidation by MnO_2 .

2.2.1 Reactivity of Reducing Acids with MnO_2

Studies of the kinetics of MnO_2 dissolution with oxalic, glycolic, and glyoxylic acid have been reported by Wang and Stone.²⁷ The relative reaction rates reported for the reductive dissolution of Mn(III,IV) (hydr)oxides (a mixture of Mn(III) and Mn(IV) hydroxides and oxides) indicate a rate constant for reduction by glyoxylic acid that is an order of magnitude higher than the corresponding rate constant for reduction by oxalic acid. This rate constant is, in turn, an order of magnitude higher than the rate constant for manganese reduction by glycolic acid. Similarly, Furlani has reported the products of reductive acid leaching of manganese dioxide in the presence of glucose, noting the formation of a number of simple carbonaceous species (including glycolate and formate).²⁸ The relative abundance of formate over that of the other species (two orders of magnitude greater than measured glycolate concentration) in product solutions led Furlani to propose formate as a relatively stable end-product. These results suggest that formic acid is less reactive toward the reductive dissolution of manganese dioxide than glycolic acid.

Using this information, the reactivity of organic reductants towards MnO_2 is shown in Figure 2-2. Note that these results are for tests with only MnO_2 and related compounds and that the potential effects of noble metals, nitrite, and Hg were not addressed in these specific tests.

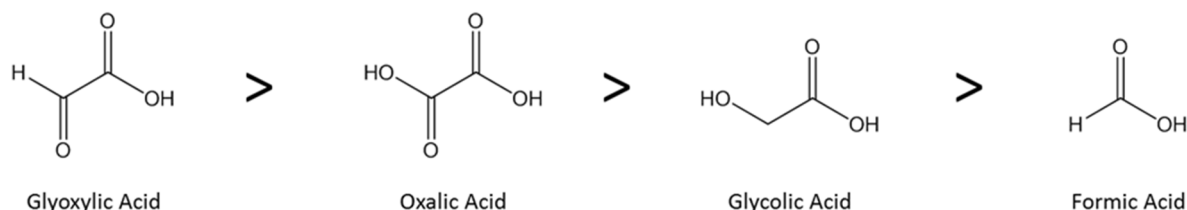


Figure 2-2. Order of Reactivity of Glycolic Acid and Products towards MnO_2 Reduction.

Because of their significantly higher reaction rates, intermediate glyoxylic and oxalic acids may not be detected in reaction mixtures because their concentrations would never be high enough to measure. This conclusion is consistent with the actual experimental results where neither was detected in the oxidation of MnO_2 .

2.3 Proposed HgO Chemistry

Like MnO_2 , HgO is theoretically capable of oxidizing glycolic acid to any of the intermediate oxidation states between glycolic acid and carbon dioxide (formate and oxalate) per these overall reactions:



In these reactions, 0.33 to 0.50 mole of glycolic acid are required to reduce one mole of HgO. However, it is likely that HgO must first be dissolved before it can be reduced.

In the NF flowsheet, the overall reduction of HgO by formic acid occurs by Reaction [35]:



Here two additional moles of any acid are required to first dissolve the HgO. The dissolution of HgO by glycolic (or any other) acid should proceed by Reaction [36]:



Reaction [35] written in terms of Hg^{2+} is:



Combination of Reactions [36] and [37] gives Reaction [35] and the hydrogen ions used in [36] are regenerated in [37] such there is no net additional hydrogen ion usage. Similar reactions can be written for glycolic or glyoxylic acid.

In addition to the complexity added by the possibility of multiple routes of reduction, the understanding of mercury chemistry is further confounded by conflicting reports about the capability of glycolic acid to reduce HgO.^{7,29}

Sequential reactions of single HgO molecules with glycolic, glyoxylic, and formic acids can be written similarly to those for MnO_2 . The possible reduction reactions of single HgO molecules are given by Reactions [35], [38] and [39]:



The reaction of HgO with glyoxylic acid to generate oxalic acid would be:



These reactions are consistent with the mechanism shown in Figure 2-1.

There is evidence showing that both Hg^{2+} and Hg_2^{2+} form complexes with glycolate.³⁰⁻³² For Hg^{2+} , the complexation can be described by Reaction [41]:



Here the value of n is 1 or 2; it may also be possible to form a negatively charged tri-glycolate complex.

2.4 Proposed Roles of Noble Metals

Noble metals (Ag, Pd, Rh, and Ru) appear to have distinguishable effects on both glycolate and formate CPC chemistry.^{11,19,20} As noted above, the presence and selection of noble metals (or precursors, in simulant testing) may have effects on the conversion of glycolate to formate and to oxalate. Additionally, an apparent effect of noble metals on NO and N_2O production has been previously suggested.¹¹ With these observations in mind, the following questions may be asked:

- 1) What effect do noble metals have (if any) on the conversion of glycolate to formate?
- 2) What effect do they have (if any) on the conversion of glycolate to oxalate?
- 3) How does the introduction of noble metals affect offgas production rates?

With these questions in mind, a series of experiments (nineteen in total) were designed to investigate the reactivity of nitrite-bearing solutions, MnO₂-bearing slurries, and HgO-bearing slurries with nitric acid and glycolic acid. Special attention was given to experimental planning in order to ensure strategic sampling for anion and soluble metal analysis. The purpose of this report is to highlight the findings from these experiments and discuss their implications for the glycolic flowsheet.

2.5 Acid Requirements and Minimum Acid Requirement Equations

The *minimum* acid requirement (A_{\min} , mol acid / L slurry) equations developed for the NF flowsheet were the aforementioned Hsu and KMA equations. The *minimum* acid requirement is an estimate of the smallest amount of any acid (nitric or formic) that is required for a set of reactions to occur to specific extents; this value does not specify how much of each acid is required. The REDOX of the melter feed is controlled by adjusting the ratio of nitric and formic acids used as specified by the REDOX Equation [1]. The *minimum* acid amount is based on experimental data and is less than the stoichiometric amount required for the proposed reactions. The reactions required to be performed are the criteria for the definition of *minimum* acid. Reactions [2]–[5] showed the acid-base reactions that are included in the Base Equivalents and Total Inorganic Carbon (TIC) terms in the acid equations. The criteria for *minimum* acid are shown in Table 2-2.

Table 2-2 Comparison of Minimum Acid Equation Terms and Coefficients

Requirement	Hsu Equation	KMA Equation	Glycolic Minimum Acid (GMA) Equation (Proposed)
Neutralize (acidify) sludge hydroxides and carbonates to modify rheology Base Equivalents TIC Insoluble Ca and Mg	Yes 1.0 Total: 2 NA	Yes 1.0 Soluble: 1.0 1.5	Yes 1.0 Either
Reduce nitrite concentration in SRAT product to < 1000 mg/L supernate	Yes 0.75	Yes 1.0	Needed?
Reduce a percentage of MnO ₂ to mitigate melter foaming	Yes, 40% 1.2	Yes, 50% 1.5	Yes (to be determined in this work)
Reduce HgO to Hg ⁰ for removal by steam stripping	Yes 1.0	Yes 1.0	Yes (to be determined in this work)
SRAT and SME H ₂ generation rates must not exceed limits	Yes	Yes	Not Applicable

The reduction of the nitrite concentration to less than 1000 mg/kg supernate in the SRAT assures that the maximum H₂ generation is seen in the SRAT where there is sufficient air purge rather than in the SME. In the Hsu and KMA equations for the NF flowsheet, the rheology requirements reduce the yield stress and consistency (viscosity) of the SME slurry sufficiently to meet DWPF pumping requirements. High acid additions much greater than the minimum requirements can result in slurries that are too ‘thin’ such that frit is not well suspended. This upper limit on acid is not set by the *minimum* acid equations. The SRAT and SME H₂ generation limits are never exceeded at the *minimum* acid; the H₂ generation rates from experimental testing determine the upper acid addition limit. The percentage of MnO₂ reduction in the equations was chosen somewhat arbitrarily and was based on the actual conversion attained in experimental studies. In actual DWPF operation, extended slurry boiling often results in catalytic destruction of formate and from reaction with nitrate to generate ammonium,^{33,34} which increase pH such that the Mn that had

been dissolved reprecipitates. It has not been determined if this reprecipitated Mn has actually been re-oxidized to MnO₂ or if it is different insoluble Mn species.

The Hsu equation was the first equation derived for the *minimum* acid requirement, and is currently used by DWPF.¹²

$$A_{\min} = [\text{Base Equivalents} + 2 \times \text{Total TIC} + 0.75 \times \text{Nitrite} + \text{Hg} + 1.2 \times \text{Mn}] \quad [42]$$

where A_{\min} is the minimum acid requirement in mol/L of sludge.

As previously described, the theoretical coefficient on nitrite would be 0.66 for disproportionation, so the assumed coefficient provides some excess acid. The coefficient of 1.2 on Mn was based on the assumption that 40% of the MnO₂ would need to be reduced (40% x 3.0 stoichiometric).

Koopman¹¹ proposed the revised KMA calculation given by Equation [43] based on analysis of significantly more data for the *minimum* acid requirement (KMA). One impetus for this revised equation, in addition to potentially being more chemically accurate, is that the Hsu equation sometimes underestimated the acid requirement such that nitrite was not sufficiently destroyed. The acid requirement from the KMA equation is almost always higher.

$$A_{\min} = [\text{Base Equivalents} + \text{Soluble TIC} + \text{Nitrite} + 1.5 \times (\text{Ca} + \text{Mg}) + \text{Hg} + 1.5 \times \text{Mn}] \quad [43]$$

Koopman showed that Base Equivalents and Total TIC double-counted some of the TIC during the Base Equivalents titration and proposed that use of the Soluble TIC would be more accurate. He also incorporated terms for Ca and Mg (mostly insoluble) to account for CaCO₃ (s) in Total TIC and also insoluble Mg(OH)₂. Koopman also increased the coefficient on Nitrite from 0.75 to 1.0 to account for the REDOX reaction of formic acid with nitrite to generate N₂O that uses more acid per nitrite than the disproportionation Reaction [6]. Koopman increased the acid requirement for Mn from 1.2 to 1.5 on the assumption of 50% reduction of MnO₂. The coefficients on Base Equivalents and Hg are the same as the Hsu equation.

Koopman also proposed a *nominal* or *stoichiometric* acid requirement in Equation [44] based on these additional data that might be a more accurate first principles calculation of the stoichiometric requirement. In this equation, additional acid is required for: 1) nitrite to account for higher catalytic destruction; 2) Ca and Mg for greater dissolution; and 3) Mn for 100% reduction.

$$A_{\min} = [\text{Base Equivalents} + \text{Hg} + \text{Soluble TIC} + 1.1 \times \text{Nitrite} + 1.8 \times (\text{Ca} + \text{Mg}) + 3 \times \text{Mn}] \quad [44]$$

This stoichiometric amount should always conservatively overestimate the acid requirement.

A revised *minimum* acid requirement (Glycolic Minimum Acid, or GMA) might be written for glycolic acid based on proposed glycolic acid reactions where the additional reducing power of glycolic acid, significantly less formation of N₂O, and generally greater reduction of Mn is accounted for in the coefficients on the species involved in REDOX reactions (nitrite, Hg, Mn):

$$A_{\min} = [\text{Base Equivalents} + \text{Soluble TIC} + \alpha \times \text{Hg} + \beta \times \text{Nitrite} + 1.5 \times (\text{Ca} + \text{Mg}) + \delta \times \text{Mn}] \quad [45]$$

where α , β , and δ are coefficients to be determined.

Equation [45] could also be written based on the Hsu equation:

$$A_{\min} = [\text{Base Equivalents} + 2 \times \text{Total TIC} + \alpha \times \text{Hg} + \beta \times \text{Nitrite} + \delta \times \text{Mn}] \quad [46]$$

These proposed equations for glycolic acid will be discussed further in Section 4.5 in light of the results of this current work. The results from the SB9-NG simulant testing will be used to compare the proposed equations.

3.0 Experimental Procedure

The experimental equipment used in this testing, the calculations of simulant compositions and acid requirements, the preparation of simulants, experimental run parameters, offgas sampling and analysis, and liquid sampling and analysis are described in this section. Research and Development (R&D) Directions, raw data, and data analysis spreadsheets are stored permanently in the ELN experiment T7909-00035-15.

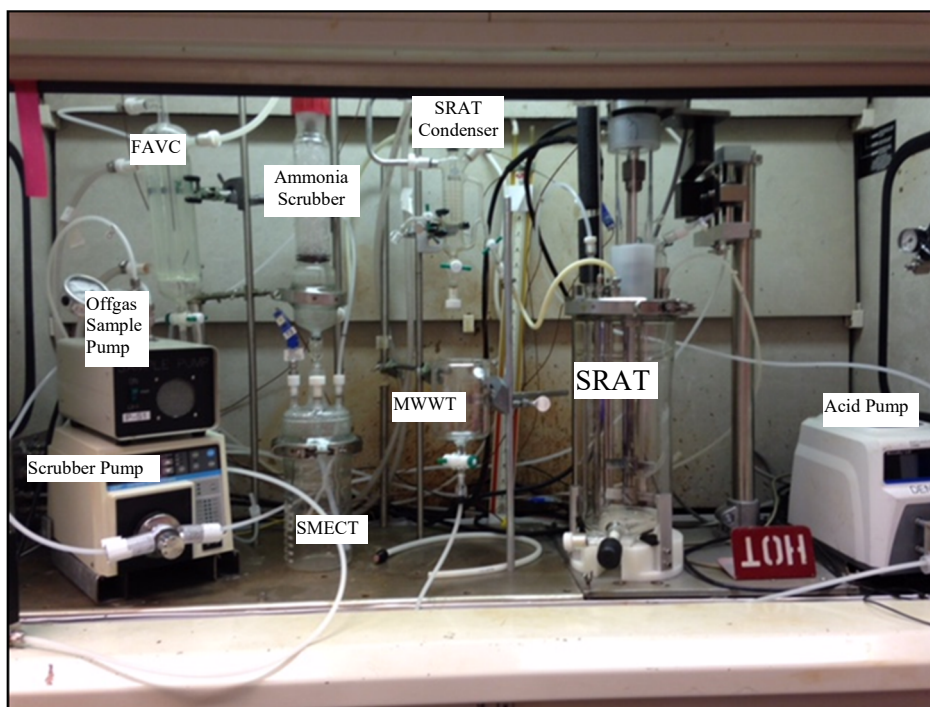
3.1 Experimental Set-up

Four series of tests were performed during this study and are described below. As shown, the series were identified as A through D. The scale of the tests is indicated by 4-L or J-Kem. “J-Kem” refers to runs that were performed using a J-Kem® reactor apparatus, which is described in more detail below.

1. Initial Nitrite Tests (A Series, 4-L)
2. Initial J-Kem Tests (B Series, J-Kem)
3. Final J-Kem Tests (C Series, J-Kem)
4. Combined Species Tests (D Series, 4-L)

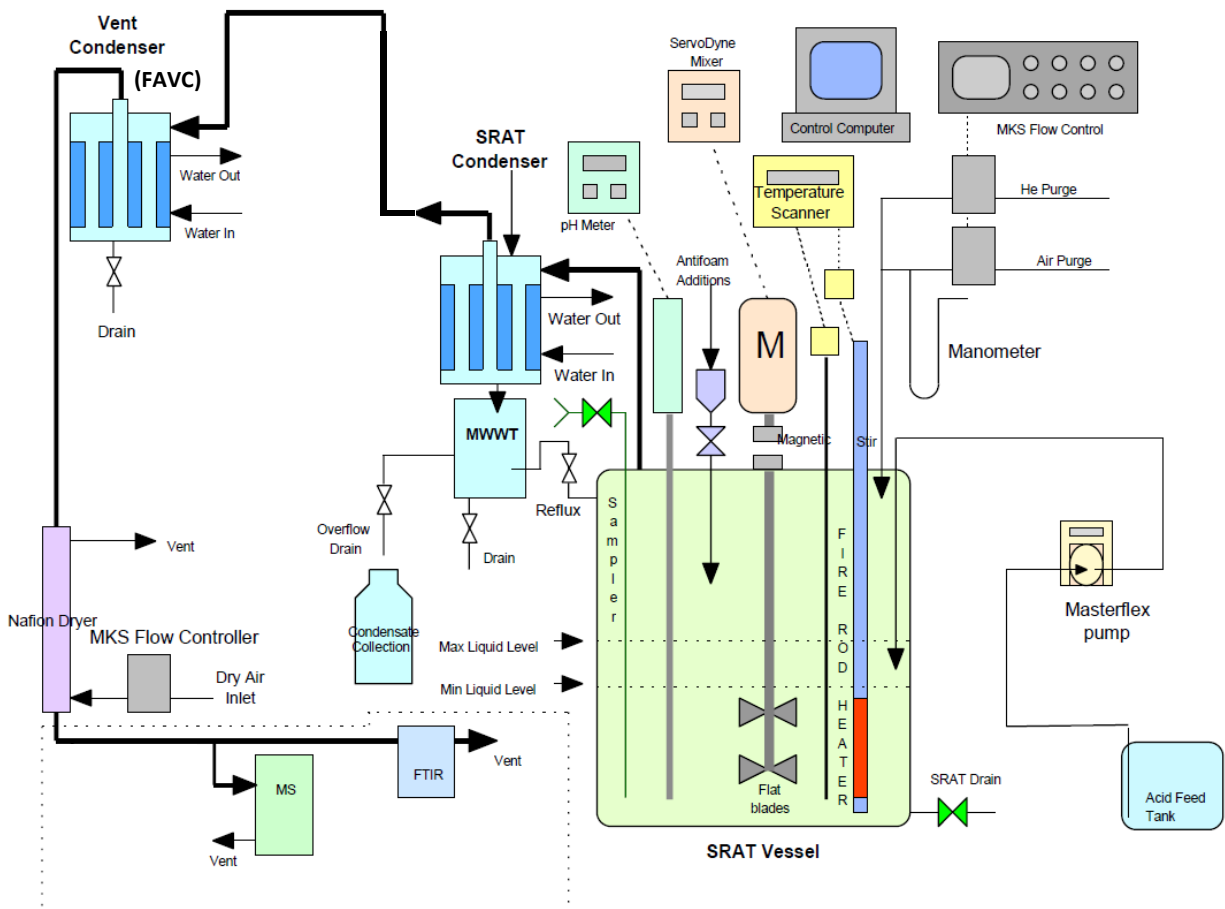
3.1.1 Initial Nitrite Tests

Initial nitrite tests were performed in the same 4-L equipment used for simulant flowsheet studies. Figure 3-1 shows a typical SRAT simulation setup. A process flow diagram is given below in Figure 3-2. Note that the Ammonia Scrubber was not used during these tests.



(Note: Formic Acid Vent Condenser (FAVC); Slurry Mix Evaporator Condensate Tank (SMECT))

Figure 3-1. Photograph of 4-L SRAT Apparatus Used for CPC Simulations.



(see text below for new acronyms)

Figure 3-2. Schematic of 4-L Apparatus Used for Initial Nitrite Testing.

In these tests, reagent solutions were added directly to the reaction vessel (SRAT), stirring was performed using a drive motor with a sealed magnetic drive assembly, and purge gas composed of air and He was added to simulate DWPF operation and to enable offgas analysis. Once the reaction mixture reached the desired temperature (93 °C), nitric (10.472 M) or glycolic (11.962 M) acid was added below the surface of the reaction mixture from the acid feed tank via the Masterflex® acid addition pump at a specified volumetric flow rate. Gases generated from the reactions were swept into the offgas system with the purge gas to the SRAT condenser, which was held at 25 °C. In the SRAT condenser, condensate is collected and drops into the Mercury Water Wash Tank (MWWT) where it then refluxes back into the SRAT vessel. In several tests, the MWWT was removed and the condensate from the SRAT condenser was drained directly to the SRAT vessel via a dip tube that prevented gas bypassing. This arrangement was used to eliminate the periodic emptying of the MWWT overflow that caused spikes in NO_x in the vapor phase. Vapors in the SRAT condenser proceed to the FAVC, which is held at 4 °C. Following the FAVC, gases are passed through a Nafion™ dryer to remove additional water before analysis by mass spectrometry (MS) and Fourier transform infrared spectroscopy (FTIR). Following acid addition, the reaction mixture was heated to boiling and allowed to reflux for the remainder of the experiment.

Two cylindrical stainless steel heating rods inserted through the stainless steel SRAT lid were used to heat the vessel to 93 °C and for subsequent boiling. Additionally, a glass dip tube was inserted via a port in the lid to facilitate liquid phase sampling. The liquid sampling process is described later. A pH probe was also installed to follow the solution pH during the course of the reactions.

The 4-L equipment was controlled by LabVIEW software installed on a Windows process control computer. The software controlled and recorded reaction temperature (for temperature setpoints), heat input (for heating rate setpoints), acid addition rate, SRAT impeller rate, and purge gas rates. The software monitored solution pH, temperature of the reaction solution, SRAT condenser temperature, FAVC temperature, impeller torque, heater power, and totalized acid addition volume.

3.1.2 J-Kem Tests

All J-Kem tests employed a 4-cell J-Kem[®] reactor equipped with four glass reaction vessels, a temperature-controlled heating block, and a cooling block serving as an overhead condenser that was supplied with cooling water (5 °C) from a recirculating water chiller. The apparatus is shown in Figure 3-3. It was initially intended that four reactions would be conducted simultaneously, but following more than one reaction at a time was found to not be feasible. All tests were performed at ~93 °C.



Figure 3-3. Photograph of J-Kem Vessel Used in Testing.

Each glass reaction vessel was equipped with a Teflon[™] cap machined to include six ports for processing and sampling. A photo of one of these caps is shown in Figure 3-4. The largest port (1) was designed to allow the installation of a small glass pH probe for real-time pH monitoring. The next largest port (2) allowed acid addition via micropipettes. An additional port was fitted with a stainless steel Swagelok fitting (3) to allow the addition of a purge gas. The final three ports served as access ports for a syringe for liquid sampling (4), a thermocouple for temperature monitoring (5), and a section of tubing used for offgas sampling (6).

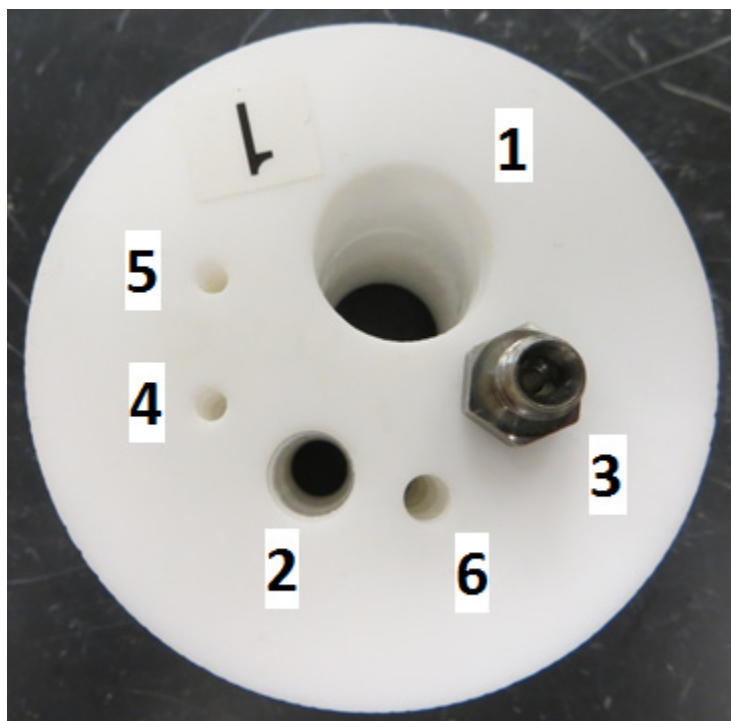


Figure 3-4. Photograph of Machined Teflon Cap for J-Kem Reactor Vessels.

During initial testing, it was proposed to incorporate purge gas and offgas sampling similar to the 4-L experiments as a source of additional data. The purges were achieved by feeding purge air (blended with 1 volume % He) at a controlled rate into four parallel rotameters and attempting to equalize the flow between the four vessels. The offgas sampling tube was moved from vessel to vessel to investigate each reaction, utilizing a gas sampling pump to draw vapors from the vessel headspace at a rate lower than the purge rate and route it to the MS and FTIR for analysis. As the J-Kem assembly had not been designed for this purpose, the development of offgas measuring capability was considered scoping work and not assumed to be quantitative in this first iteration. Unfortunately, a leak in the sample line after the sample pump resulted in the sample flow exceeding the purge flow such that significant inleakage into the vessel occurred, which more than doubled the effective purge rate. For this reason, offgas data were unable to be used in the final series of J-Kem tests.

Mixing in the vessels was provided by magnetic stir-bars in the liquids and the magnetic stirring mechanisms in the J-Kem heating block. The rate of stirring was qualitatively controlled by looking for indications of a fluid vortex in each vessel. Temperature and pH were continuously monitored using the same LabVIEW software described in the initial nitrite testing section. As mentioned above, final J-Kem testing employed the same equipment as initial J-Kem testing, with the exception that offgas analyses were not performed.

3.1.3 Combined Species Tests

The combined species testing equipment was almost identical to the equipment set-up used in the initial nitrite testing experiments, except that due to the observation of inconsistent refluxing from the MWWT in the nitrite tests, the MWWT was removed and direct reflux from the SRAT condenser to the SRAT vessel was done via a dip tube.

3.2 Solution/Slurry Preparation

For initial nitrite tests, initial J-Kem tests, and combined species tests, concentrations of reagents (nitrite, Hg, Mn, noble metals) were based on Sludge Batch (SB) 9 (SB9) flowsheet testing values. Table 3-1 gives each component used, a description of how reaction concentrations were determined, and an approximation of the final concentrations used in this testing.

Table 3-1. Derivation of Target Concentrations Used Throughout Testing

Compound	Description of Concentration Estimate ⁸	Final Concentration (mg/kg)
NO ₂ ⁻	Direct input from SB9 testing	10,200
Mn	Calculated from SB9 inputs for Mn loading (8.74% of calcined solids) and calcined solids loading (11.74% of total mass)	10,260
Hg	Calculated from SB9 simulant inputs (105% of value used in real-waste test) for Hg loading (2.48% of total solids) and total solids loading (15.25% of total mass)	3,780 or 10,000
Ag	Calculated from SB9 simulant inputs (125% of value used in real-waste test) for noble metal loadings (% of total solids): Ag = 0.0139, Pd = 0.0037, Rh = 0.0156, Ru = 0.0762 and total solids loading of 15.25% of total mass	21
Pd		5
Rh		24
Ru		116

Nitrite, Mn, and Hg were added (as applicable) to each run as pure solids (sodium nitrite, manganese dioxide, and mercuric oxide). The form of the noble metals used were added in the following fashion:

- Ag: added as silver nitrate solid
- Pd: added as a solution of palladium(II) nitrate (15.27 wt% Pd)
- Rh: added as a solution of rhodium(III) nitrate (4.93 wt% Rh)
- Ru: added as a solution of ruthenium(III) nitrosyl nitrate (1.5 wt% Ru with 1.6 wt% dissolved nitric acid)

It is important to note that in the case of J-Kem testing, the amounts of noble metals were too small to add as pure solids or solutions. In these cases, dilute solutions of noble metals were prepared from the stock reagents above and neutralized with dilute NaOH before being added to each reaction to prevent premature acidification. Neutralization was not expected to detrimentally alter the chemistry since these noble metal solutions are neutralized when added to caustic sludge simulant in CPC simulations.

Throughout final J-Kem testing, it was considered more important to generate solutions that would produce measurable concentrations of products than to be prototypic of actual waste. Therefore, the SB9 concentrations were changed in favor of higher concentrations. For example, Hg concentrations in initial J-Kem testing were targeted at 3,780 mg/kg, but were increased to over 10,000 mg/kg in final J-Kem testing.

3.3 Offgas Sampling and Analysis

All experiments were monitored using an Extrel Core MS Model MAX300LG and an MKS Model MG2030 FTIR. Some preliminary tests were also monitored by gas chromatograph (GC), but observed periods of offgas generation were so brief that the relatively long time between GC samples (~4 minutes) prevented sufficient resolution for reliable quantification. GC monitoring was therefore discontinued for the remainder of this testing. A helium tracer gas (added at 0.5% for testing in 4-L rigs and 1% in J-Kem tests, measured by MS) was used to calculate offgas generation rates by material balance. Table 3-2 gives the offgas species of interest in this testing and the measurement technique by which they were observed.

Table 3-2. Offgas Components by Analysis Technique

Offgas Component	MS	FTIR
Ar	X	
H ₂	X	
He	X	
CO ₂	X	X
N ₂	X	
NO	X	X
N ₂ O		X
NO ₂	X	X
O ₂	X	

3.4 Liquid Sampling and Analysis

For the 4-L scale runs, liquid sampling was performed by connecting a sample trap to a dip tube placed below the liquid level and pulling a slight vacuum with a syringe. This arrangement allowed the sample to be collected with minimum exposure to laboratory atmosphere and mitigated the likelihood of inleakage during sampling. Samples for anion analysis by IC were immediately quenched with caustic solution (typically 4 g of 50 wt% NaOH for every 20 g of solution sample) in order to stop or slow any reactions that were occurring in the acidic process.³⁵ These samples were generally ~20 mL. Samples for metals analysis by inductively-coupled plasma atomic emission spectroscopy (ICP-AES) were collected directly into 15 mL centrifuge tubes. These samples were then immediately centrifuged for ~7 minutes at 3500 rpm. Once centrifuged, the clear liquid supernate above the solid phase was transferred into a sample bottle via disposable pipette. These samples were typically ~5-8 mL. No further chemical reaction, such as precipitation of MnO₂ or HgO, of the supernate was assumed to occur in the samples.

During J-Kem testing, liquid samples were pulled from the reaction vessels directly into plastic syringes via 1/8" outside diameter (OD) metal syringe tips equipped with Leur lock heads. Once extracted, the sample was either added directly to a sample bottle with a pre-weighed amount of caustic solution for IC samples or transferred to a centrifuge tube, centrifuged, and decanted into sampling bottles for ICP-AES samples. The volumes of these samples were generally 5-8 mL.

Liquid samples were submitted to the SRNL Process Science Analytical Laboratory (PSAL) for IC and ICP-AES analysis. Samples were affixed with unique numbers for identification to mitigate the possibility of confusion. None of the samples analyzed for metal content by ICP-AES were additionally treated, such as to add nitric acid; these samples were diluted to appropriate concentrations and analyzed directly. This method is what has historically been used for supernate samples from CPC simulations. The soluble concentrations of Mn were found to be biased low for many samples that were clear solutions. The soluble concentrations should have equaled the calculated total concentrations, but were found to be lower. The Mn concentration was typically about 70% of the expected value. It appears that the excess of glycolate may be affecting these analyses in some way.

Recommendation: The cause of the low bias in soluble Mn concentration measurements in supernate samples containing glycolic acid should be determined, and a method developed to assure accurate measurements.

3.5 pH Measurement

Throughout testing, Thermo Scientific Orion pH meters were used to monitor the activity of hydronium ions (H₃O⁺) free protons in solution. These meters were used in tandem with glass pH probes rated for use up to 120 °C. Each pH probe/meter combination was calibrated using buffer solutions at pHs of 4, 7, and 10. The slope of this calibration response (mV/pH) was then automatically calculated in terms of the Nernst

slope (percent of -59.16) and used with process temperature data to calculate a temperature corrected pH, according to the equation below:

$$pH_{T\text{-corrected}} = 7 + \frac{mV}{\left(\frac{T_S + 273.15}{T_R + 273.15}\right)} \left(-59.16 \frac{mV}{pH} \frac{\% \text{ slope}}{100}\right) \quad [47]$$

where $pH_{T\text{-Corrected}}$ is the estimated pH of the solution at the process temperature, mV is the output of the pH meter (in mV), T_S is the process temperature (in °C), T_R is the reference temperature (25 °C), and % slope is the calibration slope of the pH meter/probe combination (% of Nernst slope, -59.16 mV/pH unit).

4.0 Results and Discussion

4.1 Destruction of Nitrite

Seven 4-L scale experiments were performed in order to gain an understanding of nitrite destruction chemistry in the CPC. Parameters varied were acid selection, acid loading relative to nitrite concentration (referred to as stoichiometry), acid addition rate, solution volume, and air purge rate. A summary of results from nitrite destruction testing is shown in Table 4-1 and Table 4-2. The acid stoichiometry was defined by the non-REDOX disproportionation Reaction [6] where 1 mole of any acid is required per mole of nitrite, but since 1/3 of nitric acid is generated, only 2/3 of a mole of acid is actually required. This amount is referred to as 66% acid stoichiometry, which is the minimum required. (SRNL did not redefine 2/3 of a mole of acid required to be “100%” to avoid confusion and because it was not known if this would actually be the true minimum acid).

Table 4-1 shows the experimental parameters and the final pH, molar rate of peak NO_x generation ranked in order of magnitude, and the acid addition duration. Both Table 4-1 and Table 4-2 have been organized by Run ID and also grouped to compare nitric and glycolic acid results and to compare the effects of feedrate and headspace volume (HSV). The column headings in Table 4-1 have been abbreviated in Table 4-2 to allow more columns of results to be displayed. Table 4-2 shows the nitrite destruction, nitrite to nitrate conversion, nitrite to nitrate conversions adjusted to the actual nitrite destruction, closure of the nitrogen balance, the overall NO/NO_x offgas ratio, and the ratio of NO_x generated to nitrite destroyed. Except for Run 3A, the closure of the nitrogen balances were less than 100%, indicating that the nitrite or nitrate concentration or the NO_x evolution values were lower than actual.

Table 4-1. Run Parameters and Results for Nitrite-Only Tests

Run ID	Acid	Stoichiometry (%)	Target Acid Addition Rate (mL/min)	Target Solution Volume (L)	Target Headspace Volume (L)	Air Purge Rate (sccm)†	Final pH	Peak NO _x Molar Rate Rank	Acid Addition Duration (min)
1A	Nitric	66	4.5	2.0	3.04	232	1.6	2	9
2A	Nitric	66	4.5	3.6	1.44	418	1.9	1	18
3A	Nitric	33	4.5	2.0	3.04	232	5.5	3	4.5
4A	Nitric	66	0.2	2.0	3.04	232	1.1	*	150
5A	Nitric	66	0.2	3.6	1.44	232	1.2	*	270
6A	Glycolic	66	4.5	2.0	3.04	232	4.1	4	7
7A	Glycolic	33	4.5	2.0	3.04	232	5.1	5	7
Compare Acids									
1A	Nitric	66	4.5	2.0	3.04	232	1.6	2	9
6A	Glycolic	66	4.5	2.0	3.04	232	4.1	4	7
3A	Nitric	33	4.5	2.0	3.04	232	5.5	3	4.5
7A	Glycolic	33	4.5	2.0	3.04	232	5.1	5	7
Compare Feedrate & Vessel Headspace									
1A	Nitric	66	4.5	2.0	3.04	232	1.6	2	9
2A	Nitric	66	4.5	3.6	1.44	418	1.9	1	18
4A	Nitric	66	0.2	2.0	3.04	232	1.1	*	150
5A	Nitric	66	0.2	3.6	1.44	232	1.2	*	270

† sccm = flow rate of gas in cubic centimeters per minutes at standard conditions of 1 atm and 21.11 °C (70 °F)

* no NO peak at low acid addition rate

Table 4-2. Run Parameters and Additional Results for Nitrite-Only Tests

Run ID	Acid	Stoich. (%)	Acid (mL/min)	Sol. Vol. (L)	HSV (L)	Air (sccm)	Nitrite Destruction (%)	Nitrite to Nitrate Conversion (%)	Corrected Nitrite to Nitrate Conversion (%)†	Nitrite/NO _x Balance Closure (%)*	NO/NO _x (%)	NO _x / (Nitrite Destroyed) (%)
1A	Nitric	66	4.5	2	3.04	232	100	43.1	43.1	90	96	47
2A	Nitric	66	4.5	3.6	1.44	418	100	38.6	38.6	83	93	45
3A	Nitric	33	4.5	2	3.04	232	70.5	43	61.0	102	87	42
4A	Nitric	66	0.2	2	3.04	232	100	76.4	76.4	91	78	15
5A	Nitric	66	0.2	3.6	1.44	232	100	62.9	62.9	95	62	32
6A	Glycolic	66	4.5	2	3.04	232	96.9	55.4	57.2	89	90	31
7A	Glycolic	33	4.5	2	3.04	232	76	40.5	53.3	87	65	29
Compare Acids												
1A	Nitric	66	4.5	2	3.04	232	100	43.1	43.1	90	96	47
6A	Glycolic	66	4.5	2	3.04	232	96.9	55.4	57.2	89	90	31
3A	Nitric	33	4.5	2	3.04	232	70.5	43	61.0	102	87	42
7A	Glycolic	33	4.5	2	3.04	232	76	40.5	53.3	87	65	29
Compare Feedrate & Vessel Headspace												
1A	Nitric	66	4.5	2	3.04	232	100	43.1	43.1	90	96	47
2A	Nitric	66	4.5	3.6	1.44	418	100	38.6	38.6	83	93	45
4A	Nitric	66	0.2	2	3.04	232	100	76.4	76.4	91	78	15
5A	Nitric	66	0.2	3.6	1.44	232	100	62.9	62.9	95	62	32

† Adjusted nitrite to nitrate conversion is the conversion to nitrate of the nitrite actually destroyed

* Closure based on nitrite, nitrate generated, and NO_x. Nitrate from nitric acid is excluded from the balance.

@ HSV: Headspace volume

4.1.1 Effect of Acid Selection

Results from Table 4-1 and Table 4-2 suggest that nitrite destruction is independent of the acid selected. Run 1A employed nitric acid at 66% stoichiometry and effectively destroyed 100% of the original nitrite, whereas Run 6A used the same loading of glycolic acid and achieved 97% destruction of the original nitrite. Likewise, Run 3A yielded 70.5% destruction of nitrite at 33% stoichiometry with nitric acid, while Run 7A exhibited destruction of 76% of nitrite at the same stoichiometry with glycolic acid. Assuming a linear response between nitrite destruction and stoichiometry, these data suggest that an acid stoichiometry of about 50% (relative to the nitrite loading) is sufficient to remove all nitrite. These results confirm the hypothesis represented by Reactions [12]–[14] that either or both internal recycle of HNO₃ in the headspace and external recycle of HNO₃ from the SRAT condenser contributes additional acid such that the actual acid requirement is lower than represented by Reaction [6]. By combining Reactions [6], [12], and [14] in varying proportions, the overall acid stoichiometry can be adjusted. To achieve an overall acid requirement of 50%, 1/3 times each of Reactions [12] and [14] can be added to Reaction [6] gives Reaction [48].



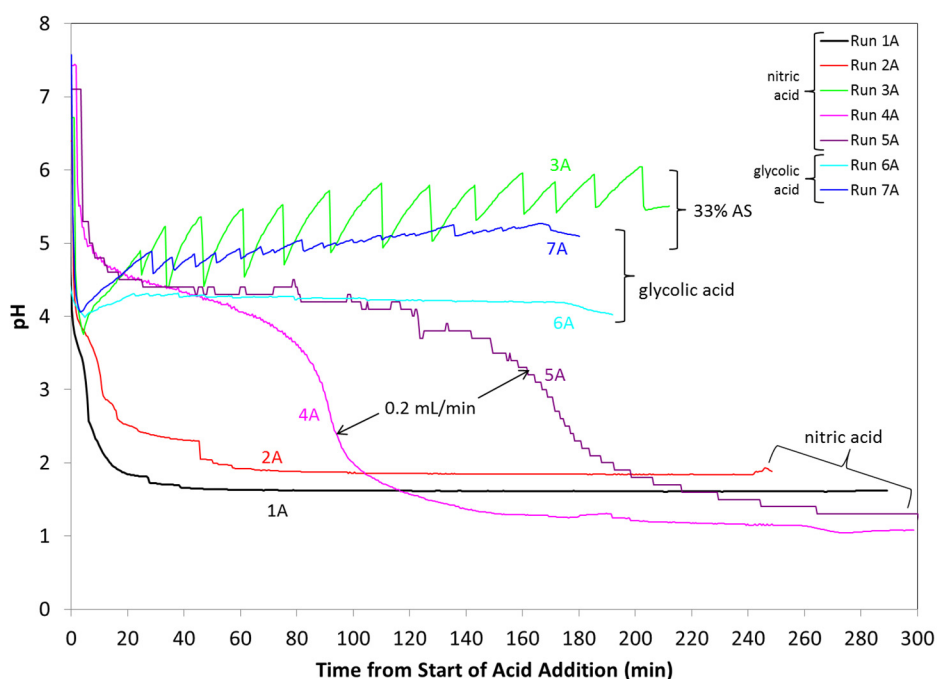
The acid stoichiometry of Reaction [48] is then the net acid consumed, or $(\text{HNO}_2 - \text{HNO}_3) / \text{HNO}_2 = (\frac{8}{3} - \frac{4}{3}) / \frac{8}{3} = 50\%$. The summation of these equations can be adjusted to achieve

any acid stoichiometry actually measured. Note that Reaction [12] actually may proceed to a greater extent than shown above to make NO_2 that remains in the vapor phase and is not scrubbed out in the SRAT headspace or condenser as HNO_2 and HNO_3 .

Comparing Run 1A to 6A and Run 3A to 7A, the nitrite to nitrate conversions did not show any correlation to the acid used. The data for nitric acid shown at the bottom of Table 4-2 comparing the results by acid feedrate and headspace volume show that larger headspace volume gives slightly higher nitrite-to-nitrate conversion for both 4.5 and 0.2 L/min acid feedrates. Relatively higher headspace volume has been hypothesized to result in more internal refluxing of nitric acid (Reactions [12]–[14]), and these results are consistent with this hypothesis, although not definitive.

The lower feedrate at both headspace volumes results in higher nitrite-to-nitrate conversion. This result can be explained by the rate at which NO gas is generated at the two feedrates. At the high feedrate, NO is generated at a rate high enough to completely consume all of the O_2 available so that relatively less is converted to NO_2 by Reaction [12] and thus not be scrubbed out as NO_2 . At the lower feedrate, there is more opportunity for NO to be oxidized to NO_2 because the NO generation rate is lower.

Figure 4-1 shows the pH profiles of Runs 1A–7A as a function of time (with $t = 0$ being defined as the start of acid addition). The jagged profiles exhibited by Runs 3A, 5A, and 7A are due to the periodic reflux of acidic condensate to the vessel from the MWWT. These results imply the periodic refluxing was of greater magnitude in these runs. It is not apparent why there would have been greater refluxing for these particular runs. The end of acid addition for Runs 1A, 3A, 6A and 7A was at less than 10 minutes and can be seen by inflection points or changes in slope of the pH curves. Run 2A acid addition ended at 17 min and the later inflection can be seen in Figure 4-1. The slow acid addition Runs 4A and 5A gave inflections that were much more gradual and have the appearance of titration curves.

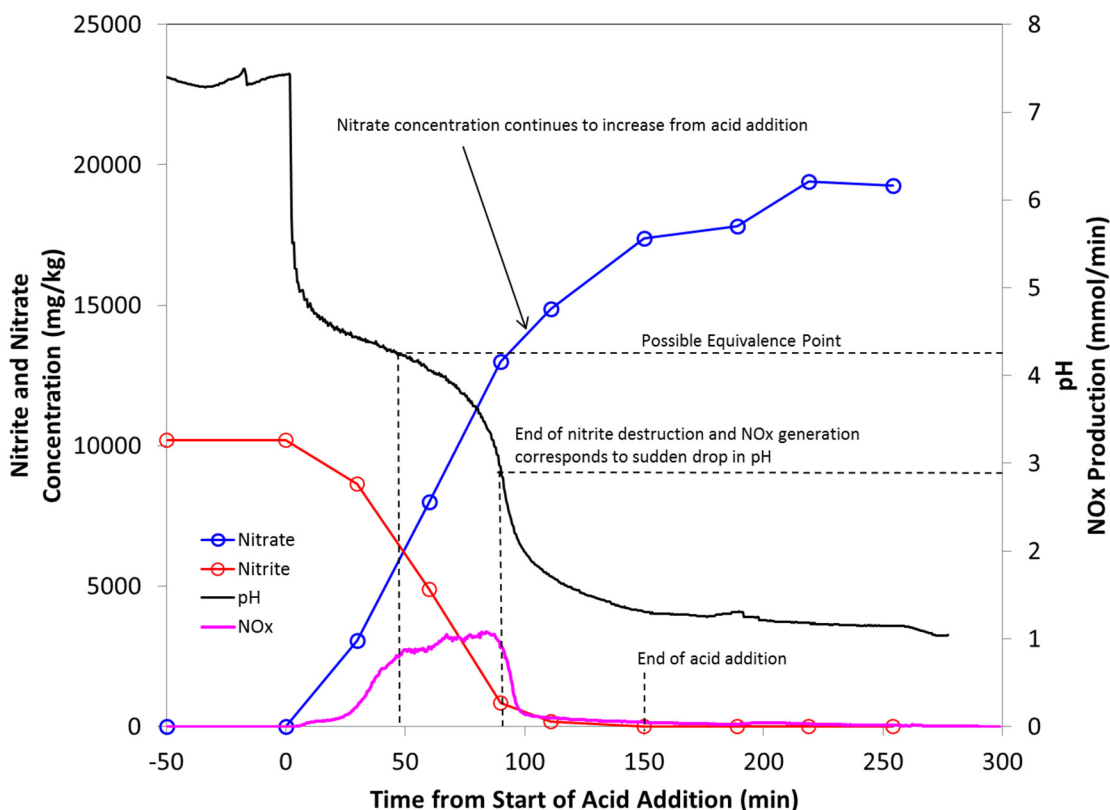


The “jagged” lines are due to the inconsistent return of condensate from the MWWT.

Figure 4-1. pH Profiles of Initial Nitrite Tests 1A-5A (Nitric Acid) & 6A-7A (Glycolic Acid).

Runs 3A and 7A at 33% acid stoichiometry and less than 90% nitrite destruction exhibit a continually increasing pH after completion of acid addition. The remainder of the runs equilibrate at a pH within one of two ranges (pH=1-2 for Runs 1A, 2A, 4A, and 5A with nitric acid; pH=4 for Run 6A with glycolic acid). These values correspond reasonably well to the pKa values of the acids employed. Because insufficient acid to total destroy nitrite in Runs 3A and 7A, the pH gradually increased indicating the consumption of hydronium ions as nitrite was destroyed. These results are consistent with the idea that the protonated nitrite (nitrous acid) is the active reagent in nitrite destruction.

Additionally, an inflection point can be seen in the pH profiles of Runs 4A and 5A. This point seems to correspond to a pH of approximately 4.2 for the slower acid addition rates, and is due to the buffering effect of nitrous acid/nitrite equilibrium in solution. Similar inflections in the pH data of Runs 1A and 2A are seen, but at pH ~3.7, and much earlier due to the high rate of acid addition (Figure 4-4). Comparison of the pH profile of Run 4A with measurement of nitrite concentration and NO_x offgas generation rates add further support for the apparent pH-dependent behavior of nitrite destruction. This comparison is shown in Figure 4-2. Note that the NO_x measured was about 80% NO and 20% NO₂, with negligible N₂O. The results for Run 5A are very similar. Runs 1A–3A had similar pH and nitrite profiles except that the drops are much quicker because of the much faster feedrate. The NO_x distributions for Runs 1A–3A are, however, significantly different. The NO constitutes about 95% of the total NO_x because it is evolved at such a high rate that depletion of O₂ occurs such that most of it cannot be oxidized to NO₂.



(66% Acid Stoichiometry, 2 L Reaction Volume, 4.5 mL/min HNO₃ Addition Rate)

Figure 4-2. Concentrations of Nitrite & Nitrate, NO_x Rate, and pH During Run 4A.

It is clear from Figure 4-2 that the beginning of offgas generation of nitrogen oxide species begins immediately upon acid addition when the pH drops to below 5. Generation of NO_x then slowly increases until it reaches a plateau at the apparent equivalence point where nitrite/nitrous acid buffers the pH. The

end of NO_x generation and the drop in pH indicating the destruction of the nitrous acid buffer correspond to the pH drop at about 90 minutes. Even though nitrite is destroyed by 110 minutes, the nitrate concentration continues to increase until about 250 minutes. The nitrate concentration continues to rise because nitric acid is added until 150 minutes; the increase in nitrate concentration after this time may be due to water loss during boiling from 150 to 250 minutes.

The reaction of nitrite with nitric acid in Run 4A was approximated using the electrolyte chemistry software OLI Studio.³⁶ The Mixed Solvent Electrolyte (MSE) thermodynamic framework was used. Two models were generated: 1) a simple acid-base model assuming no REDOX reactions occur; and 2) a model where nitrogen REDOX and gas phase products were allowed. For this second model, oxygen was excluded because its presence would oxidize all species in OLI. In the models, 1 L of 0.222 M nitrite (10,200 mg/kg) was reacted with 0.500 moles of nitric acid at 95 °C.

The results of the simple model and the REDOX model are shown in Figure 4-3 (a) and (b), respectively. In the acid-base model, nitrous acid is the product, whereas NO and nitrate are the products when REDOX is included. In Figure 4-3 (b) at about 0.15 moles HNO_3 added, there is a slight inflection in the moles of HNO_3 and the increase in the moles of NO generated ceases. At this point, 1/3 mole of nitrate and 2/3 mole of NO have been generated per mole of nitrite reacted, which is exactly the stoichiometry assumed (67%) and given by Reaction [6]. Further addition of nitric acid is predicted to result in reabsorption of some of the NO to form HNO_2 , which would not happen in the open experimental system.

The inflection point in the pH in Figure 4-3 (a) where the concentrations of nitrite and nitrous acids are equal is the equivalence point, or pK_a , of nitrous acid at 95 °C and has a value of about 2.7. The pK_a at 25 °C is about 3.2, and the OLI software accurately predicted this value. The model with REDOX in Figure 4-3 (b) has an equivalence point at about pH 5.6. The possible equivalence point in Run 4A was about 4.2, which is half way between the acid-base and REDOX models of the reactions. The modeling results suggest that the actual pH behavior is between the purely acid-base and REDOX behaviors. Ultimately, the product distribution matches the REDOX model. These results would indicate that the REDOX reactions are slower than the essentially instantaneous acid-base reactions, as expected.

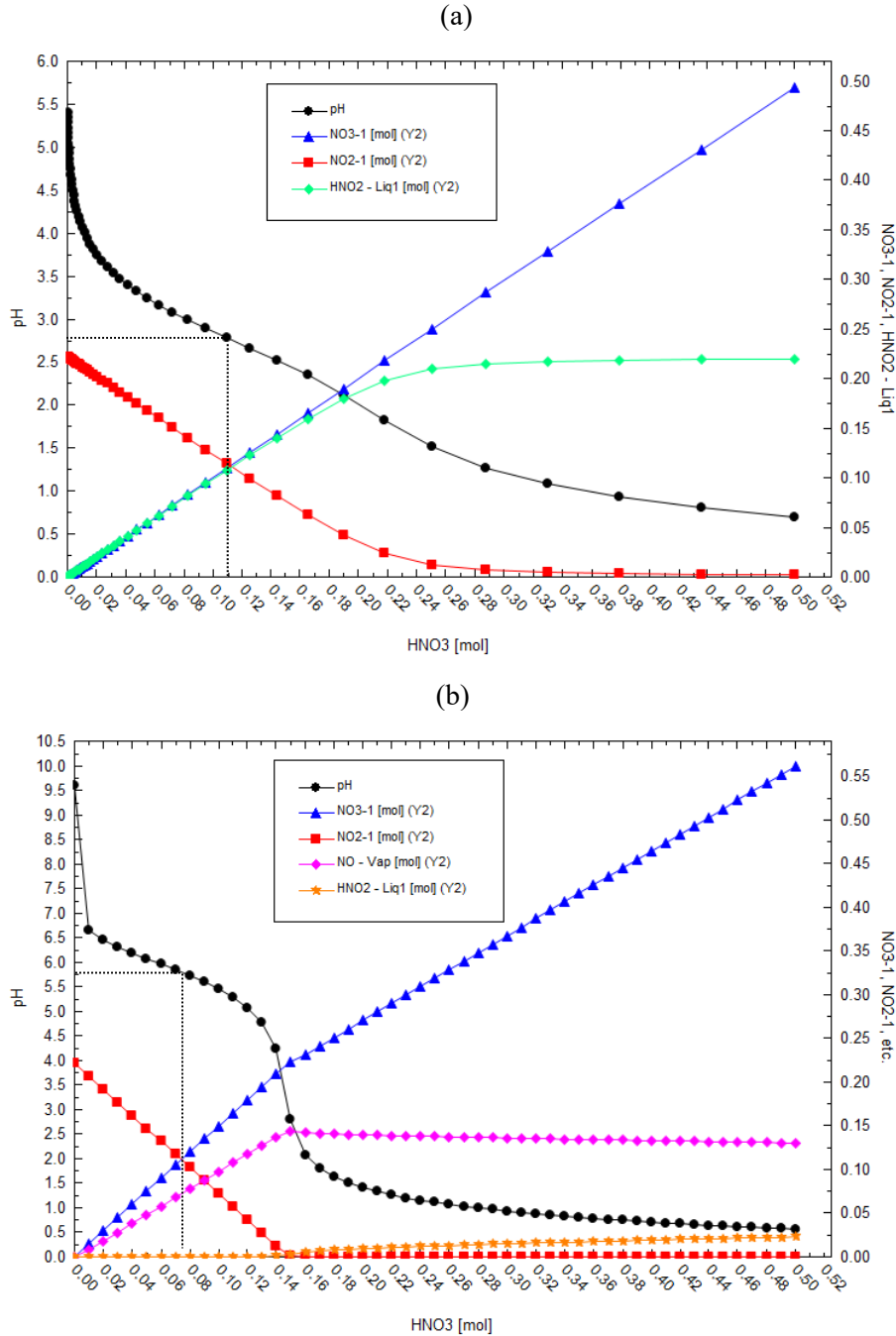
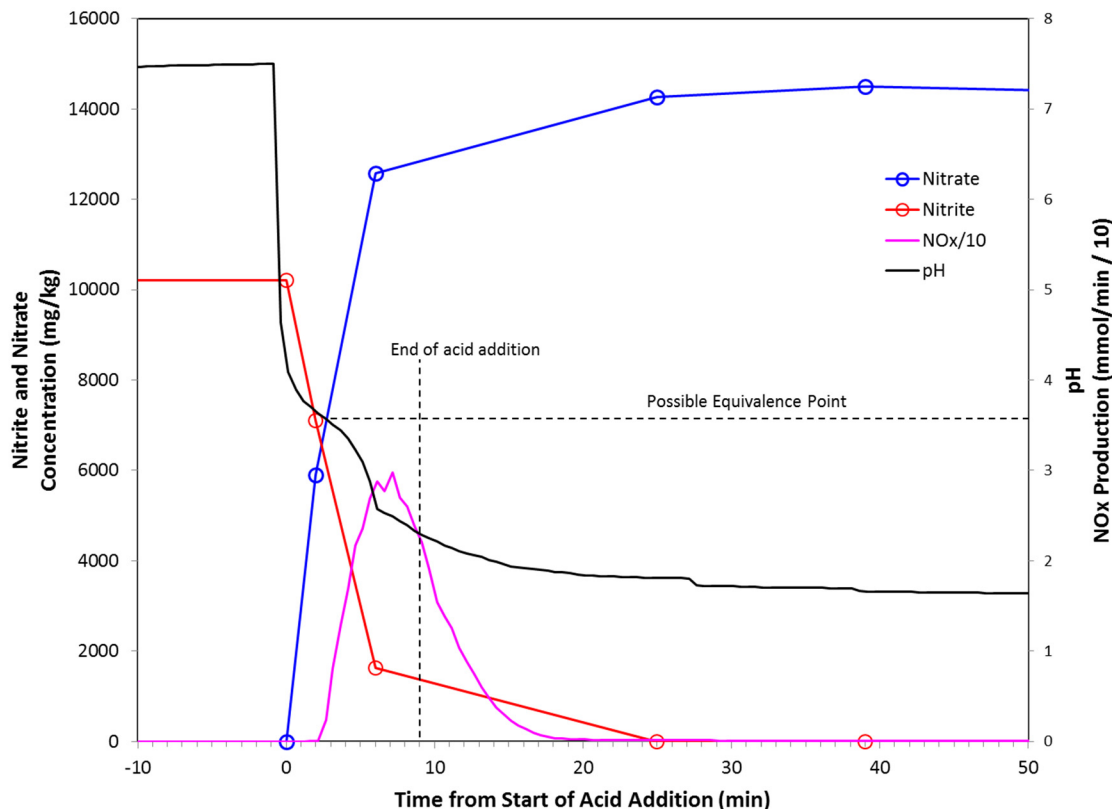


Figure 4-3. OLI Models of Reactions in Run 4A

Results for Run 1A, similar to Run 4A (Figure 4-2), at the much faster feedrate are shown in Figure 4-4. The NO_x emissions end before the end of acid addition indicating that excess acid was added. As previously mentioned, the nitrous acid equivalence point appears to be at about pH 3.7.



(66% Acid Stoichiometry, 2 L Reaction Volume, 0.2 mL/min HNO₃ Addition Rate)

Figure 4-4. Concentrations of Nitrite & Nitrate, NO_x Rate, and pH During Run 1A.

These results agree with the hypothesis that nitrite destruction is pH-dependent, supporting a nitrous-acid disproportionation mechanism that can use any acid. The disproportionation reactions proposed in Reactions [6] and [7] are shown again below:



The predominance of NO as the major NO_x species, especially at 95% at the high acid feedrate, suggests Reaction [6] occurs to a much greater extent than [7], and that the NO₂ measured is mostly due to the oxidation of NO by O₂.

In addition to the effect of pH, it is important to also consider the possibility of chemical reduction of nitrite by glycolic acid when glycolic acid is used. Table 4-3 gives the amount of glycolate destroyed (%), creation of formate (%), oxalate (%), and N₂O (mmol), and carbon and nitrogen mass balance closures (%), for both reported glycolic acid runs (Runs 6A and 7A) and corresponding nitric acid runs (Runs 1A and 3A) for comparison.

Table 4-3. Selected Results from Initial Nitrite Testing

	Run 1A	Run 3A	Run 6A	Run 7A
Acid Used	N	N	G	G
Acid Stoichiometry	66	33	66	33
Glycolate Destruction (%)	N/A	N/A	0	5.5
Conversion to Formate (%)	N/A	N/A	0	0
Conversion to Oxalate (%)	N/A	N/A	0	0
N ₂ O Produced (% of nitrite)	0.0	0.0	0.09	0.02
Carbon Mass Balance Closure (%)	N/A	N/A	105	94

It is clear from the data reported in Table 4-3 that the contribution of glycolate on the formation of nitrous oxide in these simple solutions is negligibly small. Some small increase (0.1-0.4 mmol) in N₂O production is seen when glycolic acid is used in place of nitric acid. However, these amounts of N₂O account for an insignificant percentage (0.2%) of the total nitrite added at the beginning of the reaction. Additionally, these small amounts of produced N₂O are appreciably smaller than the amounts of glycolic acid added to the reactions (0.1 and 0.4 mmol of N₂O vs 298 and 148 mmol of glycolic acid for Runs 6A and 7A, respectively), and could just as easily be a result of reduction by impurities in the glycolic acid such as formic acid. As a result, it can be concluded that reduction of nitrite by glycolic acid is not significant in the absence of catalysts such as noble metals or other reductants such as manganese.

4.1.2 Behavior of Nitrogen Oxide Gases in Offgas System

In addition to studying the liquid phase dynamics of nitrite destruction, experimental efforts were also designed to further the understanding of offgas NO_x behavior in the CPC. Figure 4-5 shows the offgas profiles for NO_x (NO+NO₂) for each run. Note that the NO_x production rate is the rate at the exit of the offgas train and not the rate exiting the reaction solution. The NO_x evolution from the reaction solution is expected to be predominantly NO, and the rate will be higher than at the offgas train exit due to scrubbing of the NO₂ formed in the headspace and condenser.

The net production rates and concentrations of NO_x at the high nitric acid feedrate were much higher than those typically seen in sludge batch simulant testing, with up to 80 vol% NO measured in the offgas. Much higher concentrations were seen because the acid addition rate was significantly higher than normally used.

As shown in Table 4-2, in the measured NO_x at the condenser exit, NO predominated (90-96% NO) at the higher acid feedrate with 66% acid stoichiometry for both acids. The lowest NO fractions were for nitric acid at the lower feedrate (62% NO) and glycolic acid at the lower acid stoichiometry (65% NO); these runs had lower total NO_x concentrations, so more NO was oxidized to NO₂. The NO_x/nitrite destroyed ratio data are consistent with the nitrite to nitrate conversions, with higher NO_x/nitrite destroyed corresponding to lower nitrite to nitrate conversion.

In Run 5A, the nitric acid feed was stopped temporarily at about 102 minutes due to a small leak. It was restarted several minutes later, and at about 123 minutes, the condensate built up in the MWWT was quickly drained back to the SRAT vessel. At this time there was a relatively large surge in the NO_x evolution caused by the recycled HNO₂ and HNO₃. The rate of acid addition from this recycle was significantly higher than the acid addition at 0.2 mL/min.

The NO generation shown in Figure 4-5 for each run is also ranked by magnitude in Table 4-1. More NO (larger area under the peak) was produced in Run 2A compared to 1A because the total acid added was greater by 80% and it was added over about twice the time.

Run 2A had higher peak NO than 1A because the higher air purge rate and lower headspace volume.

It was expected that the air purge rates and the vapor headspace volume to liquid volume ratio would be important experimental parameters for the measured rate of NO production. Higher air purge rate and lower

headspace volume create two effects: 1) a “peak-sharpening” effect due to the lowered residence time in the vapor headspace and 2) less time in the headspace for oxidation of NO by O₂ to form NO₂, which can be scrubbed out in the headspace and condenser.

Run 3A with half the nitric acid addition had the third largest NO peak. The glycolic acid Runs 6A and 7A both had lower peak NO rates and the NO generation was spread out over a longer time indicating that the rate of reaction of glycolic acid with nitrite is less than the rate with nitric acid. This result is expected since nitric is a much stronger acid.

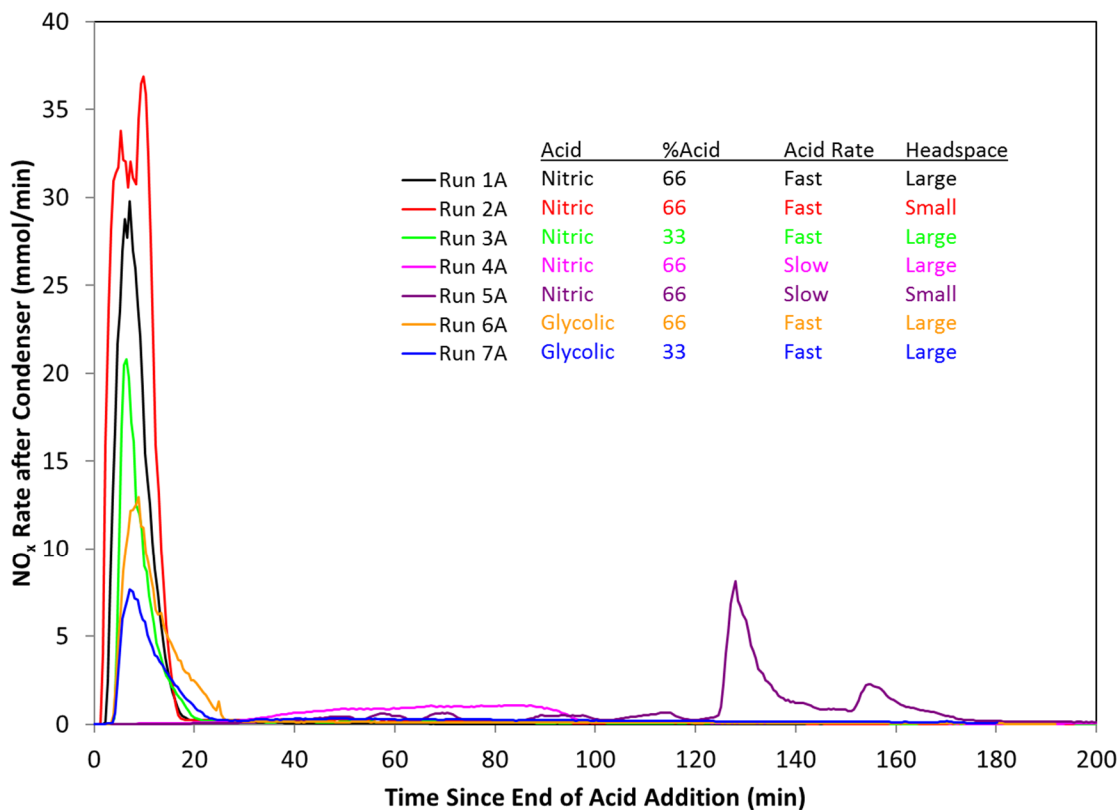


Figure 4-5. Production Rates of NO During Initial Nitrite Tests.

Further evidence for the presence of NO oxidation by O₂ is given by the O₂ rates and the depletion of O₂, both shown graphically for each run in Figure 4-6. Oxygen consumption was calculated by comparing the measured concentration of O₂ to the concentration expected based on the measured concentrations of N₂ and Ar.

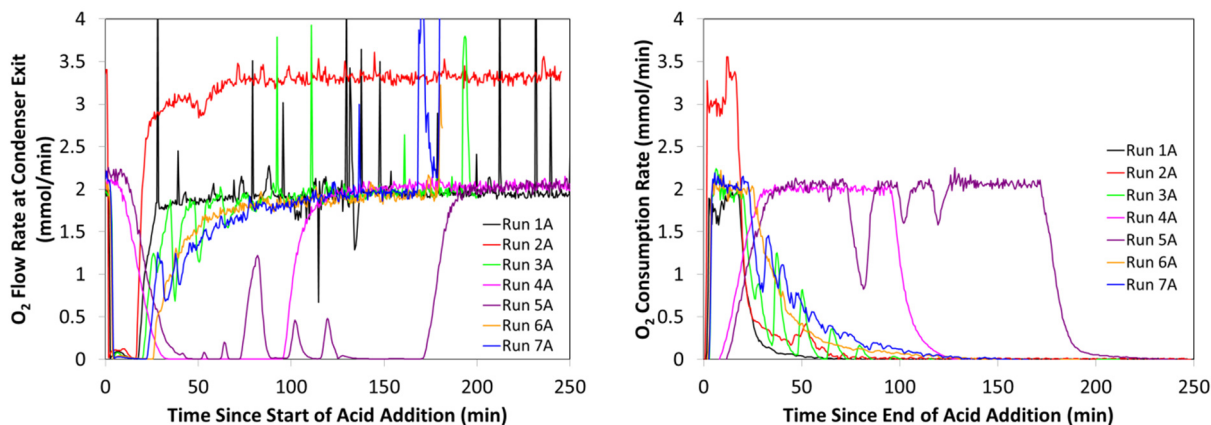


Figure 4-6. Consumption Rates of O₂ During Initial Nitrite Tests 1A-7A.

Each run experienced periods of depletion of O₂ due to the oxidation of NO. Runs 1A, 2A, 3A, 6A, and 7A experienced periods of about 50 minutes or less of O₂ depletion (indicated by a “plateau” in oxygen consumption) due to the rapid release of NO (shown in Figure 4-5) from the high rate of HNO₂ disproportionation (destruction). Note that the rates of O₂ addition in the air purge were only about 2 to 3.5 mmol/min compared to the NO generation rates of approximately 7 to 35 mmol/min, so O₂ was always the limiting reactant and as such its concentration went to zero.

Runs 4A and 5A, despite the decrease in HNO₂ disproportionation rates caused by slower acid addition, also experienced periods of complete O₂ consumption (anoxic). Even at the low acid addition rate, the molar rate of acid addition exceeded the rate of O₂ addition in the air purge. The anoxic periods in Runs 4A and 5A exhibited longer durations and delayed onsets due to the lower acid addition rate that limited the rate of NO production.

Once generated, a portion of the NO₂ is expected to be scrubbed out of the offgas stream (either in the offgas train or while still inside the vessel headspace) by some combination of the overall reactions proposed below:



Note that all of the proposed hydrolysis reactions have a direct impact on the nitrite-to-nitrate conversion. Reaction [49] generates 2 molecules of nitrate for every 3 molecules of nitrogen dioxide reacted, along with an additional molecule of nitric oxide (which can be released to the offgas stream or recycled back into the process by re-oxidation with O₂). Reaction [50] generates a molecule of nitrate and a molecule of nitrite for every two molecules of NO₂ reacted, recycling half of the scrubbed nitrogen back into the system as nitrous acid.

Of these proposed hydrolysis reactions, only one offers a hypothesis that can be tested easily. Reaction [50] proposes the simultaneous formation of nitrite and nitrate in condensate streams, whereas Reaction [49] proposes only nitrate as a condensate. The presence of this reaction was tested by taking the final MWWT sample from Run 6A and immediately quenching it with caustic solution (50 wt% NaOH), which prevented the HNO₂ from decomposing so that the sample could be analyzed for nitrite. This quench is similar to what has been done to SRAT slurry samples during acid addition to prevent the nitrite destruction reactions from further proceeding in the sample bottle. An assumption is made that all of the nitrous acid is converted to nitrite and that no other reactions occur that would bias the nitrite content.

Recommendation: When analyzing condensate samples for nitrite and nitrate, the samples should be caustic quenched to prevent decomposition of nitrous acid during storage. Comparison to unquenched samples should be performed. (Condensate samples should probably not be caustic quenched if the intended analysis is for species that are potentially volatile under caustic conditions (e.g., ammonia, formaldehyde).

This sample was found to contain about 63 mol% nitrate and 37 mol% nitrite (about 2:1 nitrate:nitrite), compared to samples that were not quenched that contained nitrate but no detectable nitrite. Note that this is the result for just one run and that the proportion may be variable depending on the run. These results indicate that a portion of NO₂ scrubbed from the offgas stream is absorbed as nitrous acid. This proportion is consistent with adding one-half of Reaction [49] with Reaction [50] so that the ratio of HNO₃ to HNO₂ is approximately 2. The distribution of nitrogen between nitrous and nitric acids probably depends on Reactions [49] and [50], and also the disproportionation Reaction [6].

These results have several important ramifications for DWPF operations or SRNL testing:

1. The formation of nitrite in the condensate from the nitrite destruction products NO and NO₂ confirms a recycle reaction pathway for both nitrite and nitrate that had been suspected. This recycle results in a minimum acid stoichiometry that is complicated by the variation in the amounts of nitrite and nitrate recycled.

This result affects both the minimum acid stoichiometry and REDOX prediction based on the equipment geometry, indicating that differing geometry between DWPF and small-scale testing can result in differences in the nitrite to nitrate conversion. This effect has been previously reported.^{19,20}

2. The concurrent formation of nitrous and nitric acids in the MWWT during NO₂ scrubbing will cause additional gas-generating chemistry to occur in the MWWT, primarily the disproportionation of nitrous acid. The potential for this chemistry highlights the need to quench condensate samples designated for ion chromatography with caustic solution so that further reaction does not occur before analysis. (Note that caustic quenching may not be desired for other analyses such as ammonia, volatile organics, etc.)

This result affects SRNL CPC simulations where condensate samples are taken to be analyzed.

3. This chemistry has the potential to re-oxidize any elemental mercury present in the MWWT, causing it to re-dissolve and be transferred back to the SRAT or to the SMECT rather than collect in the MWWT as desired. Such dissolutions have been described in the literature.³⁷

This result affects the collection of mercury in the MWWT in DWPF.

Evidence for gas-generating chemistry in the MWWT has been observed previously.¹⁴ Figure 4-7 shows a photograph of the MWWT during SRAT-cycle processing from SB9 glycolic flowsheet testing. Bubbles can clearly be seen evolving on the glass surface, indicating formation of gases in the solution.



Figure 4-7. Photograph of Bubbles Forming in MWWT Condensate During CPC Run SB9-NG57

4.1.3 Effect of MnO_2 on Nitrite

During the literature investigation, the previously unconsidered possibility of nitrite oxidation by manganese dioxide (reductive dissolution of manganese) was proposed, according to the mechanism below:^{38,39}



This reaction, if it occurs to a significant extent, could impact on the calculation of a minimum acid stoichiometry.

Run 1C in the J-Kem system (Table 4-4) was performed to isolate and identify this synergistic effect. The stoichiometry of Reaction [51] suggests that two equivalents of sodium nitrite and four equivalents of acid are required to completely react with one equivalent of manganese dioxide (Mn: NO_2^- : HNO_3 1:2:4). Run 1C employed 23 mmol MnO_2 , 69 mmol sodium nitrite, and 138 mmol nitric acid per mole of MnO_2 (Mn: NO_2^- : HNO_3 ~1:3:6), allowing a 50% excess of both acid and nitrate to compensate for the expected concurrent disproportionation destruction of nitrite by nitric acid. After addition of nitrite to the MnO_2 slurry, addition of nitric acid initiated the rapid evolution of orange gas (presumably NO_2) and vigorous bubbling. After addition of half of the specified acid amount, the solution was noticeably clearer and nearly free of solids. An image of this moment in processing is captured in Figure 4-8.

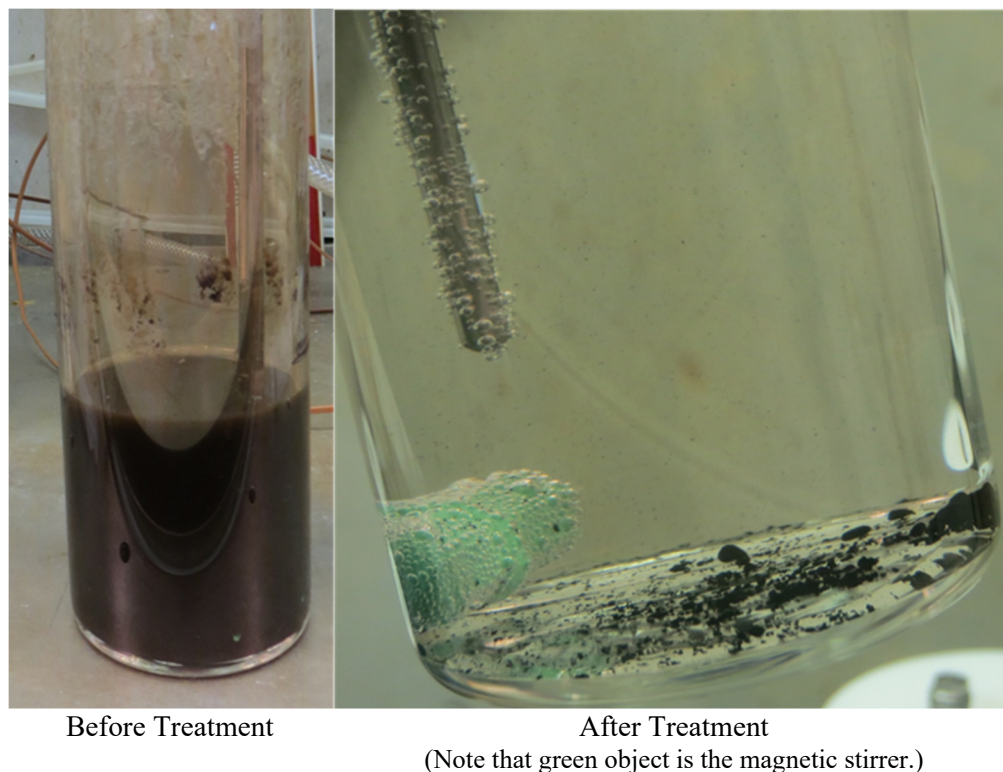


Figure 4-8. Photographs of MnO₂/Nitrite Slurry Before and After Treatment with Nitric Acid.

The observation that most of the Mn appears to have been dissolved after addition of half of the specified acid is not conclusive, but may suggest a lower stoichiometric requirement than given by Reaction [51]. A lower acid requirement could be the result of some of the NO₂ being converted to HNO₂ and HNO₃ by Reactions [49] and [50].

If NO₂ were completely converted to give only HNO₃ as the oxidized nitrogen product as shown in Reaction [52], the reaction stoichiometry would be Mn: NO₂⁻:HNO₃ = 1:1:2 rather than the value of 1:2:4 for Reaction [51].



The actual course of this reaction appears to be somewhere between Reaction [51] and Reaction [52].

The effects of pH on the oxidation of nitrite with MnO₂ in sludge simulant were not determined in this limited study. It is not known if this reaction is a major or minor contributor to the chemistry in the CPC, although the Combined Species tests described in Section 4.4 showed a significant amount of MnO₂ can be dissolved by addition of nitric acid.

Recommendation: Further testing targeting the role of direct oxidation of nitrite by manganese and other metal oxides in the CPC should be investigated.

4.1.4 Summary of Observed Nitrogen Chemistry

Through literature review²¹⁻²⁵ and simple chemical testing of sodium nitrite reactions, a mechanism for nitrite destruction in acid solution has been proposed, suggesting three process steps:

1. Disproportionation of nitrous acid (dependent on pH and nitrite concentration):



2. Oxidation of nitric oxide (dependent on the purge flow rate and available O₂):



3. Hydrolysis of nitrogen dioxide (dependent on the concentration of available NO₂ and water):



Reaction [49] can be shown to be a linear combination of the other equations, so only Reactions [6], [12], and [50] are required to describe the chemistry of nitrous acid. Reaction of nitrite with MnO₂ has not been explicitly considered in the current minimum acid equations, but the contribution of this reaction is likely dominated by the direct reactions of MnO₂ with formic and glycolic acids.

A visual representation of the model is given in Figure 4-9, and assumes the following steps:

1. Following protonation, nitrite (nitrous acid) decomposes in solution to form aqueous NO and NO₂.
2. NO is less reactive than NO₂ in aqueous solution (which forms HNO₃), so it is more likely to be evolved to the vapor space.
3. Once vaporized, NO is free to react with available O₂ to form gaseous NO₂.
4. Aqueous and gaseous NO₂ are released and absorbed, respectively, as a function of solution and vapor space composition.
5. Aqueous NO₂ undergoes hydrolysis to form nitric acid and reform nitrous acid (nitrite) ions.

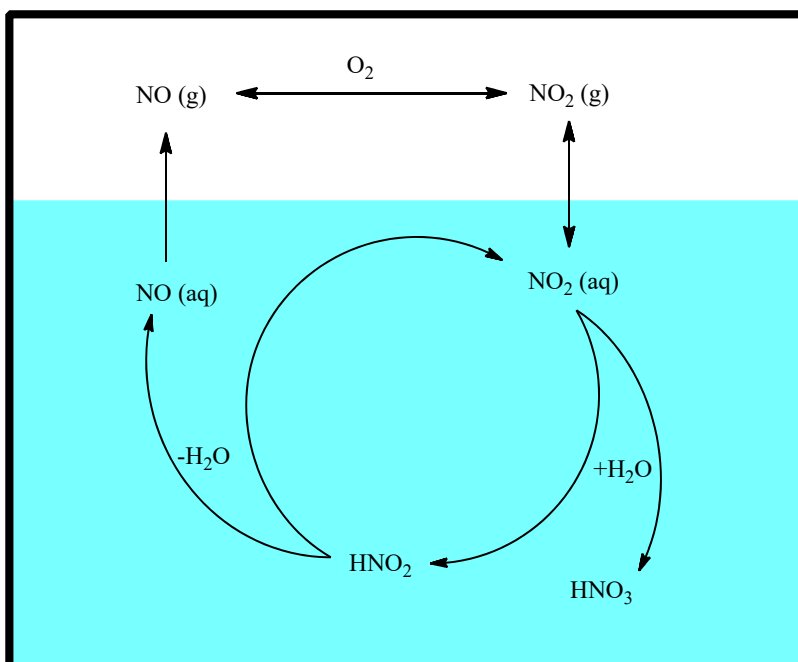


Figure 4-9. Proposed Model for Nitrite Destruction by Nitrous Acid Disproportionation in the Absence of Other Reactants.

It is important to note that these three reactions do not necessarily best describe the actual physical behavior of nitrite decomposition in terms of mechanistic reaction equations, accurate rate constants, and kinetics. They are simply a tool to describe physical phenomena in terms of process parameters (e.g., effect of purge flow rate on NO oxidation, effect of pH on nitrite-to-nitrate conversion, etc.). This model is proposed as a simple foundation for further development of computational models being developed by SRNL and DWPF personnel.

In addition to the nitrite destruction chemistry mentioned above, it is also possible to develop a model that incorporates the observed effects of manganese dioxide on nitrite oxidation. Since this reaction is proposed as strictly an oxidation of nitrite, it can be accounted for by adding an alternative pathway for the creation of NO₂ from nitrite. This alternative mechanism is shown in Figure 4-10. Note that MnO₂ and H⁺ are reactants and Mn²⁺ and H₂O are products.

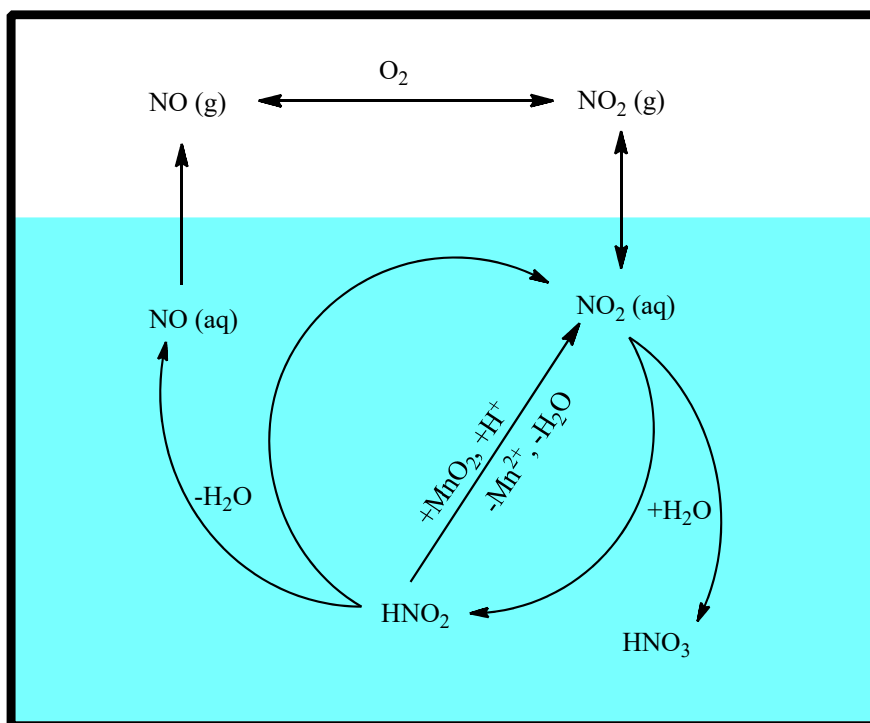


Figure 4-10. Proposed Model for Nitrite Destruction in the Presence of MnO₂ Particles.

It is important to note here that although the reaction arrow is drawn from nitrous acid, it is not known at this time if the reaction can occur with nitrite ion or if only the protonated form (nitrous acid) is reactive toward this path. This uncertainty has implications for behavior of sludge at neutral and basic pHs, and should be investigated before incorporation into chemistry modeling efforts.

In addition to the chemistry discussed above, this testing has also investigated the possibility of direct reduction of nitrite to N₂O by glycolic acid and concluded that any such direct reduction is negligible when accounting for destruction of nitrite. Note that evolution of N₂O from reduction of nitrite by other organics or metals could be possible.

4.2 Reduction of MnO₂

This work studied the distribution of reaction products from glycolic acid (CO₂, formic acid, oxalic acid) with MnO₂ as the only reactant and also with HgO and nitrite present. Tests to determine the minimum

amount of total acid (nitric + glycolic) and of only glycolic acid required were performed. Reduction of MnO₂ by nitrite in acidic solution was also tested.

Six 120 mL scale experiments using slurries of MnO₂ were performed to gain an understanding of manganese reduction/dissolution chemistry in the CPC. The parameters acid stoichiometry, pH, nitrite concentration, and noble metals concentrations were varied during this testing. Experiments were carried out until visual confirmation of manganese dissolution was achieved. Runs 1B, 2B, and 3B were performed by instantaneously adding a predetermined amount of glycolic acid to the reaction mixture; Run 3B included nitrite. Run 1C was performed similarly but with nitric acid and included nitrite (Section 4.1.3). Run 3C was performed by adding dilute glycolic acid dropwise until all of the MnO₂ dissolved. Run 4C was performed by instantaneously adding nitric acid at about the same number of moles of glycolic acid that had been used in Run 3C, followed by dropwise addition of a solution of dilute sodium glycolate; nitrite was not used. A summary of results from manganese reduction/dissolution testing is shown in Table 4-4. The amounts of acid and nitrite added are expressed as the molar ratio to manganese added. Note that the destruction and conversion percentages are given as inequalities because of uncertainty in measured values due to water loss during the experiments.

Table 4-4. Run Parameters and Results for J-Kem MnO₂ Testing.

Run ID	Acid	Acid Addition Rate	Nitrite to Mn Molar Ratio	Acid to Mn Molar Ratio	Glycolate to Mn Molar Ratio	Glycolate Destruction (%)†	Conversion to Formate (%)†	Conversion to Oxalate (%)	Noble Metals? (Y/N)
1B	Glycolic	Instantaneous	0	2.3	2.3	≥19	≤15	0	N
2B	Glycolic	Instantaneous	0	2.3	2.3	≥8	≤13	0	Y
3B	Glycolic	Instantaneous	1.2	3.1	3.1	≥-4	0	0	N
1C	Nitric	Instantaneous	3.0	6.0	0	N/A	N/A	N/A	N
3C	Glycolic	Dropwise	0	2.3	2.3	≥6	≤13	0	N
4C	Nitric & Glycolate	Nitric Inst.*, Glycolate Dropwise	0	2.2 (N)@	0.9	≥42	≤16	0	N

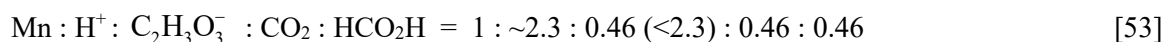
† Partial inequalities (“≤” and “≥”) are used to indicate bounding values calculated with uncertainty from water loss due to poor condenser efficiency.

* Instantaneous. @ N: nitric acid; G: glycolic acid.

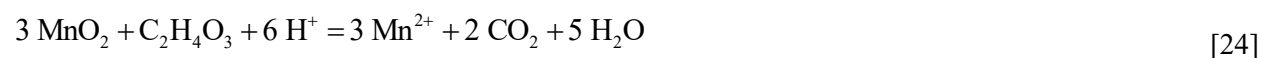
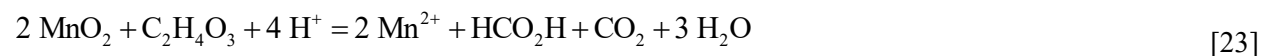
4.2.1 Reduction by Glycolic Acid

In every case tested, glycolic acid successfully reduced and dissolved MnO₂. The results from Runs 1B, 2B, and 3C show that at least 2.3 moles of any acid per mole of MnO₂ are required. The actual glycolate destruction of about 20% indicates that 0.46 moles of glycolate were destroyed per mole of MnO₂, so the actual glycolate requirement is greater than 0.46 and less than 2.3 moles. The lower value only indicates how much glycolate was consumed and not whether an excess would be required.

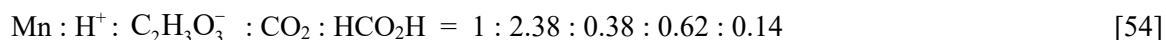
These results suggest an acid stoichiometry of about:



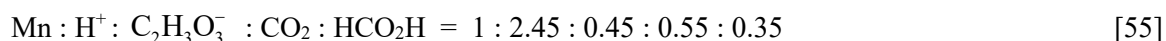
This stoichiometry is close to the stoichiometry of Reaction [23]. In these runs, the fraction of formate generated to glycolate destroyed was ranged from <80% to <217%, so it is reasonable to choose 100% as the conversion within the large error. This value is also consistent with Reaction [23].



In Run 4C where nitric acid supplied the acid requirement and glycolate was then added, about 0.9 moles of glycolate were required to reduce 1 mole of MnO₂. This value is about twice the value given by Equation [53], showing that at least a 100% excess of glycolate was required for reduction. For this run, there was less conversion of glycolate to formate, so Reaction [23] does not account for all of the reactions; Reaction [24] must be included. About 0.45 moles of glycolate were destroyed per mole of MnO₂, but only 0.14 moles of formate were produced, so Reaction [23] would comprise about 31% of the overall reaction. The stoichiometry for this run, based on the formate generated is:



Based on the glycolate destroyed, the stoichiometry is:



The glycolate requirements in these equations is the amount consumed. These equations are bounded by Reactions [24] and [23], but the actual excess glycolate requirement is about 140% for Equation [54] and 100% for Equation [55].

4.2.2 Generation of Oxalate and Formate

When no nitrite was present during the reaction, formate was observed in the final product, yielding conversions calculated between 13 and 16 percent, which is consistent with Reaction [23] to form equimolar amounts of formic acid and CO₂. However, when nitrite was added to the reaction mixture, no formate was observed in the final product, suggesting that formate was either never produced during the reaction or that it was destroyed upon formation. The former scenario is possibly explained by the earlier observation that nitrite can play an active role in manganese reductive dissolution (Table 4-4 Run 1C). If the available nitrite participated in the reduction of MnO₂, it would be expected that less glycolate would be needed to reduce the remainder of the MnO₂. This possibility would lead to lower glycolate destruction and formate conversion values (possibly indicated in the results from Run 3B). Alternatively, it is possible that the presence of the nitrite in solution added a barrier to the reaction pathway involving the generation of formate from Mn reduction.

These results are consistent with the results of full sludge simulant testing in CPC demonstrations GN51-56 and GN58-59.²⁰ In these GN runs, no noble metals or Hg were used. The conversion of glycolate to formate was up to 100% for KMA acid stoichiometry of 100%; these results are consistent with Reaction [23] where one mole of both formate and CO₂ are formed per mole of glycolate. The GN runs done at 125% KMA acid stoichiometry had only about 17% conversion to formate, indicating that with excess acid, Reaction [24] that forms two moles of CO₂ per mole of glycolate predominated.

It is known that oxalate is formed during CPC simulations performed with sludge simulant and glycolic acid (presumably as an oxidation product of glycolic acid). Since no oxalate was formed with MnO₂ and nitrite, it appears that the presence of other species such as noble metals, mercury, or other metals, which were not tested in the aforementioned results, may be required to produce oxalate.

4.3 Reduction of HgO

In this work, the ability of glycolic acid to reduce HgO to Hg⁰ metal was studied with and without MnO₂ and nitrite present to determine if glycolic acid alone can reduce HgO or if additional species are necessary. Three 120 mL experiments were conducted in the J-Kem equipment to better understand this chemistry. Runs 4B and 5B were performed by adding glycolic acid directly to slurries of HgO in water. The initial pH of the HgO in water was 7.7. The molar ratios of glycolic acid to HgO used were 2.3, as described above, and 5.6.

Run 2C was performed at a higher slurry concentration (to maximize the probability of observing small changes in chemical composition) by adding glycolic acid to a slurry of HgO in water (2C-a) followed by an addition of formic acid (2C-b). The same ratio of glycolic acid to HgO from run 5B was used, and approximately the same molar ratio of formic acid was used in run 2C-b. Results from these runs are given in Table 4-5.

Table 4-5. Run Parameters and Results for J-Kem HgO Testing.

Run ID	Hg (mmol)	Glycolic Acid (mmol)	Acid to HgO Molar Ratio	Glycolic Acid Destruction (%)	Formic Acid (mmol)*	Formic Acid Destruction (mmol / %)	Conversion to Oxalate (%)	Conversion to Formate (%)
4B	2.3	5.3	2.3	0	NA	NA	0	0
5B	2.3	10.6	4.6	0	NA	NA	0	0
2C-a	9.3	42.6	4.6 (glycolic)	0	NA	NA	0	0
2C-b	9.3	NA	5.1 (formic)	0	47.5	9.7 / 20.4%	0	NA

* Basis adjusted for samples taken prior to formic acid addition

It should be noted that in every case, HgO was rapidly dissolved by addition of glycolic acid, changing the physical appearance of the reaction mixture from that of an orange slurry to a clear, colorless solution.

4.3.1 Reaction of HgO with Glycolic Acid

In Runs 4B, 5B, and 2C-a, HgO was rapidly dissolved upon the addition of glycolic acid, changing the physical appearance of the reaction mixture from that of an orange slurry to a clear, colorless solution. It was also observed that no vapors (as bubbles) were generated as a result of this addition, suggesting that production of CO₂ was zero or small. This observation, combined with the fact that none of the three runs generated formate or oxalate, suggests that the reduction of HgO by glycolic acid is slow or negligible without the presence of other species. This hypothesis is further validated by the fact that none of the three glycolic acid runs demonstrated any appreciable destruction of glycolate. The only reaction that appears to occur to any significant extent is the dissolution of HgO to form Hg²⁺, which may be present as glycolate complexes.

In run 4B with 2.3 mole glycolic acid to HgO, the solution initially and quickly became clear, but after about an hour, an orange precipitate was seen suspended in the liquid that looked similar to the initial HgO. It seems unlikely that HgO could have re-precipitated at the low pH with the slight excess of glycolic acid. The orange precipitate could have been some other undetermined Hg compound; anecdotal evidence from cleaning offgas system glassware has shown that mercury deposits can turn orange during cleaning in 8M nitric acid where no HgO could exist. After several months of standing, the orange precipitate had turned black, which could possibly indicate the formation of miniscule droplets of Hg⁰ metal, which looks black at small particle sizes; however, this precipitate could also be some other Hg species. Run 5B with 4.6 moles of glycolic acid per mole of HgO remained clear after several months.

The conclusion to be drawn from this testing is that glycolic acid by itself is probably incapable of directly reducing HgO.

4.3.2 Reaction of HgO with Formic Acid

It had previously been proposed that some other species created from glycolic acid is responsible for the reduction of HgO.²⁹ A hypothesis was proposed that formic acid produced from the reaction of MnO₂ with glycolic acid was responsible for the reduction of HgO to elemental mercury. To test this hypothesis, the dissolved mercury from Run 2C-a was treated with approximately 48 mmol of formic acid (Run 2C-b).

Upon the addition of formic acid, immediate evolution of gas was observed, followed by precipitation of silver-colored droplets of Hg⁰ suspended in the solution (Figure 4-11).



Before formic acid addition, solution was homogeneous and colorless, exhibiting no production of gas. After addition of formic acid, gases were rapidly released and the silver color shown above was observed within seconds.

Figure 4-11. Photograph of HgO-Glycolic Acid Solution After Treatment with Formic Acid.

IC analysis of the resulting product revealed that about 20% of the added formic acid had been destroyed during the reaction and that no additional glycolate had been destroyed. The amount of formic acid destroyed was about 9.7 mmol compared to the 9.3 mmol of Hg that was present, or approximately a 1:1 molar ratio. The oxidation of formate to CO₂ provides the same number of electrons required for reduction of HgO to elemental Hg (two-electron transition) as shown in Reaction [35]:



The observation that precipitation of Hg metal occurred only after formic acid addition indicates that formic acid and not glycolic acid is responsible for the reduction of HgO.

4.4 Combined Species Testing

To confirm the observations made in earlier testing, and to observe any synergistic effects, three combined species tests were performed in the 4-L scale rigs. All three runs were performed with Mn at ~10,300, Hg at ~3,850, and nitrite at ~10,200 mg/kg of slurry. Runs were performed entirely at 93 ± 2 °C; the solutions were never boiled. Acids were added at 0.5 mL/min. The acid requirements per species that were assumed are shown in Table 4-6 and are compared to the requirements for the KMA and Hsu minimum acid equations and Koopman's Cation stoichiometric equation (approximation of 100% actual stoichiometry versus minimum acid stoichiometry).

Table 4-6. Comparison of Stoichiometric Requirements

Species	This Work	KMA	Hsu	Cation
Nitrate	0.67	1.00	0.75	0.50
MnO ₂	2.33	1.50	1.20	3.00
HgO	0.33	1.00	1.00	1.00
Total	3.33	3.50	2.95	4.50

Note that for this work, the acid requirements were intended to be the stoichiometric amounts and not minimum amounts. Based on the discussion in Section 4.3, it may have been appropriate to choose a value for HgO of 2.33 rather than 0.33.

A summary of run parameters and results from these tests is given in Table 4-7. The glycolate destruction was calculated from the measured glycolate concentration and volume in the final product. Some uncertainty is introduced when accounting for samples removed, and the glycolate concentration measurements have been shown in some cases to be biased low, so the glycolate destroyed values may be high.²⁰ The conversion to formate was very low in all three tests and the final oxalate conversions were all zero. The carbon balances closed within 69-85%, with less carbon in the products than in the glycolic acid added (consistent with low glycolate measurements). The amount of glycolate carbon that would be converted to CO₂ by MnO₂ reduction by Reaction [56] was 254 mmol for Runs 1D and 2D. This amount is very close to the amount of CO₂ generated in each of these runs.

For all tests, the nitrite destruction was 100%. The nitrogen balances closed within 81-106%. The N_yO_x generated included NO, NO₂, and N₂O. Measurements of any N₂ or NH₃ formed could not be done, but formation of these is considered unlikely. Again, the generation of N₂O was minimal.

Table 4-7. Run Parameters and Results from Combined Species Testing.

Run ID	1D	2D	3D
Reducing Acid (%)	100	100	74
Noble Metals? (Y/N)	N	Y	Y
Nitrite Destruction (%)	100	100	100
Nitrite to Nitrate Conversion (%)	67	71	96
Glycolate Destruction (%)	13	12	12
Conversion to Formate (%)	0.9	2.2	1.8
Conversion to Oxalate (%)	~0	~0	~0
Peak CO ₂ Production (mmol/min)	2.96	2.49	2.07
Peak NO _x Production (mmol/min)	0.41	0.58	0.30
	(mmol)	(mmol)	(mmol)
Mn Dissolved/Reduced	381	382	381
Hg Dissolved	39	39	39
Hg Precipitated as Hg ⁰ (Reduced)	25	18	15
HgO Reduced (%)	65%	46%	38%
Measured Mn Dissolved (%)	70%	86%	75%
Glycolate Carbon Added	2410	2410	1808
Glycolate Carbon Destroyed (Measured)	306	290	217
Glycolate Carbon Converted to CO ₂ by MnO ₂ Reduction	254	254	*
CO ₂ Generated	238	247	149
Formate Generated	10	~0	~0
Oxalate Generated	~0	~0	~0
Carbon Unaccounted For	58	43	68
Carbon Accounted For as Percentage of Glycolic Acid Destroyed	81%	85%	69%
Nitrite Destroyed	451	451	451
Nitrate Generated	304	340	433
N _y O _x N Generated	59	69	46
Nitrogen Unaccounted For	88	42	-29
Nitrogen Balance Closure (%)	81%	87%	106%

* Some Mn reduced by nitrous acid

With the exception of the addition of noble metals, Runs 1D and 2D were effectively identical, yielding similar results for nitrite-to-nitrate conversion (67% and 71%) and glycolate destruction (13% and 12%).

Run 3D was performed by first metering in nitric acid (26% of the acid stoichiometry), followed by glycolic acid. This change appeared to have a noticeable effect on the nitrite-to-nitrate conversion, increasing it to 96% (relative to 71% observed at 100% glycolic acid).

Figure 4-12 gives instantaneous values calculated for anion conversions and metal solubilities observed during Run 1D as a function of time; Figure 4-14 shows similar results for Run 2D. Note that the instantaneous conversion (glycolate destroyed, glycolate converted to formate or oxalate) is the amount of the species converted or destroyed divided by the cumulative amount of glycolate added. As such, this ratio or percentage will decrease just by dilution as more glycolate is added even there are no reactions occurring. Figure 4-13 shows these same data plotted as the number of mmol of each species as a function of time.

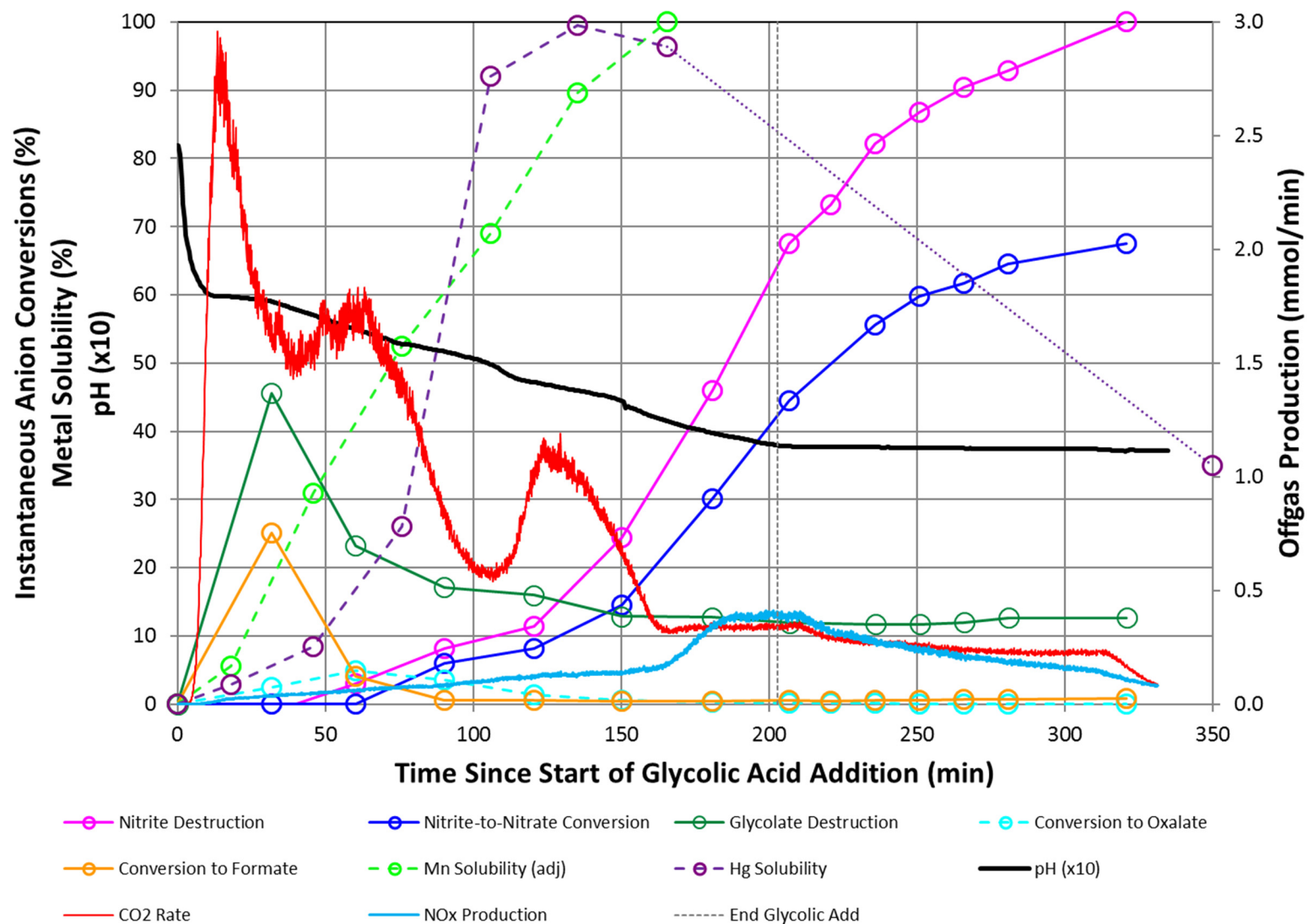


Figure 4-12. Anion Conversions, Offgas Production, Metal Solubilities, and pH of Run 1D as a Function of Processing Time.

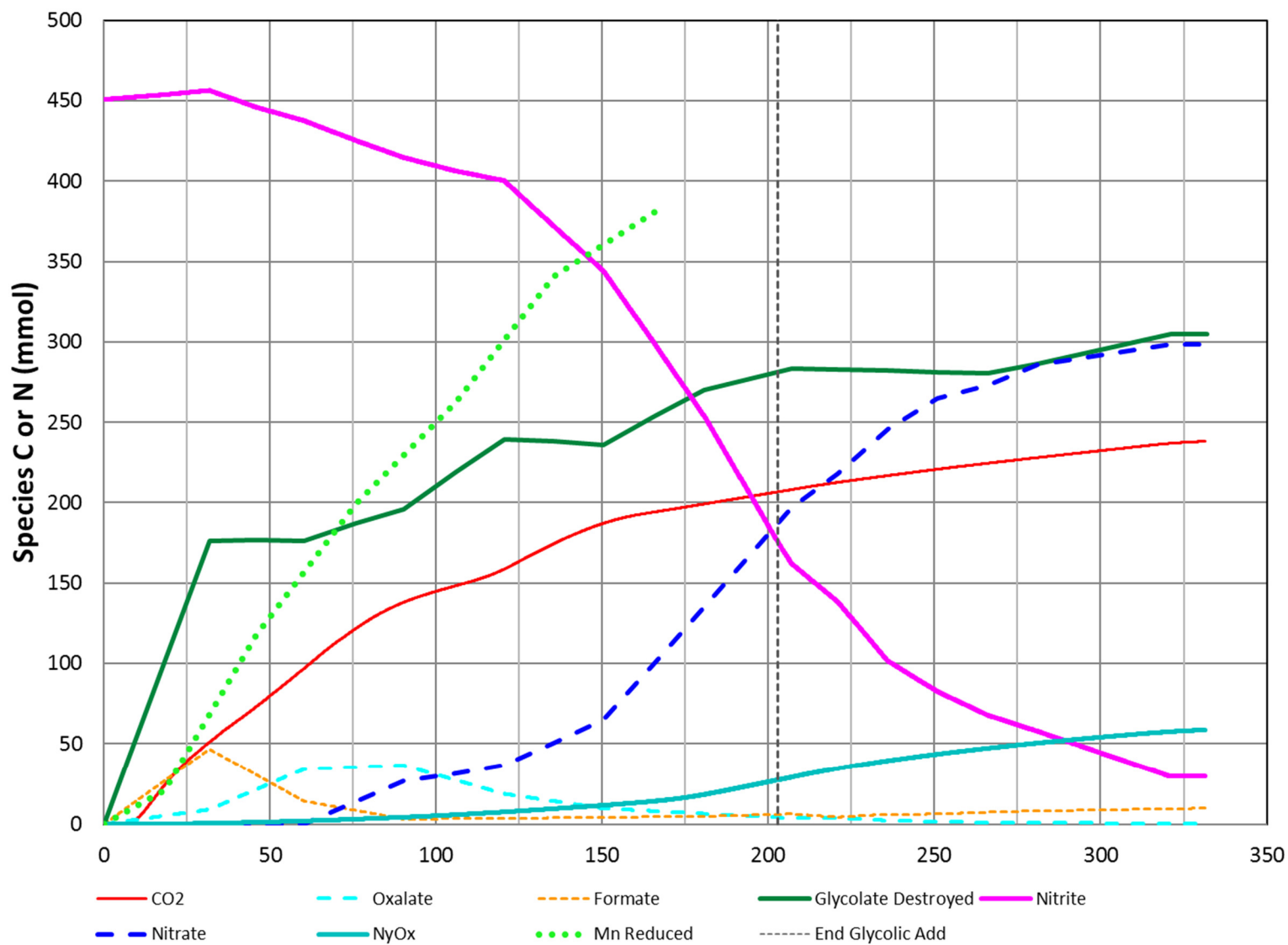


Figure 4-13. Species Quantities for Run 1D as a Function of Processing Time.

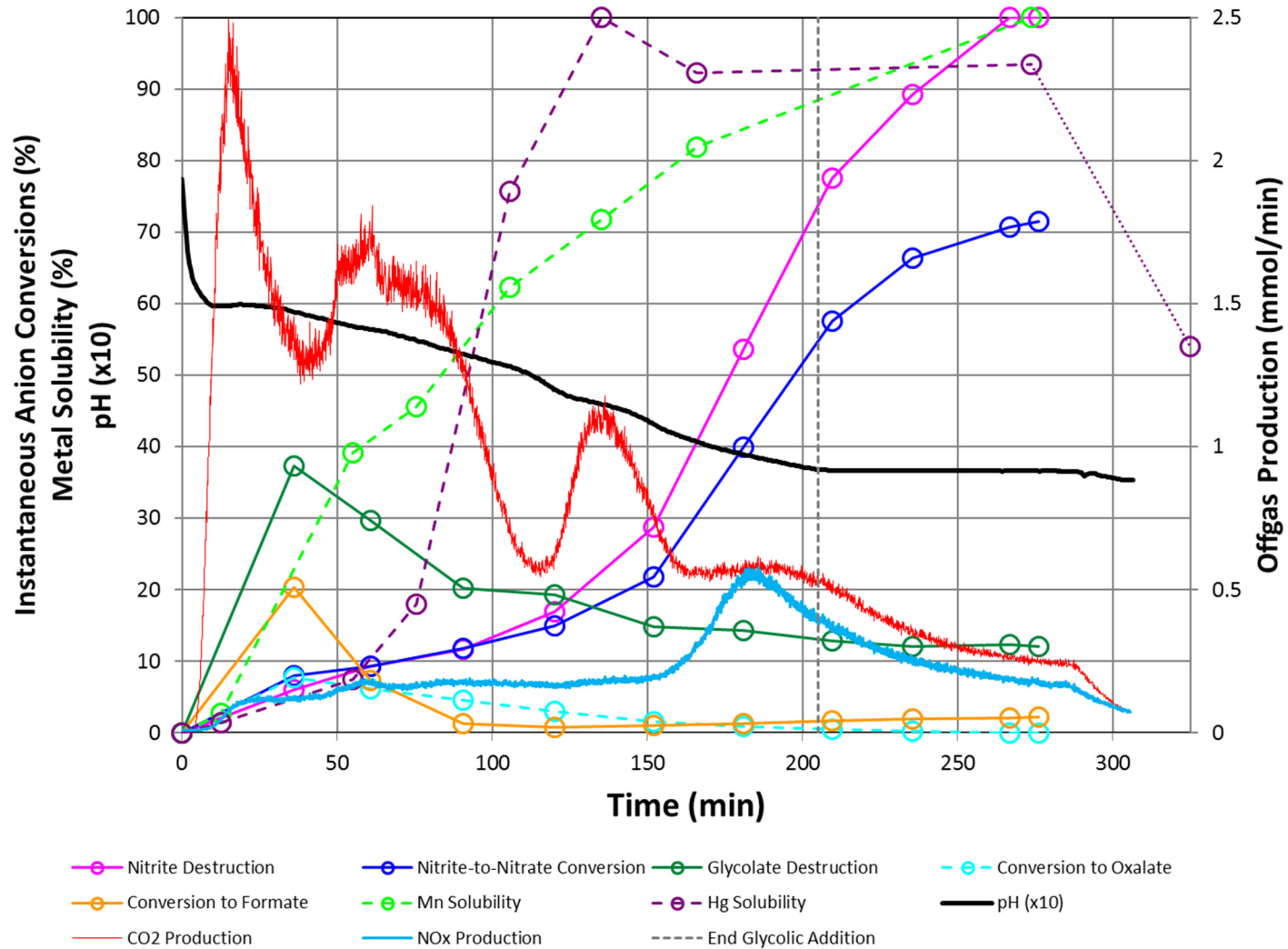


Figure 4-14. Anion Conversions, Offgas Production, Metal Solubilities, and pH of Run 2D as a Function of Processing Time.

Figure 4-12 also shows the offgas generation rates of CO₂ and total NO_x, as well as the pH (multiplied by a factor of ten). The solubility of HgO after the run was completed is shown at 350 min and is connected by a dotted line to indicate that this is not actually the concentration measured at that time. This solubility is based on the recovery of elemental Hg⁰ from the product. Note that the apparent measured solubility of Hg can be misleading. Upon complete dissolution of HgO to form Hg²⁺ or complexes, the measured solubility will be the entire amount of Hg added.

Reduction of the Hg²⁺ to Hg⁰ can generate microscopic droplets of Hg⁰ that will appear as though they are totally dissolved and are thus indistinguishable from Hg²⁺. Only when the droplets coalesce to sufficiently large sizes can they be separated, and the measured solubility will then decrease. Samples that were optically transparent were not subjected to centrifuging that might have removed the Hg⁰. Therefore, the complete solubility of Hg did not necessarily mean that the Hg²⁺ had not been reduced, only that it had not formed a macroscopic Hg⁰ liquid phase.

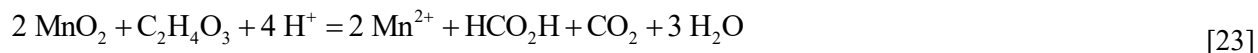
In Figure 4-12, during the first 8 minutes, where the pH drops from about 8.2 to 6.0, only neutralization and possibly protonation of nitrite is occurring. CO₂ generation and MnO₂ dissolution begin when the pH drops below 7.1. Although the final percentage of glycolate destroyed during Run 1D is approximately 13%, the instantaneous glycolate destruction reaches much higher values during the earliest processing times (>40% destroyed at 30 minutes into reaction). This peak corresponds well to the rapid evolution of CO₂ during this time, suggesting that glycolate is quickly oxidized while reducing MnO₂. The maximum glycolate destruction occurred at the peak in CO₂ concentration. During the first 60 minutes, the dissolution of HgO begins, but there is insignificant destruction of nitrite. Nitrite is probably insufficiently protonated to begin disproportionation until about 60 minutes when the pH has begun to drop below about 5.3. The reaction of MnO₂ and glycolic acid to form CO₂ uses up most of the available hydrogen ions until it is complete.

Also, although the amount of formate observed in the final product was very low, the instantaneous conversion to formate during processing is observed to be ~25% at 30 minutes. During this time, the pH remains steady until the glycolate destruction rate and formate generation rates peak. The CO₂ evolution rate then steadies out until the formate concentration significantly decreases, the rate of dissolution of HgO accelerates, and the oxalate concentration peaks at 35 mmol or about 5% conversion of glycolate. The formic acid made and destroyed during this period most likely reduced MnO₂ and not HgO since there was very little dissolved Hg at this time. The observation that oxalate is formed in these experiments but is not formed in simpler reactions involving only MnO₂, HgO, or nitrite with glycolic acid implies that additional reactions are occurring that are not seen in the simpler experiments.

The low generation of formate in these tests are consistent with full sludge CPC demonstrations with noble metals and Hg present.²⁰ Very little formate has been shown to be generated when noble metals and Hg are present, but no demonstrations with only noble metals or only Hg have been conducted, so it has not been possible to determine which of these causes low formate generation. The current work has shown that with Hg present, formate generation is low (compare 1D and 2D to 1B, 2B, and 3C).

Recommendation: Three full sludge demonstrations should be performed with 1) both noble metals and Hg present; 2) with only noble metals present; and 3) with only Hg present to verify that it is the presence of Hg that results in low conversion of glycolate to formate.

Figure 4-13 shows that at about 25 minutes, approximately equimolar amounts (40 mmol) of MnO₂ reduction, formate generation, and CO₂ formation have occurred, but that about 175 mmol of glycolate carbon have been destroyed. About 75 mmol of glycolate carbon destroyed are unaccounted for at this time, suggesting that some other carbon-containing species was present such as glyoxylic acid (which might have been unmeasurable—Section 4.2). Reaction [23], which produces equimolar amounts of CO₂ and formic acid is the closest to this stoichiometry:



Reaction [23]: 1 : 2.0 : 0.5 : 0.5 : 0.5

Observed: 1 : NA: 3.5 : 1.0 : 1.0

The amount of MnO_2 reduced is half the amount expected from the formic acid and CO_2 production, and no other species (HgO , nitrite) appears to have been reduced.

In Figure 4-12, at about 70 minutes, the rate of CO_2 generation drops significantly, the rate of nitrite destruction increases and HgO is dissolved. The rate of CO_2 generation then peaks again when HgO is completely dissolved and most of the MnO_2 is also dissolved. The CO_2 rate then drops down to a relatively steady rate until the end of the test. From 70 min until the end of the run, the moles of CO_2 evolved parallel the moles of glycolate carbon destroyed, indicating that the reactions occurring are generating one mole of CO_2 per mole of glycolate carbon destroyed (Reaction [24]). From the start of dissolution, the rate of MnO_2 dissolution was relatively constant at about 2.4 mmol/min.

The rate of HgO dissolution is initially lower than the rate of MnO_2 dissolution, but it increases significantly from about 75-110 minutes (Figure 4-12). This rate then slows as all of the HgO is dissolved by 140 minutes; reduction of Hg^{2+} may then be starting. From 165 minutes to the end of the run, about 44 mmol of CO_2 are produced and 25-39 mmol of Hg^{2+} are reduced to Hg^0 (25 mmol corresponds to the solubility shown at 350 min; 39 mmol would be complete reduction to Hg^0). The reduction of Hg^{2+} by formic acid has 1:1 stoichiometry. During this time period, glycolic acid is being oxidized slowly, presumably to generate formic acid and CO_2 , but the species oxidizing the glycolic acid is not apparent. The MnO_2 and HgO oxidants are completely spent, leaving only nitrite or nitrous acid, which were shown not to participate in REDOX reactions with glycolic acid in the nitrite only tests. It appears again that the combination of reactants must be causing different reactions to occur compared to the single component tests.

The results for Run 2D with noble metals, shown in Figure 4-14, are very similar to the Run 1D results. One noticeable difference is the rate of MnO_2 dissolution, which is initially similar to Run 1D, but then slows to less than half the rate of Run 1D. The rate of CO_2 generation after the third peak (~120-130 min) was higher in Run 2D while MnO_2 was still being dissolved than in Run 1D where the dissolution of MnO_2 was complete.

Oxalate was only detected in these combined species runs when MnO_2 , HgO , and nitrite were all present. No oxalate was found when only these individual species were used. Glycolate from glycolic acid is consumed during reaction with MnO_2 , but it is not consumed in the reactions with HgO or nitrite. These observations suggest that oxalate is formed from a product of the oxidation of glycolic acid by MnO_2 by a pathway that is only available with HgO (and possibly nitrite) present. Recall that with MnO_2 and nitrite, no formic acid or oxalate were generated. No tests were performed with MnO_2 and HgO without nitrite present, so it was not determined if nitrite is required to produce oxalate.

Figure 4-12 and Figure 4-14 also show the time dependent behavior of nitrite destruction and nitrite-to-nitrate conversion. Unlike glycolic acid, all of the nitrite employed is present at the beginning of the reaction. Therefore, values for nitrite destruction and nitrite-to-nitrate conversion are calculated relative to the amount of nitrite used, not the amount destroyed at a given time. It is interesting to note that there appear to be two regions of nitrite chemistry: 1) the initial region (up to ~120 min) where nitrite destruction and nitrite-to-nitrate conversion track closely, indicating high instantaneous nitrite-to-nitrate conversion, and 2) the later region where nitrite destruction significantly exceeds nitrite-to-nitrate conversion and NO_x evolution is increased. Note that the time of this transition coincides with the end of high CO_2 generation and metal dissolution. While MnO_2 and HgO are being dissolved, these reactions consume both acid (H^+) and glycolate (as a reductant), limiting the amount of acid available to cause the destruction of nitrite by

disproportionation of HNO_2 . Insufficient HNO_2 is formed until the pH gets below about 4.5-5. Therefore, it is reinforced here that the primary mechanism of nitrite destruction and nitrite-to-nitrate conversion is pH-driven and not reductively-driven.

Run 3D differed from Runs 1D and 2D in that two acids were employed (nitric and glycolic) instead of just glycolic, making it more similar to a traditional CPC simulation. Both acids were metered in at 0.5 mL/min with a 10 mL water flush between additions. Run 3D included noble metals as did 2D. Table 4-7 above lists results from Run 3D compared to the other runs. Run 3D results for anion conversion, offgas production, metal solubility, and pH as a function of time are shown graphically in Figure 4-15. Note that the pH in Run 3D drops to about 3.1 compared to 3.8 for Runs 1D and 2D due to the stronger nitric acid used.

In Run 3D, the pH drops quickly to less than 5, which is where HgO dissolution and nitrite destruction became significant in Runs 1D and 2D. HgO begins to dissolve almost immediately upon addition of nitric acid, showing that it is the stronger nitric acid and lower pH that drives both HgO dissolution and nitrite destruction. Note that the initiation of MnO_2 dissolution also occurs prior to the addition of the reducing acid (glycolic acid addition begins around 60 minutes). The formation of nitrous acid that occurs causes the dissolution of MnO_2 as was described in Section 4.1.3 and Reaction [51]. The direct reaction between MnO_2 and HNO_2 would indicate that less than the proposed stoichiometric amount of glycolic acid should be needed. MnO_2 reduction up to 100 min was faster than with only glycolic acid, but the rate then decreased significantly until reaching 100%. About 50 mmol of formic acid could have been produced from MnO_2 reduction from about 140 minutes on. This amount of formic acid is reasonably close to the amount of Hg^0 produced (~35 mmol), so a 1:1 reaction of Hg^{2+} and formic acid is consistent.

Upon addition of glycolic acid, the pH actually increased slightly before continuing to decrease. The solubility of Hg quickly decreased, possibly indicating that the addition of glycolic acid after nitric acid can reduce dissolved Hg^{2+} to Hg^0 sufficiently to see an actual decrease in overall solubility. However, the solubility of Hg then increased to about 100%, which casts doubt on the prior formation of Hg^0 . Several explanations could be given for this behavior: 1) Hg^0 is formed but is re-oxidized and re-dissolved by HNO_2 as more acid is added; 2) Hg^{2+} was not actually reduced, but temporarily converted to a relatively insoluble Hg(II) salt such as mercuric oxalate $\text{Hg}(\text{C}_2\text{O}_4)$ (the oxalate would be detected by IC analysis) that then dissolves as the pH decreases. The behavior of Hg in Run 3D after reaching maximum solubility was very different than the other runs. In Run 3D, the solubility of Hg actually decreased during the experiment to about 40% indicating Hg^0 formation and coalescence. Recall that in Runs 1D and 2D there was insignificant accumulation of Hg^0 until the reaction mixtures were cooled and sat for a period of time.

CO_2 produced from the oxidation of glycolic acid is immediately observed from the reduction of MnO_2 when glycolic acid is added. The small amount of CO_2 observed before glycolic acid addition is likely due to the acidic release of CO_2 that was absorbed during the preparation of the experiment. Just as in Runs 1D and 2D, the production of NO_x gas increases as the initial surge of CO_2 from reduction decreases and Mn solubility is maximized.

Interestingly, measurable accumulation of formate was not observed at any point during Run 3D. Given that formate has been shown to be a product of the reduction of MnO_2 , this result is consistent with there being a reduced amount of MnO_2 present at the start of glycolic acid addition, and with reduction of MnO_2 by nitrous acid.

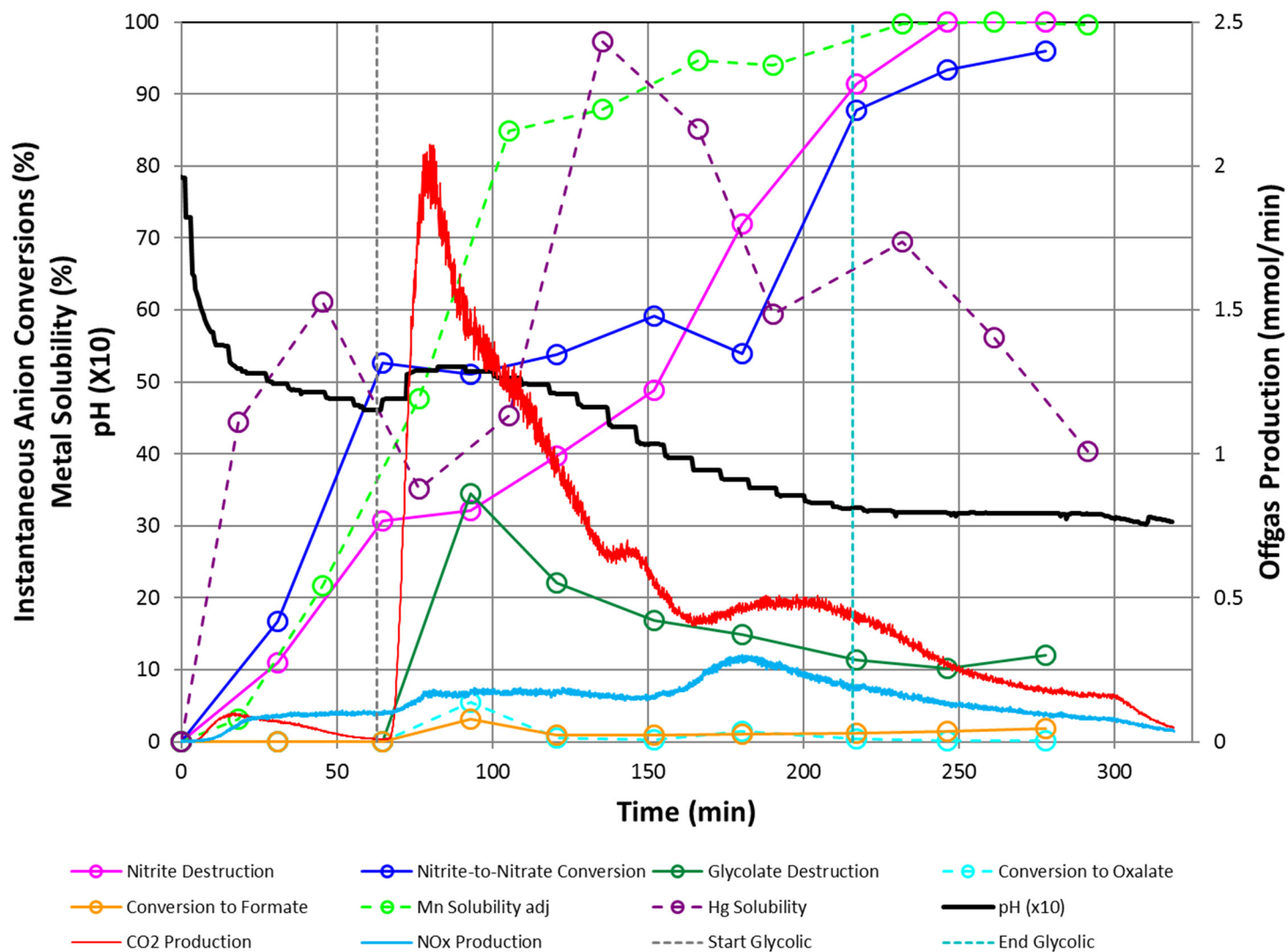


Figure 4-15. Anion Conversions, Offgas Production, Metal Solubilities, and pH of Run 3D as a Function of Processing Time.

The results of this current work suggest that HgO cannot be reduced by glycolic acid without the presence of additional species that appear to generate the apparently necessary formic acid. Runs 1D–3D tested only the combination of MnO₂, HgO, and nitrite. No tests with only MnO₂ and HgO or with only HgO and nitrite were performed. These tests should be performed to deconvolute the effects of each species that could not be determined from the testing with all three present.

Recommendation: Tests with only MnO₂ and HgO and with only HgO and nitrite should be performed to understand the effect of each on the chemistry.

4.4.1 Reduction of HgO in Supernate Only Tests from 2012

Six supernate only tests were performed in 2012 to evaluate the effects on the reduction of HgO of the presence of nitrite, noble metals, and chloride in RuCl₃.²⁹ The moles of chloride in the RuCl₃ was in excess of the moles of HgO used. No MnO₂ was included in this testing. The simulant used contained representative amounts of supernate cations and anions as shown in Table 4-8. Mercury oxide was added at 1.5 wt% of total solids (TS) in GF39a-d and at the same mass in GF39e (2.57 wt% TS). Both nitric and glycolic acids were used in series.

Table 4-8. Composition of Supernate Simulant for Runs GF39a–GF39e

Anion or Cation (mg/kg)	Runs GF39a–d	Run GF39e
Nitrite	21600	0
Nitrate	15800	16300
Carbonate	6050	6250
Oxalate	351	363
Sulfate	1890	19510
Free Hydroxide	3560	3560
Na	27100	27100
K	153	153

Table 4-9 shows additional run parameters and mercury recovery results. For all runs, formate was below the quantification limit (but may have been present; note that in the current work, below quantification values were used). Oxalate appears to have been made in these tests, but the results are ambiguous because oxalate generation was measured at the end of nitric acid addition where it could not have occurred. (At the time of these tests, the Caustic Quench method for glycolate and oxalate had not been developed so the measurement of these concentrations was unreliable.) No formate was detected in any of these tests.

Table 4-9. Runs GF39a-e Parameters and Results

Parameter	Run 39a	Run 39b	Run 39c	Run 39d	Run 39e
% KMA Acid Stoichiometry	100	100	100	80	100
% Reducing Acid	70	70	70	74	65
Rh, Pd, Ag	No	Yes	Yes	Yes	No
RuCl ₃	No	Yes	No	Yes	No
Hg ⁰ Recovery in Offgas Condensate (%)	18	0	13	0	29
Hg ⁰ Recovery in Vessel (%)	43	NA	57	NA	NA
Hg ⁰ Not Recovered (%)	39	NA	30	NA	NA
Hg in Vessel Appearance	Metal	NA	Black	NA	NA
Appearance of Vessel Contents after Dissolution of HgO	Clear until Hg ⁰ precipitation, then cloudy	Opaque purple, then transparent purple	Not noted	Not noted	Clear, appearance not noted after Hg ⁰

In Runs 39a and 39e, the solutions became totally clear upon dissolution of HgO, whereas the solutions with noble metals were purple. Run 39b changed from an opaque purple to transparent purple. Photos of Runs 39a and 39b are shown in Figure 4-16. Reduction of HgO to Hg⁰ definitely occurred in Runs 39a, 39c, and 39e. Runs 39b and 39d with Cl in excess of Hg appear to have possibly made calomel Hg₂Cl₂ that remained in the vessel. The appearance of Hg in the Run 39c product may have been finely divided Hg⁰, which can appear black.



Figure 4-16. Photos of Runs GF39a and 39b Before and After HgO Dissolution

The only significant REDOX active species in the Runs 39a–d simulant was nitrite; oxalate could also participate in REDOX reactions, but its concentration was very low. Nitrate is relatively inert under the mild acidity conditions used. None of the other supernate species used should participate in REDOX reactions. The REDOX reactivity of the noble metals is unknown.

Runs 39a with nitrite definitely produced Hg⁰, apparently showing that the presence of nitrite is sufficient for glycolic acid to reduce HgO. The combination of HgO and nitrite was not tested in the current work.

The most confusing result is Run 39e where nitrite was removed from the simulant and noble metals were not used. In this run, HgO was still reduced to Hg⁰ by a combination of nitric and glycolic acids, which is contrary to the results of the current work for the combination of HgO and glycolic acid. Note that in the current work, nitric acid followed by glycolic acid was not tested for the reduction of HgO.

Adding nitric acid first, followed by glycolic acid, could generate nitrous acid by reduction of the nitric acid and oxidation of the glycolic acid, much like nitric and formic acids will eventually generate nitrous acid. Dissolved metal ions (such as Hg²⁺) may catalyze the formation of nitrous acid under these conditions. Run 39e may have progressed by formation of nitrous acid after both nitric and glycolic acids were added, and then nitrous acid with glycolic acid was then able to reduce HgO to Hg⁰.

Recommendation: The reaction of HgO with glycolic acid should be studied with prior addition of nitric acid to dissolve the HgO to determine if Hg⁰ is formed and if the presence of nitrate is sufficient to cause HgO reduction.

Recommendation: The reduction reactions of MnO₂, HgO and nitrite should be studied further using full supernate simulants to better understand what conditions can result in reduction of HgO. Addition of Fe³⁺ as Fe(OH)₃ solids should also be considered since significant Fe dissolution occurs at high acid stoichiometries, which might indicate reduction of Fe³⁺ to Fe²⁺.

4.5 Minimum Acid Equations for the NG Flowsheet

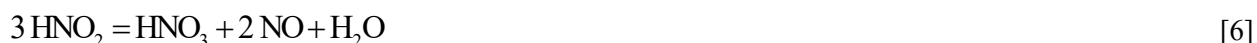
The proposed GMA minimum acid equations for glycolic acid were:

$$A_{\min} = [\text{Base Equivalents} + \text{Soluble TIC} + \alpha \times \text{Hg} + \beta \times \text{Nitrite} + 1.5 \times (\text{Ca} + \text{Mg}) + \delta \times \text{Mn}] \quad [45]$$

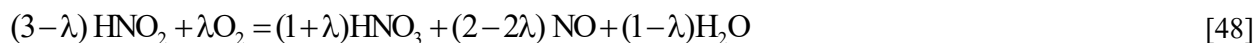
$$A_{\min} = [\text{Base Equivalents} + 2 \times \text{Total TIC} + \alpha \times \text{Hg} + \beta \times \text{Nitrite} + \delta \times \text{Mn}] \quad [57]$$

where α , β , and δ are coefficients to be determined.

The reactions proposed for the reduction of nitrite, MnO₂, and HgO form the basis for the determination of the coefficients in an acid equation for the NG flowsheet. These reactions are repeated here for convenience. Reactions [12], [14], and [48] for nitrite have been written in terms of a variable amount of acid recycle denoted by λ . Reaction [48] is the sum of Reactions [6], [12], and [14].



where $0 \leq \lambda \leq 1$



The variable λ can be adjusted to achieve any overall acid stoichiometry from 67% for no recycle ($\lambda=0$) to zero % for complete conversion of NO to NO₂ and recycle of acid ($\lambda=1$). The actual amount of recycle found during this current work gave a stoichiometry of about 50% ($\lambda=0.33$). These results indicate that the coefficient β on nitrite should be somewhere between 0.5 and 0.67. Note that these values differ from the 0.75 and 1.0 values for the NF flowsheet where the higher values account for the REDOX reaction between nitrite and formic acid to generate both NO and N₂O.

Because glycolic acid by itself does not appear to be able to reduce HgO, the reductions of HgO and MnO₂ are coupled because products of the reaction of glycolic acid with MnO₂ (glyoxylic acid or formic acid) are the reactants with HgO. The reduction reactions of MnO₂ and HgO are rewritten below.



where ξ_i is the extent of reaction i in moles. Note that the possible combinations of reactions is complicated. E.g., glyoxylic acid made from glycolic acid (ξ_1) could then reduce HgO (ξ_4) to generate formic acid, which could then reduce more MnO₂ (ξ_3); the formic acid could also reduce HgO (ξ_5). The relative amounts of each reaction would be dictated by the reaction kinetics.

The total (any) acid requirement (mol any acid/mol MnO₂) for Reactions ξ_1 and ξ_2 is 2 each and for ξ_3 it is 3. When these reactions are combined to reduce 3 moles of MnO₂ with one mole of glycolic acid, the overall acid requirement is 2.33 as shown previously in Equation [30]. The glycolic acid requirement for MnO₂ is independent of the distribution of the reactions and is 1 mole per 3 moles of MnO₂ (0.333). The total any acid requirement is significantly higher than the glycolic acid requirement.

The net any acid for HgO is zero (0) for Reaction ξ_4 and 1.0 for ξ_5 . The glycolic acid requirement is constant at 1 mol of glycolic acid per 3 moles of HgO (0.333), which is the same as for MnO₂. (Both MnO₂ and HgO require 2 electrons for reduction and glycolic has 6 electrons available.) Note that although Reaction ξ_4 requires no net any acid, it does require 0.333 mol of glycolic acid per HgO, so this requirement restricts the range of any acid to HgO to 0.333 to 1.0.

Using the reasoning employed for the Hsu and KMA equations, this value of 2.33 should then be multiplied by the percentage of MnO₂ reduction that is desired or expected, and this value inserted into the GMA equation.

Reactions ξ_4 and ξ_5 are coupled with reactions ξ_1 – ξ_3 by glyoxylic acid (C₂H₂O₃) and formic acid. If 100% reduction of MnO₂ to Mn²⁺ is assumed, then:

$$\begin{aligned} \{\text{MnO}_2\}_o &= \{\text{Mn}^{2+}\} = \xi_1 + \xi_2 + \xi_3 \\ \text{where } \{\text{MnO}_2\}_o &= \text{initial moles of MnO}_2 \\ \{\text{Mn}^{2+}\} &= \text{final moles of Mn}^{2+} \end{aligned} \quad [58]$$

With MnO₂ alone $\xi_1 = \xi_2 = \xi_3$.

Similarly to MnO₂, a balance on Hg is:

$$\begin{aligned} \{\text{HgO}\}_o &= \{\text{Hg}^0\} = \xi_4 + \xi_5 \\ \text{where } \{\text{HgO}\}_o &= \text{initial moles of HgO} \\ \{\text{Hg}^0\} &= \text{final moles of Hg}^0 \end{aligned} \quad [59]$$

If no net formation of glyoxylic acid is assumed, then:

$$\{\text{C}_2\text{H}_2\text{O}_3\} = 0 = \xi_1 - \xi_2 - \xi_4 \quad [60]$$

The net amount of remaining formic acid is:

$$\{\text{HCO}_2\text{H}\} = \xi_2 + \xi_4 - \xi_3 - \xi_5 \quad [61]$$

The requirement of any acid is:

$$\text{Any Acid} = 2\xi_1 + 2\xi_2 + 3\xi_3 + \xi_5 \quad [62]$$

Simultaneous solution of Equations [58]–[62] for initial amounts of MnO_2 and HgO and a desired amount of residual formic acid will give the resulting extents of reaction ξ_1 to ξ_5 . There will be multiple solutions to these equations for any pairs of values of initial MnO_2 and HgO ; i.e., there will not be unique solutions. In reality, there would probably be a unique solution for any pair of values that would depend on the kinetics of each reaction. The total requirement for any acid is $\frac{7}{3}\{\text{MnO}_2\} + \frac{1}{3}\{\text{HgO}\}$, and Figure 4-17 shows the requirement for any acid for MnO_2 versus the requirement for HgO for different molar ratios of MnO_2/HgO . Note that the MnO_2/HgO ratio in sludges is typically about 10.

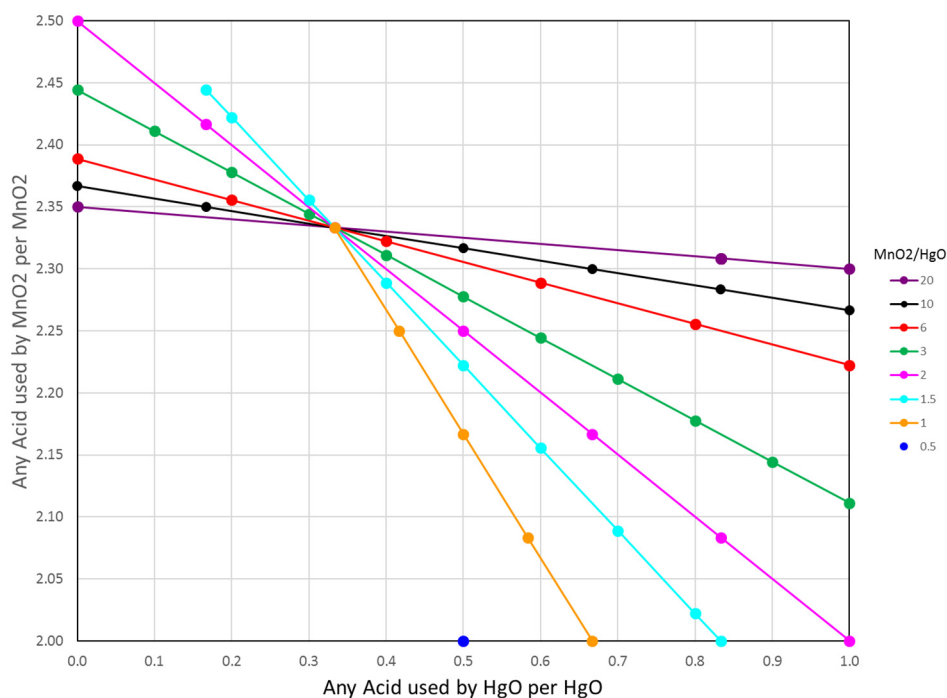


Figure 4-17. Requirement for Any Acid for MnO_2 versus HgO

For typical sludge, the any acid requirement for MnO_2 ranges from about 2.36 to 2.27 mol/mol MnO_2 while the any acid requirement for HgO ranges from 0 to 1 mol/mol HgO . This complicated relationship shows that the overall stoichiometric coefficients on MnO_2 and HgO will vary over ranges that depend on the relative amounts of each of these.

For the typical ratio of MnO_2 to HgO , the any acid requirement for MnO_2 actually varies over a small range, so choosing an average value should be sufficiently accurate. An average value of about 2.3 should be reasonable. The actual coefficient for minimum acid requirement will be some fraction of this value depending on the amount of MnO_2 reduction assumed.

The acid requirement for HgO has a wider range from 0.333 to 1.0, so the choice of value is not as obvious. If HgO is exclusively reduced by formic acid, the value is 1.0, while if by glyoxylic acid it is 0.333. Because the actual distribution of reactions is not known and may vary depending on other factors, the recommended stoichiometric coefficient for HgO is 1.0, which is the same as for the NF flowsheet.

The proposed GMA acid equations based on the KMA [45] and Hsu [46] equations are shown below.

$$A_{\min} = [\text{Base Equivalents} + \text{Soluble TIC} + \alpha \times \text{Hg} + \beta \times \text{Nitrite} + 1.5 \times (\text{Ca} + \text{Mg}) + \delta \times \text{Mn}] \quad [45]$$

$$A_{\min} = [\text{Base Equivalents} + 2 \times \text{Total TIC} + \alpha \times \text{Hg} + \beta \times \text{Nitrite} + \delta \times \text{Mn}] \quad [46]$$

Values for the constants α , β , and δ were chosen based on the previous discussion. The values of these constants and the resulting minimum acid percentages were calculated for the SB9-NG and SC-18 data and are shown in Table 4-11. The concentration inputs to the acid equations are shown in Table 4-10. The equations based on KMA are named # KMA GMA where # is 1 to 5; similarly, the equations based on the Hsu equation are named # Hsu GMA. For all of these, the values are β and δ are shown in parentheses. The value of α was unity for all of the calculations except for 1 KMA GMA, where it was 0.33. The coefficients on Soluble TIC, Total TIC, and Ca+Mg are also given. Values for Mn and Fe solubility, SRAT total solids, SRAT yield stress (up curve) and consistency (up curve) are also shown.

Table 4-10. Concentration Inputs for Table 4-11

Equation Input	Value (mol)
Base Equivalents (mol)	1.421
Soluble TIC (mol)	0.395
Total TIC (mol)	0.445
Hg (mol)	0.0642
Nitrite (mol)	0.732
Base Equivalents (mol)	0.195
Soluble TIC (mol)	0.616

Table 4-11. Calculated Minimum Acid for Proposed Equations

Equation	Coefficients							Calculated Minimum Acid (%)										
	α	β	δ	Base Equiv.	Soluble TIC	Total TIC	Ca+Mg	NG58	SC18	NG51	NG53	NG55	NG55A	NG56	NG57	NG52	NG54	NG59
KMA	1	1	1.5	1	1	0	1.5	77	78	84	84	100	100	100	100	116	117	123
Hsu	1	0.75	1.2	1	0	2	0	80	87	88	87	105	105	105	104	122	122	129
1 KMA GMA (.75 .80 {.33}) ^a	0.33	0.75	0.8	1	1	0	1.5	93	94	101	99	121	121	121	121	138	138	149
2 KMA GMA (.75 .47)	1	0.75	0.47	1	1	0	1.5	98	99	106	106	127	127	127	127	148	148	156
3 KMA GMA (.75 1.4)	1	0.75	1.4	1	1	0	1.5	82	84	89	89	107	107	107	107	124	125	132
4 KMA GMA (.67 .47)	1	0.67	0.47	1	1	0	1.5	100	101	109	108	130	130	130	130	151	151	160
5 KMA GMA (.67 1.4)	1	0.67	1.4	1	1	0	1.5	83	86	91	91	109	109	109	109	126	127	134
1 Hsu GMA (.75 .47)	1	0.75	0.47	1	0	2	0	92	99	100	100	119	119	119	119	139	139	147
2 Hsu GMA (.75 1.4)	1	0.75	1.4	1	0	2	0	78	84	85	85	101	101	101	101	118	118	125
3 Hsu GMA (.67 .47)	1	0.67	0.47	1	0	2	0	93	101	102	101	121	121	122	121	141	141	150
4 Hsu GMA (.67 1.4)	1	0.67	1.4	1	0	2	0	79	86	86	86	103	103	103	103	119	120	127
5 Hsu GMA (.67 .80)	1	0.67	0.8	1	0	2	0	88	95	95	95	114	114	114	114	133	133	140
Mn Solubility (%)	NA	NA	NA					23	18	19	21	53	38	69	50	49	50	66
Fe Solubility (%)	NA	NA	NA					0.2	0.0	0.1	0.3	2.9	2.7	4.1	6.0	11.	5.7	15.
SRAT Total Solids (wt%)	NA	NA	NA					29.8	24.6	30.8	29.9	34.2	19.8	30.9	31.0	26.4	27.7	18.7
SRAT Yield Stress (Pa) ^b	NA	NA	NA					0.6	0.0	1.0	0.5	1.3	0.1	0.8	0.5	11.5	11.7	9.7
SRAT Consistency (Pa) ^b	NA	NA	NA					5.6	2.8	9.5	9.0	10.5	2.6	6.6	5.1	32.7	28.3	17

^a Equation proposed in Lambert, et al.⁸ ^b DWPF SRAT product design range: 1.5-5.0 Pa, 5-12 cP

The value of unity for α was chosen per the previous discussions, except for 1 KMA GMA which was the equation proposed in the SB9-NG report.⁸ The values for β were chosen to be the stoichiometric amount 0.67 determined from this work and a conservatively larger value of 0.75. The Mn term coefficient δ was chosen based on the amount of MnO_2 dissolved. For a theoretical acid requirement of 2.33 moles of acid per mole of MnO_2 , values corresponding to 20% and 60% conversion (solubility) were chosen; these values are 0.47 and 1.4, respectively.

Note that the coefficients in any minimum acid equation should have values that assure sufficient acid to perform each of the desired conversions (Table 2-2). The variations calculated in Table 4-11 use the approximate actual MnO_2 dissolution as the basis for the value of δ . The minimum acid values based on the KMA and Hsu equations are plotted in Figure 4-18 and Figure 4-19, respectively. In most cases, the values based on the KMA equation give higher GMA values than those based on the Hsu equation for the same data points.

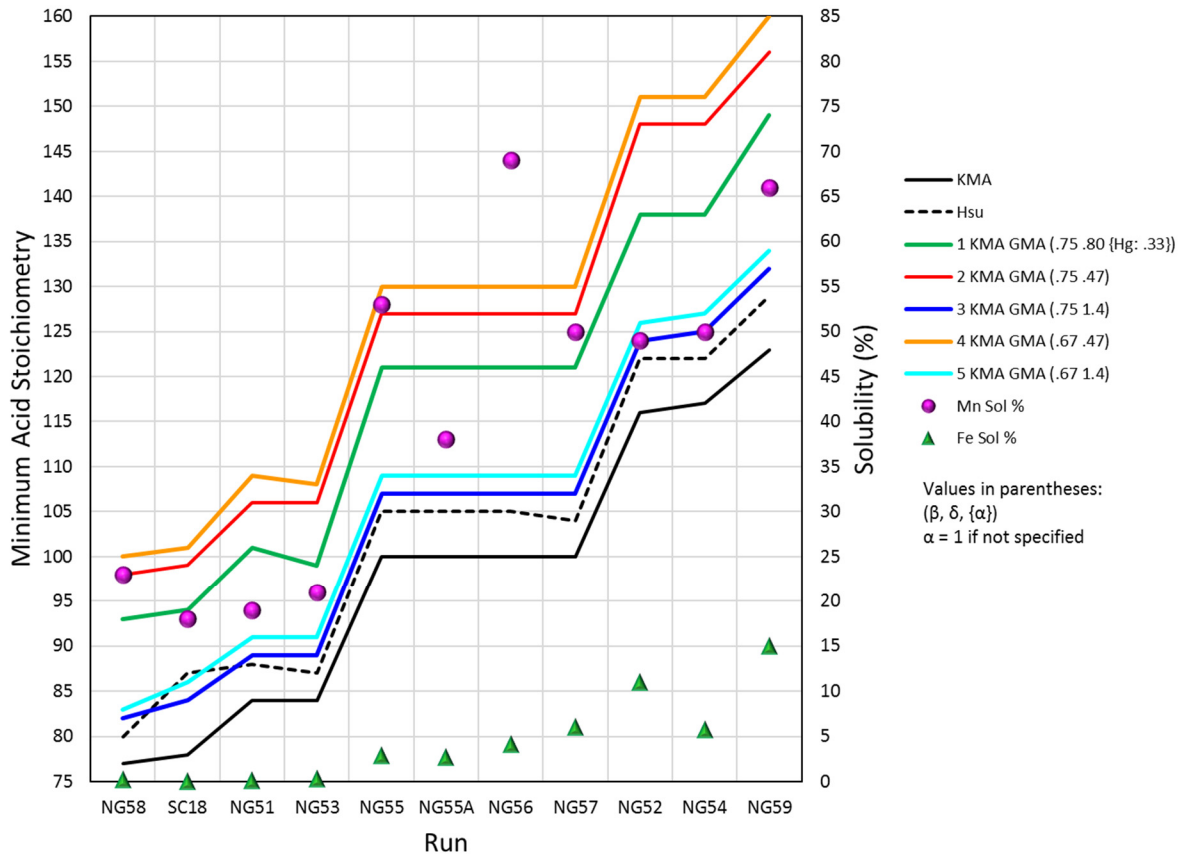


Figure 4-18. GMA Minimum Acid Stoichiometry Based on KMA Equation

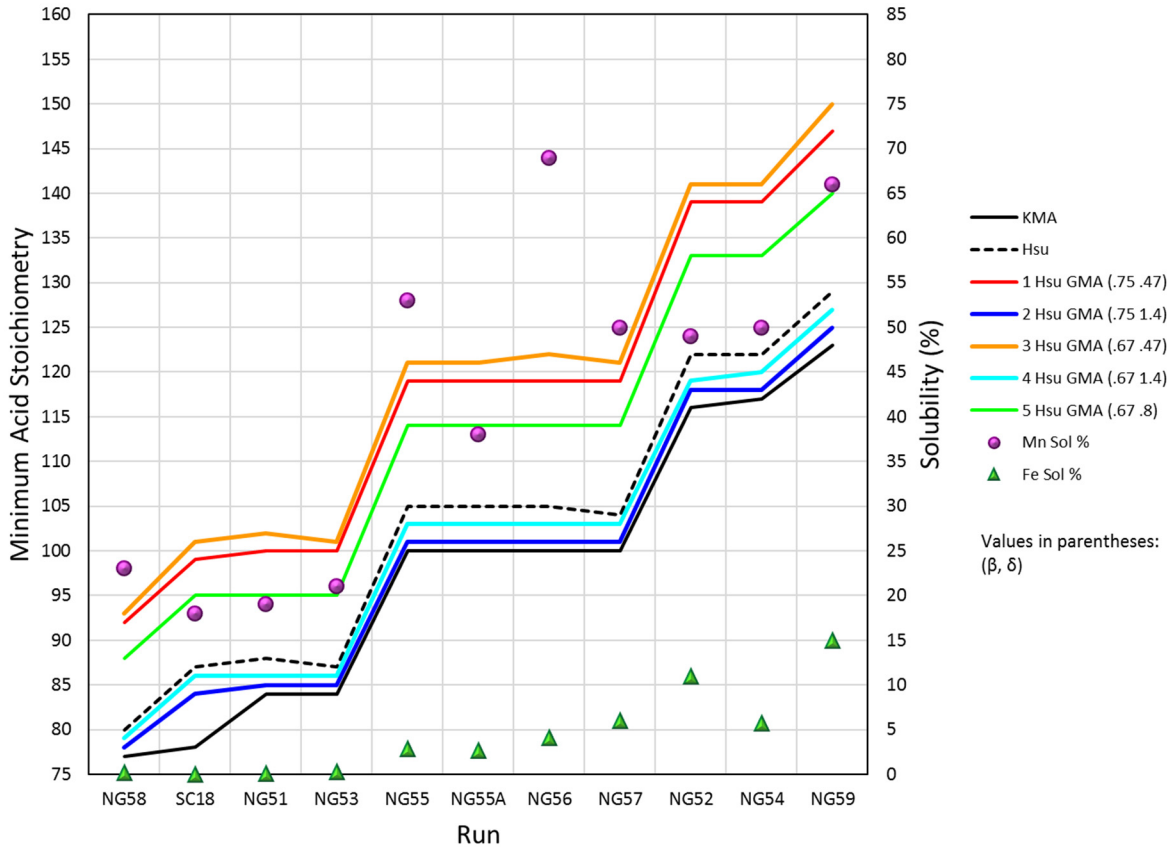


Figure 4-19. GMA Minimum Acid Stoichiometry Based on Hsu Equation

In all of the SB9-NG runs and the SC-18 run, the requirements from Table 2-2 were achieved, except for: 1) the dissolved Mn for the lower acid tests (NG58, SC18, NG51, and NG53) was about 20% versus the Hsu and KMA targets of 40-50%; and 2) the yield stress was either below or above the desired range for all runs (NG55 was close to the lower end value); and 3) the consistency values at the higher acid values (KMA>115) were too high and two runs were too low (SC18 and NG55A). Note that the total solids content of NG55A and NG59 were low compared to the other runs. The Mn solubility was greater than 38% for all KMA values of 100% and higher. Therefore, to achieve at least 40% Mn dissolution it appears that a KMA value of 100% (Hsu ~104%) may be sufficient. The acid requirement to meet the rheology specifications appear to be between KMA 100% and 116% (Hsu ~105-122%). Perhaps at about KMA 105% (Hsu 110%) the rheology would be within specifications. Unfortunately, no tests were done in this intermediate region.

Ignore for the moment that the rheological properties were not met, and assume that 20% dissolution of Mn is acceptable, then which proposed GMA equations would result in runs NG58, SC18, NG51 and NG53 having stoichiometry values of 100% indicating acceptability? The 1 Hsu GMA and 3 Hsu GMA equations fit these runs' data best as expected since the 0.47 coefficient corresponds to 20% dissolution of Mn. These same fits using the KMA basis give values greater than 100%.

Using the 2 Hsu GMA or 2 KMA GMA and 4 Hsu GMA or 4 KMA GMA equations (for 60% Mn solubility) give less than 100% but are slightly higher than KMA and similar to Hsu. These equations for the 100% KMA tests give from 100–103% for 2 Hsu GMA and 4 Hsu GMA; the comparable 2 KMA GMA and 4 KMA GMA values are about 107–109%. The 5 Hsu GMA fit using the 0.8 Mn coefficient (~35% solubility) does not match either proposed 100% fit requirement.

It appears that to achieve about 40-60% dissolution of Mn, the original KMA equation will work along with the 2 Hsu GMA and 4 Hsu GMA equations; all of these match this solubility to about 100% acid and meet the other requirements except for the rheology. Both Figure 4-18 and Figure 4-19 show that Mn solubility does not change significantly from 100% KMA to 123% (NG59). Therefore, the additional acid added from 100% to 123% KMA does not necessarily increase the amount of dissolved Mn.

Table 2-2, Figure 4-18, and Figure 4-19 also show the percentage of dissolved Fe. As previously stated, it is not known if dissolved Fe, which would come from dissolution of $\text{Fe}(\text{OH})_3$ or $\text{FeO}(\text{OH})$, is complexed Fe^{3+} or if the Fe has been reduced to Fe^{2+} and subsequently complexed by glycolic acid. The Fe solubility at 100% KMA was 2.7–6.0% and was 5.1–15.0% at 116% KMA and higher. It appears that additional acid results in dissolution of Fe (and probably other metal species), and perhaps the increase in dissolved metals increases the yield stress and consistency. The yield stress and consistency and Fe solubility are plotted versus KMA in Figure 4-20. The lines are drawn to approximate the trends; the bends are arbitrary since there is no data in the KMA 100–115% region.

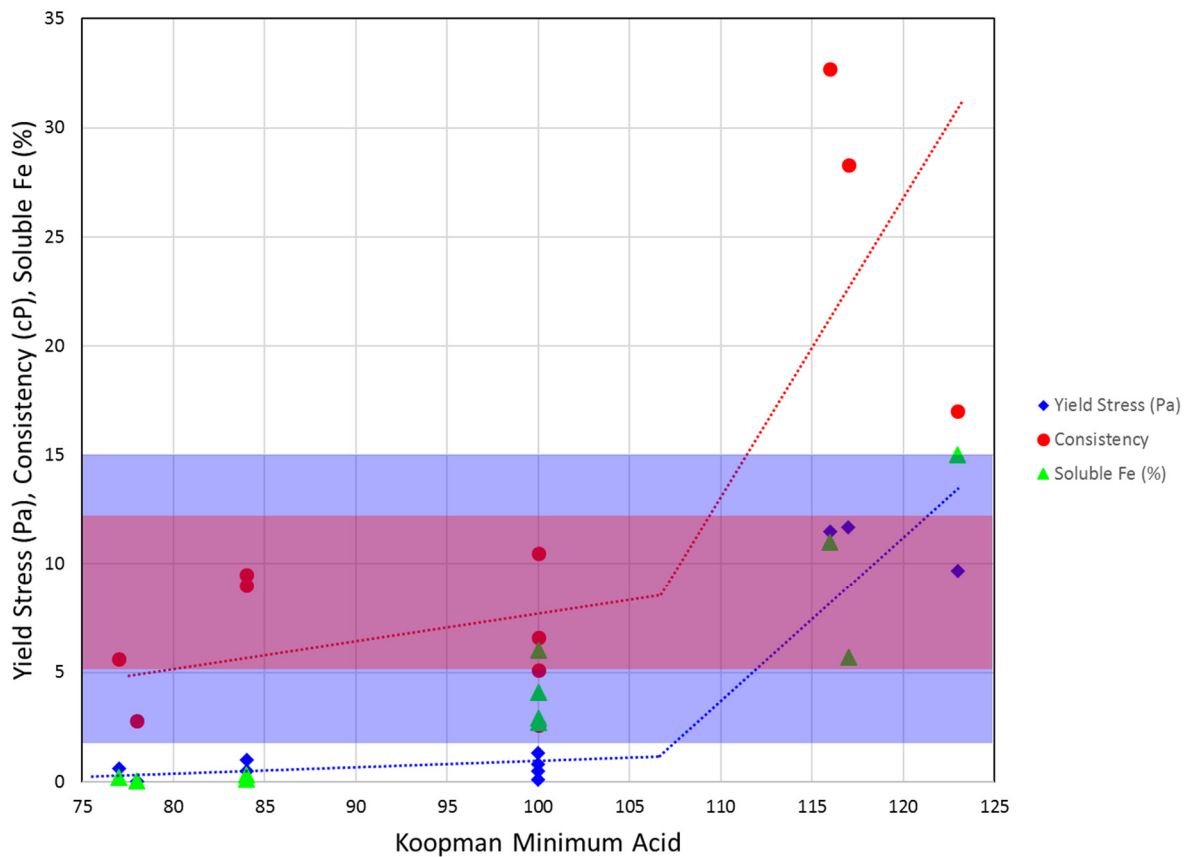


Figure 4-20. SB9-NG and SC-18 Yield Stress and Consistency versus Koopman Minimum Acid

The region in which both yield stress and consistency are within the specifications (shaded areas) lies somewhere between KMA 100–115%. It does appear that there may be a very sudden and steep increase in these values as a function of KMA. The Fe solubility trends similarly to yield stress and consistency and may be indicative of increases in these values. Higher yield stress is believed to be caused by decreased particle size from partial dissolution, and higher consistency is believed to be due to the increased concentration of dissolved metals.

It appears that the acceptable range of KMA may begin at about 105% and extend to about 115%. Ideally, the GMA equation chosen should give the minimum acid requirement at a value of 100%. None of the

alternatives tested gave a GMA value less than the KMA value because the impetus had been to create a GMA equation that gave higher values when KMA was around 80 (since at 80, the nitrite was destroyed and Hg was reduced). To create a GMA equation that would require more acid would require that one of the coefficients in the equation be increased, but there appears to be no chemical basis to increase any of the proposed coefficients (e.g., Mn coefficient should not be increased artificially to give more acid that would not actually increase the Mn solubility). Rather, it appears that the equation may need an additional term to account for the desired increases in yield stress and consistency. It appears that this term could be related to the amount of Fe dissolved. A possible equation could be:

$$A_{\min} = [\text{Base Equivalents} + 2 \times \text{Total TIC} + \alpha \times \text{Hg} + \beta \times \text{Nitrite} + \delta \times \text{Mn}] + \phi(\text{Fe}) \quad [63]$$

where $\phi(\text{Fe})$ is a function that generates a specific quantity of dissolved Fe as a function of the Fe in the feed. I.e., the desired result is not a percentage of the Fe present but is a fixed amount (such as some mg/kg slurry) of dissolved Fe, so that the percentage needed to be dissolved depends on the amount in the sludge. An empirical alternative would be to develop an equation that has fixed value that adequately approximates the additional acid needed. Such an equation would require additional testing with varying sludge compositions.

Recommendation: Further work on the relationships of Mn solubility, Fe solubility, yield stress, and consistency should be performed with additional sludge compositions to develop correlations between these variables and acid requirement.

Examination of additional historical data for the NG flowsheet (other than SB9-NG) should be included in analyses of data similar to that done in this work.

More real waste data is needed because the dissolution of Fe is likely to be different than in simulants.

Recommendation: Future testing should cover the range of KMA values from 100–115% because this appears to be the range that may result in acceptable rheological properties.

Recommendation: The basis for increasing the amount of acid above that from the KMA or one of the proposed GMA equations should be studied further. It appears that this increased acid may be needed to dissolve Fe (and possibly other metals) to a certain extent that results in the desired rheology.

Conclusion: A GMA minimum acid equation similar to the KMA or Hsu equation can be developed for the NG flowsheet that will account for the actual chemical reactions occurring in the NG flowsheet.

The Hsu equation appears to provide a better basis for the development of a GMA equation.

An additional term is needed in a GMA equation to account for the acid necessary to achieve specific rheological properties.

Conclusion: The Hsu and KMA equations are tentatively acceptable for prediction of the acid window with the acceptable range being between 100 and 115% minimum acid.

5.0 Conclusions

Nineteen experiments have been conducted to investigate some of the chemical interactions that occur in the CPC under the glycolic flowsheet. Parameters that were varied were: nitrite, MnO_2 , and HgO concentrations, noble metals addition, acid stoichiometry, acid addition rate, and percent reducing acid. Conclusions from this work include the following:

- The destruction of nitrite to form NO_x gases and nitrate occurs almost totally by internal disproportionation of the nitrous acid formed and not by REDOX reactions with glycolic acid.
- The acid stoichiometry of nitrite destruction is $2/3$ mole of any acid per mole of nitrite.
- Scrubbed NO_2 gas recycled as HNO_2 and HNO_3 reduced the effective acid requirement to $1/2$ mole of any acid per mole of nitrite.
- Lower acid feedrates result in higher nitrite-to-nitrate conversions because relatively more NO_2 is scrubbed to recycle HNO_2 and HNO_3 .
- The generation of HNO_2 and HNO_3 in the MWWT has the potential to dissolve previously collected Hg^0 metal.
- An offgas condensate that was caustic quenched showed the presence of both HNO_2 and HNO_3 , whereas unquenched samples (that had been stored several days or more) showed only the presence of HNO_3 , indicating that HNO_2 is probably lost as NO_x gas during storage. Condensates to be analyzed for nitrogen species other than ammonia should be caustic quenched.
- The reduction of nitrite by glycolic acid produces very small quantities of N_2O , indicating a REDOX reaction does occur but to a very low extent.
- The reduction of one mole of MnO_2 by glycolic acid requires 2.33-2.50 moles of any acid, consumes 0.33 to 0.50 moles of glycolate, but requires about 0.90 moles of glycolate, which is an excess of 100-140% depending on the reaction stoichiometry chosen.
- The reduction of MnO_2 by glycolic acid produces varying amounts of formate. Due to the limited scope of this work, the dependence of the conversion to formate on reaction parameters was not determined.
- No oxalate is generated in the reduction of MnO_2 alone or nitrite alone, or in the dissolution of HgO alone by glycolic acid.
- Oxalate is generated transiently when mixtures of MnO_2 , nitrite, and HgO are reacted with glycolic acid, indicating that there are additional reactions occurring when these three species are present together that do not occur with the individual species.
- This work did not, due to its limited scope, determine the reactions with full sludge simulants that generate measurable quantities of oxalate at the end of the SRAT cycle.
- The reduction of MnO_2 can be accomplished with nitrite and nitric acid, showing that a reducing acid is not required to reduce MnO_2 . In this reaction, nitrous acid acts as a reductant rather than an oxidant as it commonly does. It is unclear what effects this reaction has on acid stoichiometry.
- Most of the formic acid generated in the reduction of MnO_2 is consumed when HgO and nitrite are present.
- It was not determined if the reaction of MnO_2 and glycolic acid to generate two moles of CO_2 per mole of glycolate proceeds directly or through the generation of formate which subsequently reacts with MnO_2 to generate CO_2 .

- There is some evidence that the reduction of MnO_2 by glycolic acid may proceed through glyoxylic acid. Several tests showed more glycolate destruction than could be accounted for by formate and CO_2 generated.
- The presence of glyoxylic acid in samples could be missed by the IC method with caustic quenching if the glyoxylic acid is unstable in caustic solutions.
- Possible intermediate species that are non-ionic are not currently measured. If these species are unstable or volatile in caustic solutions (e.g., formaldehyde), the caustic quench preparation would remove them.
- HgO is readily dissolved by both nitric and glycolic acids.
- In the presence of MnO_2 and HgO , the reduction of nitrite by glycolic acid is delayed until these species are both dissolved.
- The presence of noble metals had no measurable effect on any of the reactions studied.
- Low generation of formate in the presence of noble metals *and* Hg in CPC demonstrations with sludge is due to the presence of Hg and not the noble metals.
- The measurement of dissolved MnO_2 in the presence of glycolic acid appears to be biased low by up to 30%.
- A GMA minimum acid equation similar to the KMA or Hsu equation can be developed for the NG flowsheet that will account for the actual chemical reactions occurring in the NG flowsheet.
- The Hsu equation appears to provide a better basis for the development of a GMA equation.
- The Hsu and KMA equations are tentatively acceptable for prediction of the acid window with the acceptable range being between 100 and 115% minimum acid.
- An additional additive term is needed in a GMA equation to account for the additional acid necessary to achieve specific rheological properties.

6.0 Recommendations

The following recommendations are divided into three categories: 1) additional fundamental R&D on simplified chemistry testing, should SRR choose to fund; 2) testing that would be incorporated into other SRR requested testing such as sludge batch qualification for the NG flowsheet; 3) flowsheet optimization that would occur after transition to the NG flowsheet and throughout one or more sludge batches. None of the recommendations need to be completed prior to implementation of the NG flowsheet in DWPF.

1) Fundamental R&D:

- a. Further testing targeting the role of direct oxidation of nitrite by manganese and other metal oxides in the CPC should be investigated.
- b. Samples for IC analysis should be taken without the Caustic Quench preparation and immediately be analyzed by IC to determine if glyoxylic acid is present. If glyoxylic acid is found, its stability in caustic quenched samples should be investigated.
- c. Tests with only MnO_2 and HgO and with only HgO and nitrite should be performed to understand the effect of each on the chemistry.
- d. The reaction of HgO with glycolic acid should be studied with prior addition of nitric acid to dissolve the HgO to determine if Hg^0 is formed and if the presence of nitrate is sufficient to cause HgO reduction.

- e. The reduction reactions of MnO_2 , HgO and nitrite should be studied further using full supernate simulants to better understand what conditions can result in reduction of HgO . Addition of Fe^{3+} as $\text{Fe}(\text{OH})_3$ solids should also be considered since significant Fe dissolution occurs at high acid stoichiometries, which might indicate reduction of Fe^{3+} to Fe^{2+} .
 - f. Examination of additional historical data for the NG flowsheet (other than SB9-NG) should be included in analyses of data similar to that done in this work.
 - g. Three full sludge demonstrations should be performed with 1) both noble metals and Hg present; 2) with only noble metals present; and 3) with only Hg present to verify that it is the presence of Hg that results in low conversion of glycolate to formate.
- 2) Incorporated into other planned testing:
- a. Future testing should cover the range of KMA values from 100–115% because this appears to be the range that may result in acceptable rheological properties.
 - b. Because the results for SB9-NG indicate that acid requirements from the KMA or 2 Hsu GMA equations between 100-115% may be optimal for melter feed rheology, the basis for increasing the amount of acid above that from the KMA or one of the proposed GMA equations should be studied further. It appears that this increased acid may be needed to dissolve Fe (and possibly other metals) to a certain extent that results in the desired rheology.
 - c. The cause of the low bias in soluble Mn concentration measurements in supernate samples containing glycolic acid should be determined, and a method developed to assure accurate measurements.
 - d. When analyzing condensate samples for nitrite and nitrate, the samples should be caustic quenched to prevent decomposition of nitrous acid during storage. Comparison to unquenched samples should be performed. (Condensate samples should probably not be caustic quenched if the intended analysis is for species that are potentially volatile under caustic conditions (e.g., ammonia, formaldehyde).
- 3) Flowsheet optimization:
- a. Further work on the relationships of Mn solubility, Fe solubility, yield stress, and consistency should be performed with additional sludge compositions to develop correlations between these variables and acid requirement.
 - b. More real waste data is needed because the dissolution of Fe is likely to be different than in simulants.

7.0 References

1. E.W. Holtzscheiter, "Bounding Alternate Reductant Testing/Chemistry and REDOX Definition," Savannah River Remediation, Aiken, SC, **X-TTR-S-00024, Rev. 0**, 2014.
2. C.J. Martino and J.R. Zamecnik, "Task Technical and Quality Assurance Plan for REDOX Prediction and CPC Chemistry Testing," Savannah River National Laboratory, Aiken, SC, **SRNL-RP-2014-01183, Rev. 0**, 2015.
3. J.R. Zamecnik, "Alternate Reductant REDOX Prediction and CPC Chemistry - Path Forward," Savannah River National Laboratory, Aiken, SC, **SRNL-L3100-2014-00254, Rev. 0**, 2015.
4. "Technical Reviews," **Manual E7, Procedure 2.60, Rev. 17**, August 25, 2016.
5. "Savannah River National Laboratory Technical Report Design Check Guidelines," **WSRC-IM-2002-00011, Rev. 2**, August 2004.
6. J.R. Zamecnik and W.H. Woodham, "Savannah River National Laboratory Electronic Laboratory Notebook Experiment T7909-00035-15," 2017.
7. D.P. Lambert, B.R. Pickenheim, M.E. Stone, J.D. Newell, and D.R. Best, "Glycolic-Formic Acid Flowsheet Final Report for Downselection Decision," Savannah River National Laboratory, Aiken, SC, **SRNL-STI-2010-00523, Rev. 1**, 2011.
8. D.P. Lambert, M.S. Williams, C.H. Brandenburg, M.C. Luther, J.D. Newell, and W.H. Woodham, "Sludge Batch 9 Simulants Runs Using the Nitric-Glycolic Acid Flowsheet," Savannah River National Laboratory, Aiken, SC, **SRNL-STI-2016-00319, Rev. 0**, 2016.
9. D.P. Lambert, J.R. Zamecnik, J.D. Newell, and C.J. Martino, "Impact of Scaling on the Nitric-Glycolic Acid Flowsheet," Savannah River National Laboratory, Aiken, SC, **SRNL-STI-2014-00306, Rev. 0**, 2016.
10. J.D. Newell, J.M. Pareizs, C.J. Martino, S.H. Reboul, C.J. Coleman, T.B. Edwards, and F.C. Johnson, "Actual Waste Demonstration of the Nitric-Glycolic Flowsheet for Sludge Batch 9 Qualification," Savannah River National Laboratory, Aiken, SC, **SRNL-STI-2016-00327, Rev. 1**, 2017.
11. D.C. Koopman, D.R. Best, and B.R. Pickenheim, "SRAT Chemistry and Acid Consumption During Simulated DWPF Melter Feed Preparation," Savannah River National Laboratory, Aiken, SC, **WSRC-STI-2008-00131, Rev. 0**, 2008.
12. C.W. Hsu, "Nitric Acid Requirement for Treating Sludge," Westinghouse Savannah River Company, Aiken, SC, **WSRC-RP-92-1056, Rev. 0**, 1992.
13. J.C. Marek and R.E. Eibling, "Draft Computational Algorithms for Nitric Acid Flowsheet," Westinghouse Savannah River Company, Aiken, SC, **SRTC-PTD-92-0050**, 1992.
14. T.E. Smith, J.D. Newell, and W.H. Woodham, "Defense Waste Processing Facility Simulant Chemical Processing Cell Studies for Sludge Batch 9," Savannah River National Laboratory, Aiken, SC, **SRNL-STI-2016-00281, Rev. 0**, 2016.
15. C.M. Jantzen and M.E. Stone, "Role of Manganese Reduction/Oxidation (REDOX) on Foaming and Melt Rate in High Level Waste (HLW) Melters (U)," Westinghouse Savannah River Company, Aiken, SC, **WSRC-STI-2006-00066, Rev. 0**, 2007.
16. C.M. Jantzen, M.S. Williams, T.B. Edwards, C.L. Trivelpiece, and W.G. Ramsey, "Nitric-Glycolic Flowsheet Reduction/Oxidation (REDOX) Model for the Defense Waste Processing Facility (DWPF)," Savannah River National Laboratory, Aiken, SC, **SRNL-STI-2017-00005, Rev. 0**, 2017.
17. C.M. Jantzen, M.S. Williams, J.R. Zamecnik, and D.M. Missimer, "Interim Glycol Flowsheet Reduction/Oxidation (REDOX) Model for the Defense Waste Processing Facility (DWPF)," Savannah River National Laboratory, Aiken, SC, **SRNL-STI-2015-00702, Rev. 0**, 2016.
18. C.M. Jantzen, J.R. Zamecnik, D.C. Koopman, C.C. Herman, and J.B. Pickett, "Electron Equivalents Model for Controlling Reduction-Oxidation (REDOX) Equilibrium During High Level Waste (HLW) Vitrification," Westinghouse Savannah River Company, Aiken, SC, **WSRC-TR-2003-00126, Rev. 0**, 2003.

19. J.R. Zamecnik and T.B. Edwards, "DWPF Nitric-Glycolic Flowsheet Chemical Process Cell Chemistry: Part 1," Savannah River National Laboratory, Aiken, SC, **SRNL-STI-2015-00681, Rev. 0**, 2016.
20. J.R. Zamecnik and T.B. Edwards, "Defense Waste Processing Facility Nitric-Glycolic Flowsheet Chemical Process Cell Chemistry: Part 2," Savannah River National Laboratory, Aiken, SC, **SRNL-STI-2017-00172, Rev. 0**, 2017.
21. M.S. Rayson, J.C. Mackie, E.M. Kennedy, and B.Z. Dlugogorski, "Accurate Rate Constants for Decomposition of Aqueous Nitrous Acid," *Inorganic Chemistry*, **51** [4] 2178-85 (2012).
22. E. Abel and H. Schmid, "The Kinetics of Nitrous Acids. VI. Equilibrium of Nitrous Acid-Nitric Acid-Nitrogen Oxide-Reaction in the Relationship with Its Kinetics," *Zeitschrift Fur Physikalische Chemie--Stoichiometrie Und Verwandtschaftslehre*, **136** [6] 430-6 (1928).
23. E. Abel and H. Schmid, "Kinetics of Salpetre Acids. III. Kinetics of the Salpetre Acid Decomposition," *Zeitschrift Fur Physikalische Chemie--Stoichiometrie Und Verwandtschaftslehre*, **134** [3/4] 279-300 (1928).
24. G. Da Silva, B.Z. Dlugogorski, and E.M. Kennedy, "Elementary Reaction Step Model of the N-Nitrosation of Ammonia," *Int. J. Chem. Kinet.*, **39** [12] 645-56 (2007).
25. S.E. Schwartz and W.H. White, "Kinetics of Reactive Dissolution of Nitrogen Oxides into Aqueous Solution," *Adv. Environ. Sci. Technol.*, **12** 1-116 (1983).
26. B.R. Pickenheim, N.E. Bibler, D.P. Lambert, and M.S. Hay, "Glycolic Acid Physical Properties and Impurities Assessment," Savannah River National Laboratory, Aiken, SC, **SRNL-STI-2010-00314, Rev. 3**, 2017.
27. Y. Wang and A.T. Stone, "Reaction of Mn(III,IV) (Hydr)Oxides with Oxalic Acid, Glyoxylic Acid, Phosphonoformic Acid, and Structurally-Related Organic Compounds," *Geochim. Cosmochim. Acta*, **70** [17] 4477-90 (2006).
28. G. Furlani, F. Pagnanelli, and L. Toro, "Reductive Acid Leaching of Manganese Dioxide with Glucose: Identification of Oxidation Derivatives of Glucose," *Hydrometallurgy*, **81** [3-4] 234-40 (2006).
29. D.P. Lambert, M.E. Stone, J.D. Newell, D.R. Best, and J.R. Zamecnik, "Glycolic-Nitric Acid Flowsheet Demonstration of the DWPF Chemical Process Cell with Sludge and Supernate Simulants," Savannah River National Laboratory, Aiken, SC, **SRNL-STI-2012-00018, Rev. 1**, 2012.
30. R. Portanova, L.H.J. Lajunen, M. Tolazzi, and J. Piispanen, "Critical Evaluation of Stability Constants for Alpha-Hydroxycarboxylic Acid Complexes with Protons and Metal Ions and the Accompanying Enthalpy Changes Part II. Aliphatic 2-Hydroxycarboxylic Acids," *Pure Appl. Chem.*, **75** [4] 495-540 (2003).
31. F.J.C. Rossotti and R.J. Whewell, "Structure and Stability of Carboxylate Complexes. Part 16. Stability-Constants of Some Mercury(II) Carboxylates," *J. Chem. Soc.-Dalton Trans.*, [12] 1223-9 (1977).
32. F.J.C. Rossotti and R.J. Whewell, "Structure and Stability of Carboxylate Complexes. Part 17. Stability-Constants of Some Mercury(I) Carboxylates," *J. Chem. Soc.-Dalton Trans.*, [12] 1229-32 (1977).
33. D.C. Koopman, C.C. Herman, J.M. Pareizs, C.J. Bannochie, D.R. Best, N.E. Bibler, and T.L. Fellingner, "Spontaneous Catalytic Wet Air Oxidation During Pretreatment of High-Level Radioactive Waste Sludge," Savannah River National Laboratory, Aiken, SC, **SRNL-STI-2009-00611, Rev. 0**, 2009.
34. D.C. Koopman and M.E. Stone, "Catalyzed Ammonium Ion Formation from the Reaction of Formic Acid with Nitrate Ion During Radioactive Waste Processing at the Savannah River Site," Savannah River National Laboratory, Aiken, SC, **SRNL-STI-2010-00229, Rev. 0**, 2010.
35. T.L. White, D.P. Lambert, J.R. Zamecnik, and W.T. Riley, "Ion Chromatography (IC) Analysis of Glycolate in Simulated Waste," Savannah River National Laboratory, Aiken, SC, **SRNL-STI-2015-00049, Rev. 0**, 2015.

36. OLI Studio 9.5, OLI Systems, Inc., Cedar Knolls, NJ, 2017.
37. K.H. Tan and M.J. Taylor, "Vibrational Spectra of Mercury (I) Nitrate in Aqueous Solution and of the Crystalline Hydrolysis Products," *Aust. J. Chem.*, **31** [12] 2601-8 (1978).
38. D. Vione, V. Maurino, C. Minero, and E. Pelizzetti, "Phenol Nitration Upon Oxidation of Nitrite by Mn(III,IV) (Hydr)Oxides," *Chemosphere*, **55** [7] 941-9 (2004).
39. G.W. Luther, III and J.I. Popp, "Kinetics of the Abiotic Reduction of Polymeric Manganese Dioxide by Nitrite: An Anaerobic Nitrification Reaction," *Aquatic Geochemistry*, **8** [1] 15-36 (2002).

Appendix A Equations for the Prediction of Glycolate Destruction, Nitrite to Nitrate Conversion, and Conversions to Formate and Oxalate

The following equations are from Zamecnik and Edwards.²⁰

Equation for the prediction of glycolate destruction G_D :

$$G_D(\%) = 0.2997349 - 0.319911 * AS(\%) + 1.9179 \times 10^{-5} * \text{nitrate (mg/kg)} + 0.0232576 * Hg(\text{wt}\%)$$

where G_D = glycolate destruction (%)

AS = acid stoichiometry (%) (Koopman Minimum Acid)

nitrate = nitrate concentration in sludge (mg/kg slurry)

Hg = mercury concentration in sludge (wt% of total solids)

Equations for the prediction of glycolate to oxalate conversion G_{toOx} are shown below. Two models were found to have similar fits to the data.

Model X6:

$$G_{toOx} = 0.4459707 - 0.187849 * AS(\%) - 1.8754 \times 10^{-5} * \text{nitrite (mg/kg)}$$

Model X7:

$$G_{toOx} = 0.2182302 - 0.170654 * AS(\%) - 0.01870 \langle \text{Ru form} \rangle$$

where $\langle \text{Ru form} \rangle = +1$ if Ru nitrosyl nitrate is not present

$= -1$ if Ru nitrosyl nitrate is present

and

where nitrite = nitrite concentration in sludge (mg/kg slurry)

Similarly, two approximately equivalent models for nitrite to nitrate conversion N_C were determined:

Model N4e:

$$N_C(\%) = 1.4908845 - 0.7862982 * AS(\%) - 1.326445 * PRA(\%) - 9.075 \times 10^{-5} * \text{nitrite (mg/kg)}$$

Model N4f:

$$N_C(\%) = 1.833 - 0.802 * AS(\%) - 1.33 * PRA(\%) - 1.11 \times 10^{-4} * \text{nitrite (mg/kg)} - 0.0560 * Hg(\text{wt}\%)$$

where N_C = nitrite to nitrate conversion (%)

PRA = percent reducing acid (%) (percentage of glycolic + nitric acids that is glycolic acid)

The model for glycolate to formate conversion G_{toF} in the presence of Hg and noble metals is:

$$G_{toF}(\%) = -0.059033 + \frac{0.076181}{AS(\%)}$$

Distribution:

EDWS (records administration)

alex.cozzi@srnl.doe.gov

david.crowley@srnl.doe.gov

david.dooley@srnl.doe.gov

a.fellinger@srnl.doe.gov

samuel.fink@srnl.doe.gov

nancy.halverson@srnl.doe.gov

erich.hansen@srnl.doe.gov

connie.herman@srnl.doe.gov

david.herman@srnl.doe.gov

kevin.fox@srnl.doe.gov

john.mayer@srnl.doe.gov

daniel.mccabe@srnl.doe.gov

gregg.morgan@srnl.doe.gov

frank.pennebaker@srnl.doe.gov

william.ramsey@srnl.doe.gov

luke.reid@srnl.doe.gov

geoffrey.smoland@srnl.doe.gov

michael.stone@srnl.doe.gov

boyd.wiedenman@srnl.doe.gov

bill.wilmarth@srnl.doe.gov

jeffrey.crenshaw@srs.gov

james.folk@srs.gov

roberto.gonzalez@srs.gov

tony.polk@srs.gov

jean.ridley@srs.gov

patricia.suggs@srs.gov

kevin.brotherton@srs.gov

richard.edwards@srs.gov

terri.fellinger@srs.gov

eric.freed@srs.gov

jeffrey.gillam@srs.gov

barbara.hamm@srs.gov

bill.holtzscheiter@srs.gov

john.iaukea@srs.gov

vijay.jain@srs.gov

chris.martino@srnl.doe.gov

jeff.ray@srs.gov

paul.ryan@srs.gov

azadeh.samadi-dezfouli@srs.gov

hasmukh.shah@srs.gov

aaron.staub@srs.gov

christie.sudduth@srs.gov

thomas.colleran@srs.gov

john.iaukea@srs.gov

spencer.isom@srs.gov

maria.rios-armstrong@srs.gov

jack.zamecnik@srnl.doe.gov

maximilian.gorensek@srnl.doe.gov

dan.lambert@srnl.doe.gov

david.newell@srnl.doe.gov

wesley.woodham@srnl.doe.gov

david.henley@srs.gov

anthony.howe@srnl.doe.gov

victoria.kmiec@srs.gov